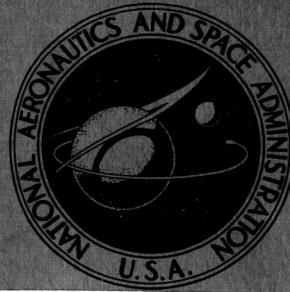


NASA CONTRACTOR
REPORT



NASA CR-126

NASA CR-126

FACILITY FORM 603

N65-12811

(ACCESSION NUMBER) _____

132

(PAGES)

(NASA CR OR TMX OR AD NUMBER)

(THRU)

1

(CODE)

13

(CATEGORY)

GPO PRICE \$ _____

OTS PRICE(S) \$ _____

Hard copy (HC) _____

Microfiche (MF) 1.00

PHOTOGRAPHY OF THE WESTERN
SAHARA DESERT FROM THE
MERCURY MA-4 SPACECRAFT

by A. Morrison and M. C. Chown

Prepared under Contract No. NASr-140 by

McGILL UNIVERSITY

Montreal, Quebec

for

PHOTOGRAPHY OF THE WESTERN SAHARA DESERT FROM
THE MERCURY MA-4 SPACECRAFT

By A. Morrison and M. C. Chown

Distribution of this report is provided in the interest of information exchange. Responsibility for the contents resides in the author or organization that prepared it.

Prepared under Contract No. NASr-140 by
McGILL UNIVERSITY
Montreal, Quebec

for

NATIONAL AERONAUTICS AND SPACE ADMINISTRATION

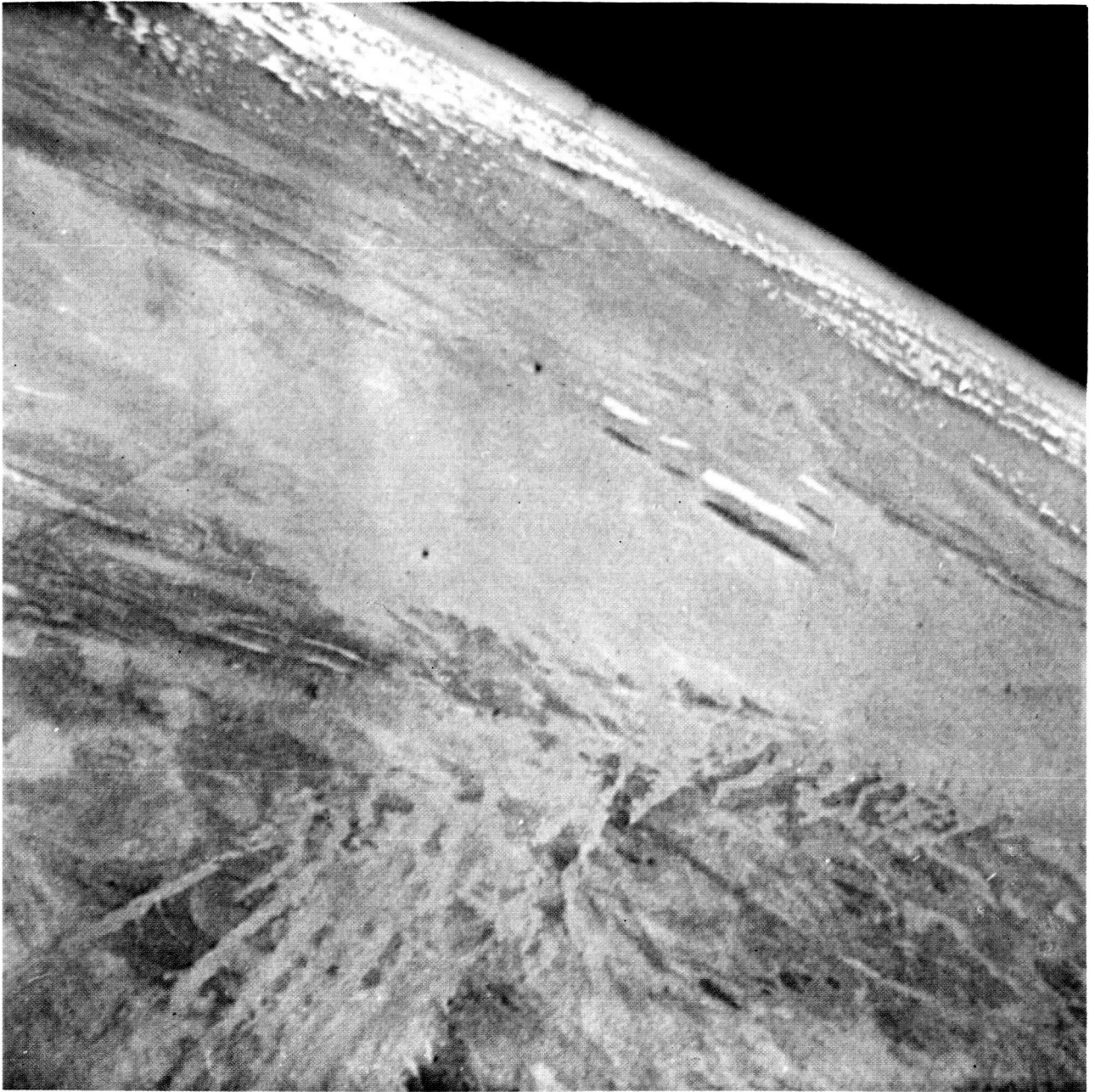
FOREWORD

This study has been supervised by Professor J. B. Bird.

The Manned Spacecraft Center of the National Aeronautics and Space Administration were responsible for the photography.

The authors acknowledge the assistance of J. Lobb of Manned Spacecraft Center, and K.M. Nagler and L.F. Hubert of National Weather Satellite Center in obtaining photographs and information; and of J.J. Donegan and C.A. Packard of NASA Goddard Space Flight Center, Data Operations Branch, who provided orbital data.

Drafting was carried out by J. Wolfe, P. Wallace, and J. Harrison.



Frontispiece. Photo 198, illustrating typical color rendering and showing the longitudinal dunes of the Erg Iguidi and part of the Eglab massif.

TABLE OF CONTENTS

SUMMARY	1
CIRCUMSTANCES OF THE PHOTOGRAPHY	1
Previous photography of the earth from space	1
Photographic system	2
Location and orientation of photographs	5
Method of determining location and orientation data	5
Accuracy of location and orientation data	8
INTRODUCTION TO THE AREA PHOTOGRAPHED	8
Climate	9
Vegetation	9
Geological structure and related landform types	14
Denudation processes and related landform types	15
Sources of information	16
INTRODUCTION TO THE SELECTED INTERPRETED PHOTOGRAPHS	18
SELECTED INTERPRETED PHOTOGRAPHS	22
COLORS	100
RESOLUTION	101
STEREOSCOPIIC EFFECT	102
Observed	102
In theory	103
INTERPRETATION	104
General	104
Geology	105
Landforms	110
Vegetation	112
Land use	112

PROPERTIES DESIRABLE IN GEOGRAPHIC SPACE PHOTOGRAPHY. 113

Area covered by a single frame 113
Ground resolution (including scale) 114
Nadir angle 115
Overlap and convergence 115
Number of wavebands used 115
Date and frequency 116
Regions photographed 116

POSSIBLE MODIFICATIONS OF THE MA-4 PHOTOGRAPHIC
SYSTEM 116

Orbital elements 116
Orientation of principal axis 117
Camera mounting 117
Camera 118
Film and filter 119
Timing of photography 120

REFERENCES 121

LIST OF FIGURES

1.	Variation along the flightline of (a) azimuth of principal axis, (b) nadir angle of principal axis, and (c) spin angle of camera about principal axis	4
2.	Method of calculating values of nadir angle	7
3.	Climatic regions of northwestern Africa	11
4.	Vegetation of northwestern Africa	11
5.	Geology of northwestern Africa	12
6.	Schematic geological cross-section across northwestern Africa . . .	13
7.	Map showing area covered by each of the selected interpreted photographs	17
8.	Key to lines used on geological overlays	21
9.	Photo 185 with overlays	23
10.	Photo 187 with overlays	27
11.	Typical geological section across the area shown in photo 187	29
12.	Photo 190 with overlays	31
13.	Photo 192 with overlays	35
14.	Photo 195 with overlays	39
15.	Typical geological section across the area shown in photo 195	41
16.	Photo 198 with overlays	43
17.	Photo 202 with overlays	47
18.	Photo 206 with overlays	51
19.	Photo 210 with overlays	55
20.	Photo 216 with overlays	59
21.	Typical geological section across the area shown in photo 216	61
22.	Photo 223 with overlays	63
23.	Photo 230 with overlays	67
24.	Photo 236 with overlays	71
25.	Photo 239 with overlays	75
26.	Photo 243 with overlay	79
27.	Photo 247 with overlays	83
28.	Photo 250 with overlay	87
29.	Photo 257 with overlay	91
30.	Photo 261 with overlay	95
31.	Photo 268 with overlay	98
32.	Structural lineaments of the northwestern Sahara	106
33.	Structural lineaments of the central Sahara	107

PHOTOGRAPHY OF THE WESTERN SAHARA DESERT
FROM

THE MERCURY MA-4 SPACECRAFT

by A. Morrison and M. C. Chown

SUMMARY

The sequence of high oblique color photographs taken by the automatic camera in the MA-4 spacecraft over the western Sahara in 1961 remains the only sequence of generally available photographs recovered from space which shows a land area of near-continental extent not obscured by cloud or haze.

The larger geological and landform patterns of the area, as well as vegetation boundaries on the south edge of the Sahara can be mapped from the photographs. One photo illustrates the potentiality of space photography for small-scale land-use mapping.

The photos appear mainly blue because no filter was used, but other colors present distinguish between geological formations which otherwise appear similar. The resolution of the original transparencies in terms of a standard test object was roughly 10-15 lines/mm. Observations and calculations show that the smallest ground features which can be seen stereoscopically on these photos are of the order of 1000 ft. high.

Much better results could be obtained using a photographic system specifically designed for mapping geographic distributions. Such systems would usually involve vertical photographs with 60% overlap; a black-and-white, infrared, or false-color film filtered to eliminate blue light; and a film of higher definition even at the cost of lower filmspeed.

CIRCUMSTANCES OF THE PHOTOGRAPHY

Previous photography of the earth from space

The photographs taken during the Mercury Atlas 4 spaceflight were the first photographs on film known to be recovered from an earth satellite. Photographs of the earth from heights practically as high as that of the Mercury spacecraft had been recovered from rocket capsules as early as the period 1946 to 1954. (ref. 2). Photographs of better quality and from greater heights had been obtained in 1954 and 1955. (refs. 3, 4). Photographs of the earth from considerably higher altitudes than those reached by the Mercury spacecraft, and covering an area in total perhaps half as large as that visible in the Mercury photos were obtained in 1959. (ref. 5). All these were recovered from the capsules of rockets which did not go into orbit, so that the

area photographed was limited by the extent of the rocket range. In addition, by the time of the MA-4 flight in September 1961, many thousands of pictures, together covering a large part of the earth's surface, and taken from considerably greater heights, had already been relayed back to earth by a television system from the Tiros series of satellites which began in 1960. (refs. 7, 8, 16). More complete accounts of space photography before and since the MA-4 flight have been given by Lowman (ref. 15), and by Bird and Morrison (ref. 14).

The MA-4 photographs are notable as the first series of photographs on film recovered from space which covered a land area of continental extent. Unlike previous aerial and Tiros photographs, they give a view of this enormous expanse which is both all-embracing and comparatively detailed. They display at a glance patterns so extensive that they can otherwise be revealed only by decades of hazardous ground travel or months of work with air photographs.

Photographic system

The Mercury-Atlas 4 (MA-4) rocket launched Mercury capsule 8A from Cape Kennedy (then Cape Canaveral), Florida, at 9 hr. 4 min. 16 sec. Eastern Standard Time on the morning of September 13th, 1961, (Lobb, personal communication) and placed it in orbit around the earth.

The orbit varied between 85.93 naut. mi. (97.99 st. mi., 159.25 km) and 120.02 naut. mi. (138.21 st. mi., 222.43 km) above the earth regarded as a sphere. Perigee was located east of Bermuda at 32.54°N lat., 43.46°W long.; apogee over S. W. Australia at 32.75°S lat., 119.44°E long. The maximum velocity reached was 24,389 ft/sec (16,629 mph, 26,606 km/hr) relative to the earth's surface below, or 25,400 ft/sec (17,320 mph, 27,700 km/hr) relative to the centre of the earth. The capsule passed around the earth once only; the retrograde rockets were fired over New Mexico at 26.22°N lat., 110.57°W long.; and the capsule splashed down in the Atlantic 161 mi. east of Bermuda, 1 hr. 49 mins. 20 secs. after launch, and was recovered. (Data Operations Branch, Manned Flight Operations Division, NASA Goddard Space Flight Center, personal communication; ref. 13, pp. 206, 148). Precise details of the orbit over northwestern Africa are given in table 1.

The capsule was not manned, but since the main objective of the flight was to test the spacecraft systems under conditions similar to those of manned orbital flight, the interior was maintained at a pressure and a temperature suitable for an astronaut.

In addition to the camera which took the photographs described in this report, the capsule carried a 16 mm camera, the 'Instrument observer camera', which continuously photographed the instrument panel; and a second 16 mm camera, the 'Periscope camera', which photographed the earth and sky every 2 seconds through the periscope optical system, which had a 178°

TABLE 1

Photo number	Time G.M.T.			Altitude above an oblate earth			Latitude	Longitude	Nadir angle of principal axis	Azimuth of principal axis	Spin angle
	Hr.	Min.	Sec.	Naut. Mi.	Stat. Mi.	Km.	° N	°	°	°	°
185	14	22	42	88.26	101.6	163.6	26.23	12.34W	72.3	22	116
187	14	22	54	88.38	101.7	163.8	25.94	11.53W	72.1	24	116
190	14	23	12	88.56	101.9	164.1	25.50	10.32W	69.2	24	118
192	14	23	24	88.68	102.1	164.3	25.20	9.53W	67.1	23	119
195	14	23	42	88.87	102.3	164.7	24.74	8.34W	64.9	20.9	121
198	14	24	00	89.06	102.5	165.0	24.26	7.16W	68.2	20.5	119
202	14	24	24	89.33	102.9	165.5	23.62	5.61W	74.0	22.6	120
206	14	24	48	89.61	103.2	166.1	22.96	4.07W	76.7	25.5	118
210	14	25	12	89.91	103.5	166.6	22.28	2.54W	75.0	27.8	115
216	14	25	48	90.37	104.1	167.5	21.23	0.29W	69.4	32	117
223	14	26	30	90.93	104.7	168.5	19.97	2.30E	67.0	29.3	119
230	14	27	12	91.53	105.4	169.6	18.66	4.84E	67.0	24	117
236	14	27	48	92.07	106.0	170.6	17.51	6.98E	71.0	17.9	115
239	14	28	06	92.35	106.3	171.1	16.93	8.04E	75.8	16	117
243	14	28	30	92.73	106.8	171.8	16.14	9.44E	77.6	25	118
247	14	28	54	93.12	107.2	172.6	15.34	10.84E	74.5	23.7	117
250	14	29	12	93.42	107.6	173.1	14.73	11.87E	69.8	25.4	118
257	14	29	54	94.14	108.4	174.5	13.40	14.26E	73.4	28	115
261	14	30	18	94.56	108.9	175.2	12.47	15.61E	77.5	33.7	119
268	14	31	00	95.33	109.8	176.7	11.0	17.96E	84.5	37	121

field of view. (Valdyke, unpublished).

The photographs described in this report were taken through the capsule window, with the aid of a mirror system, by a 70 mm camera, the

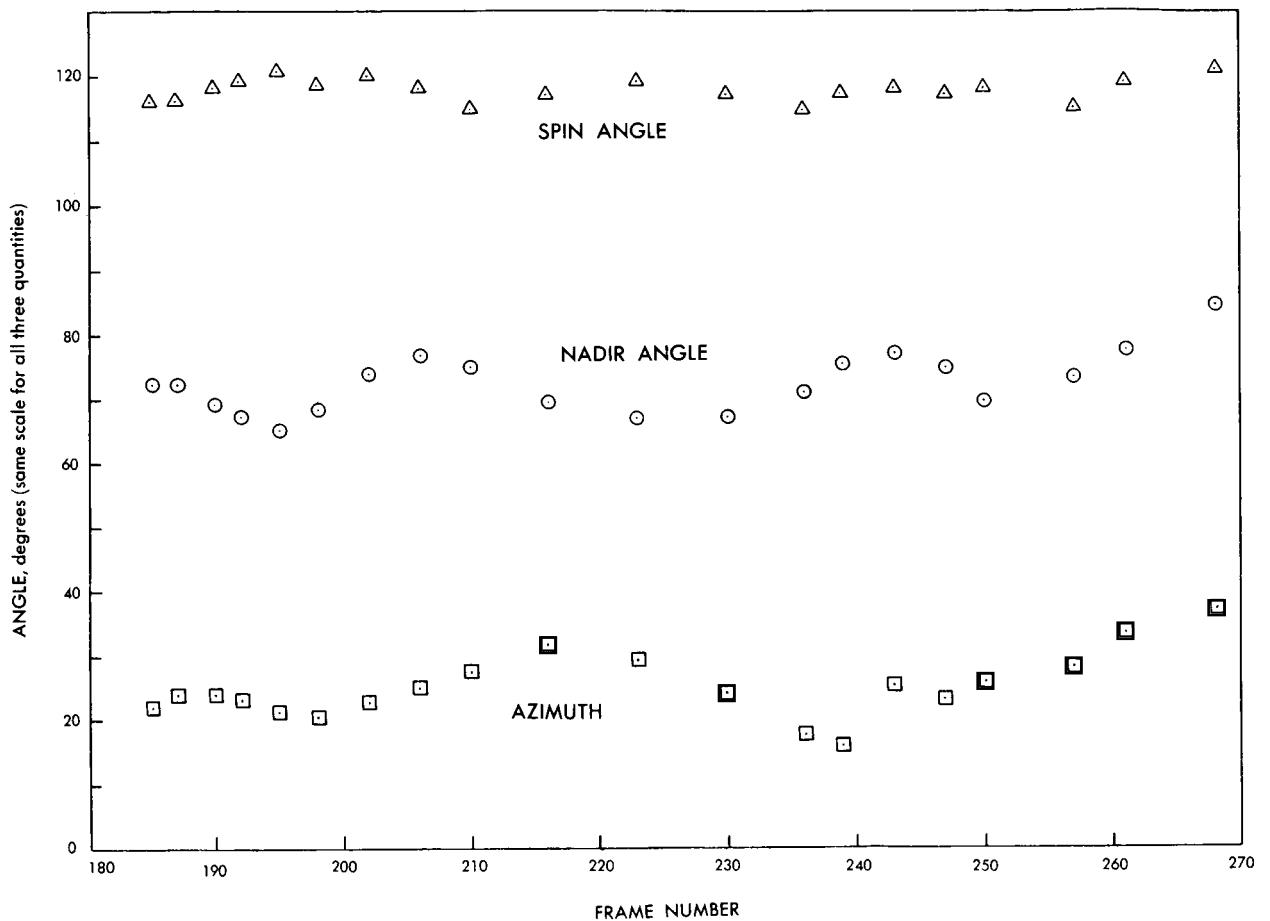


Figure 1. Variation along the flightline of (a) azimuth of principal axis, (b) nadir angle of principal axis, and (c) spin angle of camera about principal axis.

'Earth and sky camera'. Exact details of the arrangement and optical properties of the window and mirror are not available, but it is known that the window consisted of several layers of glass of flatness the same as standard plate glass. (Lobb, personal communication). Details of the window of the capsule intended for flight MA-10 have been given by O'Keefe *et al.* (ref. 10, p. 328), though this was probably not identical with that of the MA-4 capsule. It consisted of four layers, one of them set at an angle of 6° to the other three.

The camera was a Maurer 220 G time-lapse camera, serial no. 5295. The frame size was 57×57 mm ($2\frac{1}{4}'' \times 2\frac{1}{4}''$). The lens was a Fintar $f/2.8$ with focal length 75 mm. (Valdyke, unpublished). The angle of view was limited to about 44° by the field angle of the lens, which was not wide enough to reach the corners of the frame, as shown on the photos which follow.

The film used was standard Super Anscochrome color film, $2.75''$ (70 mm) wide and 100 feet (30 m.) long. No filter was used over the lens.

The filtering effect of the MA-4 spacecraft window was not measured (Lobb, personal communication), but O'Keefe et al. (ref. 10, p. 328) indicate that the window of the MA-10 capsule had a transmissivity of over 80% for all visible wavelengths, at normal incidence. The constant exposure was 1/500 sec. at f/8.

Location and orientation of photographs

The camera took photographs automatically every 6 seconds from lift-off until exhaustion of the film, which occurred over the South Indian Ocean. The path of the spacecraft during this time is shown in fig. 7 (inset). Frames 1 to 181 show the North Atlantic Ocean and the clouds over it. The latter part of the film, from frame 334 onwards, shows areas which were in darkness when photographed so that no ground detail is visible. Between frames 270 and 333, the earth's surface is obscured by broken cloud, though ground detail is visible through gaps. Continuous areas of land are visible only between frames 182 and 270. The photographs studied are from this strip, extending from the Moroccan coast to L. Tchad. In this report, Mercury "flightline" means only photographs 182 to 270.

Once in orbit the attitude of the spacecraft was stabilised by an automatic system using horizon scanners and hydrogen peroxide jets. Hence the camera pointed in roughly the same direction throughout the flightline, towards the north-northeast, obliquely downwards at an angle of about 70° from the vertical. All photographs show the horizon, which was about 1400 km (900 st. mi.) distant. The precise location of the camera station and orientation of the camera for each of the photographs reproduced in this report are given in table 1. The latitude, longitude, and altitude of the camera station must lie on a perfectly smooth curve when plotted against time. On the other hand, the orientation need not change smoothly since the hydrogen peroxide jets may have acted intermittently. Figure 1 shows that in fact the optical axis oscillated with an amplitude of about 12° in azimuth, 10° in nadir angle, and 4° in spin angle, and a period between 2 and 4 minutes.

The area covered by each of the photographs is shown in figure 7. Successive photographs overlap considerably, and allow a limited stereoscopic effect to be obtained (see p. 102), but the amount of overlap and the scale change rapidly from foreground to background. If the camera had been pointing vertically downwards, the scale of the original diapositives would have been about 1:2,200,000 (photo 185) to 1:2,400,000 (photo 268). In fact, the scale in the near foreground of the originals varies from 1:2,800,000 (photo 195) to 1:5,000,000 (photo 268), while the scale in the background is much smaller.

Method of determining location and orientation data

Measurements were made on black-and-white paper prints, 3.15 times

the linear dimensions of the original diapositives, but all measurements mentioned here have been reduced to their size on the originals.

The principal point of each of the 20 selected photos had to be located by erecting perpendiculars from the fiducial marks at the bottom and left sides of the photos, since the marks on the top and right sides could not be seen against the black background of space.

For each photo, the perpendicular from the principal point to the nearest point on the image of the horizon was produced to give the trace of the principal plane in the image. This was transferred to a 1:5,000,000 scale conformal map of the area by means of landmarks identifiable on the photo and on maps, to give a first approximation to the trace of the principal plane on the ground.

The sub-satellite path was plotted on the map from geographical coordinates provided by Data Operations Branch, Manned Flight Operations Division, NASA Goddard Space Flight Center, and assumed to be free of error. The ground traces of the principal planes were then adjusted graphically to fit the conditions (a) that they must intersect the sub-satellite path at integral multiples of a distance (about 44.5 km) representing the movement of the satellite in the 6 seconds between exposures; and (b) that the total alteration to the traces must be minimised. In this adjustment, variation in the scale of the map with latitude was taken into account, but not curvature of the ground traces of the principal lines due to the map projection, since this introduces less error than the identification and location of landmarks. In the adjustment no anomalies arose which might imply the camera did not operate at regular 6-second intervals.

The intersection of the ground trace of the principal plane with the sub-satellite path represents the picture-taking location. The latitude and longitude of this point and the azimuth of the principal plane was then read from the map. Knowing the location, the altitude and time of exposure were then found by interpolation in data provided by Data Operations Branch, NASA Goddard Space Flight Center.

The spin angle for each photograph was merely the measured obtuse angle between the image trace of the principal plane and the lower edge of the frame. Calculation of the nadir angle was more complicated, and is explained in figure 2.

The letters in figure 2 have the following meanings, all angles and distances being in the principal plane:

N is the nadir angle of the principal axis, i. e. the angle between the principal axis and the vertical, to be determined.

A is the angle between the apparent horizon and the vertical.

B is the angle between the apparent horizon and the principal axis.

f is the focal length of the camera lens, 75 mm.

b is the distance on the original diapositive from the principal point to the apparent horizon in mm., obtained by direct measurement on an enlarged print. The apparent horizon is not a sharp line on the photos, but rather a

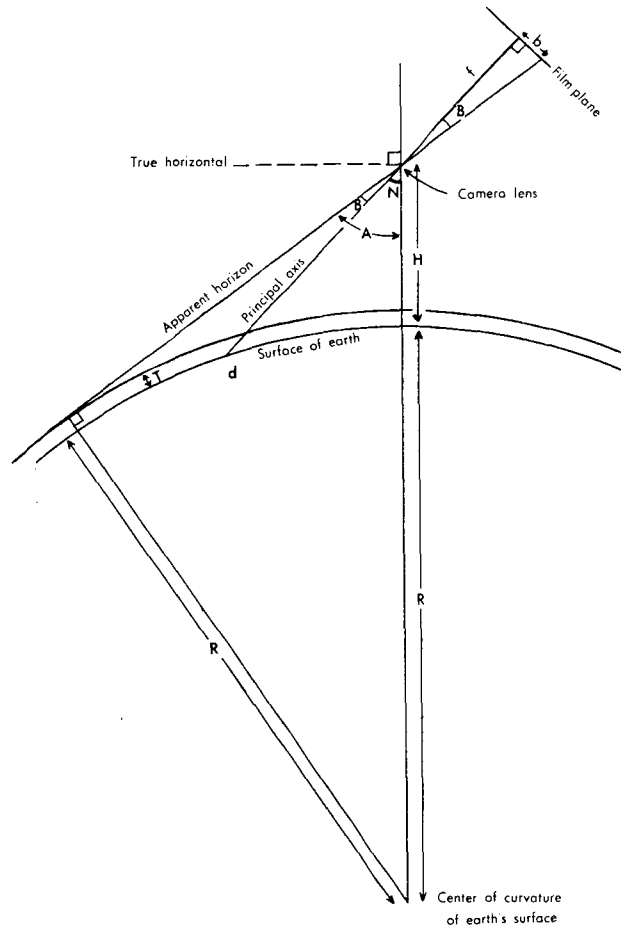


Figure 2. Method of calculating values of nadir angle given in table 1 and figure 1.

transition zone about 0.3 mm. wide. b was measured to the center of this zone, which must represent some level above the earth's surface.

T is the height of the level just referred to, above the terrestrial ellipsoid. There is no evidence on which to base an accurate estimate of T , though the MA-8 multifilter photos discussed by Soules (ref. 11) give some clues. The value 11 km., about two-thirds the height of the troposphere at this latitude, has been used.

H is the height of the satellite above the terrestrial ellipsoid, in km. These values have already been obtained.

R is the average radius of curvature of the terrestrial ellipsoid along the ray from camera to apparent horizon, in km. It is obtained from $R = R_M + \Delta R$, where R_M is the mean radius of the earth, i. e. 6368 km.,

and ΔR is read from the graph in Fujita, (ref. 6, fig. 2, p. 14), using the latitude and azimuth of the mid point of the ray.

Using the known constant values of f and T , and the known values of b , H , and R for each photograph, the value of N for each photograph was obtained from:

$$N = A - B,$$

$$\text{where } \sin A = \frac{R + T}{R + H},$$

$$\text{and } \tan B = \frac{b}{f},$$

all of which follow from the geometry of figure 2.

Figures for distance to the horizon used in figure 7 mean the arc distance d km., shown in figure 2, calculated from $d = R(\frac{\pi}{2} - A)$, where A is in radians.

Accuracy of location and orientation data

Estimates of the standard errors of the values given in table 1 are listed below. These refer to the absolute values. Differences and ratios of values appearing in the table often will have much smaller errors.

Time	\pm	0.5 sec
Altitude	\pm	1 naut mi
Latitude	\pm	.02 degrees
Longitude	\pm	.04 degrees
Nadir angle	\pm	0.5 degrees
Azimuth	\pm	0.7 to \pm 0.3 degrees
Spin angle	\pm	0.5 degrees

INTRODUCTION TO THE AREA PHOTOGRAPHED

The main part of this report consists of twenty selected photographs, interpreted by means of overlays and commentaries. As a framework for the commentaries, a summary follows of the climate, vegetation, geology, and landforms of the areas shown. This summary serves also as a glossary and as an index to photos which exemplify particular features.

Throughout the report, underlined figures are photograph numbers. The

spelling of place names follows the Times Atlas system. This means that arabic words are transliterated differently in areas which were mapped by different European powers. For instance, what is Jebel in Libya is Djebel in Morocco and Yebel in the Spanish Sahara, while Wadi becomes Oued in French areas. Foreign terms are underlined where they are explained. The terminology used for geologic time divisions is a compromise between that used in the French maps and field reports and that used by American geologists. The relationship between the terms is shown in table 2.

Climate

The majority of the photographs cover areas of true desert climate, as shown in fig. 3. They are affected by the dry northeast trade winds throughout the year and sometimes years may pass without rainfall. In general the aridity is extreme in the central part of the desert, but two mountain masses, the Ahaggar and Tibesti, rise sufficiently high to induce some rainfall in most years. Towards the edges of the desert rainfall becomes gradually more frequent, occurring mainly in winter in the north and in summer in the south, in accordance with the régimes prevailing in adjacent areas.

North of the desert lies the area of Mediterranean climate which receives rainfall in winter associated with the passage of cyclones from west to east along the Mediterranean Sea.

South of the desert lie areas which are affected during the summer by the belt of heavy equatorial rainfall. This is mainly associated with winds from the southwest, referred to as the southwest monsoon.

This average distribution of rainfall is similar to the distribution of clouds in the photographs. Most of the cloud is either in the northwest of the flight-line, (185-195), or beyond the end of the flight-line to the southeast (270-333), but there are small caps of cloud on the highest parts of the Ahaggar (230) and Tibesti (257). In fact, the only area of cloud not in a typical position is that in 216, which is over a desert lowland.

The whole area photographed experiences tropical or sub-tropical temperatures. All areas have mean monthly temperatures over 80°F (27°C) during summer, but the northern areas have mean temperatures as low as 50°F (10°C) during the winter.

Vegetation

The vegetation zones are closely related to the rainfall zones already outlined. They are shown in fig. 4. Most of the flight-line is occupied by desert with little or no vegetation. South of this, in areas with more abundant summer rainfall, Keay's map (ref. 55) indicates that the desert gives place first to sub-desert steppe (250), with widely spaced low perennial

TABLE 2

FRENCH USAGE		USED IN THIS REPORT	AMERICAN USAGE
QUATERNAIRE	Récent Quaternaire moyen Quaternaire ancien (Villafranchien etc.)	QUATERNARY Recent Late Quaternary Early Quaternary	QUATERNARY Recent Late Pleistocene Early Pleistocene
TERTIAIRE	Pliocène Miocène Oligocène Eocène	TERTIARY Pliocene Miocene Oligocene Eocene	TERTIARY Pliocene Miocene Oligocene Eocene
SECONDAIRE	Crétacé Jurassique Lias Trias	SECONDARY Cretaceous } Jurassic Triassic	MESOZOIC Cretaceous } Jurassic Triassic
PRIMAIRE	Permien Carbonifère Dévonien Silurien { Gothlandien { Ordovicien Cambrien Précambrien	PRIMARY Permian Carboniferous Devonian Silurian Ordovician Cambrian Precambrian	PALAEZOIC Permian { Pennsylvanian Mississippian Devonian Silurian Ordovician Cambrian Pre-cambrian

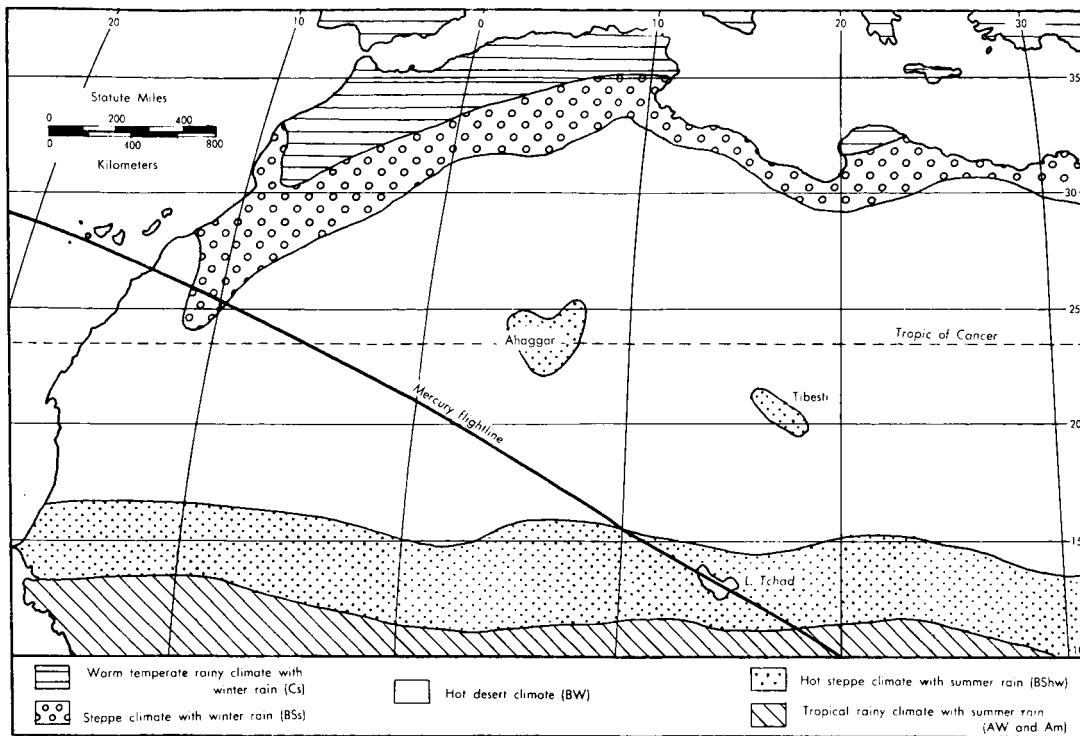


Figure 3. Climatic regions of northwestern Africa (after Köppen).

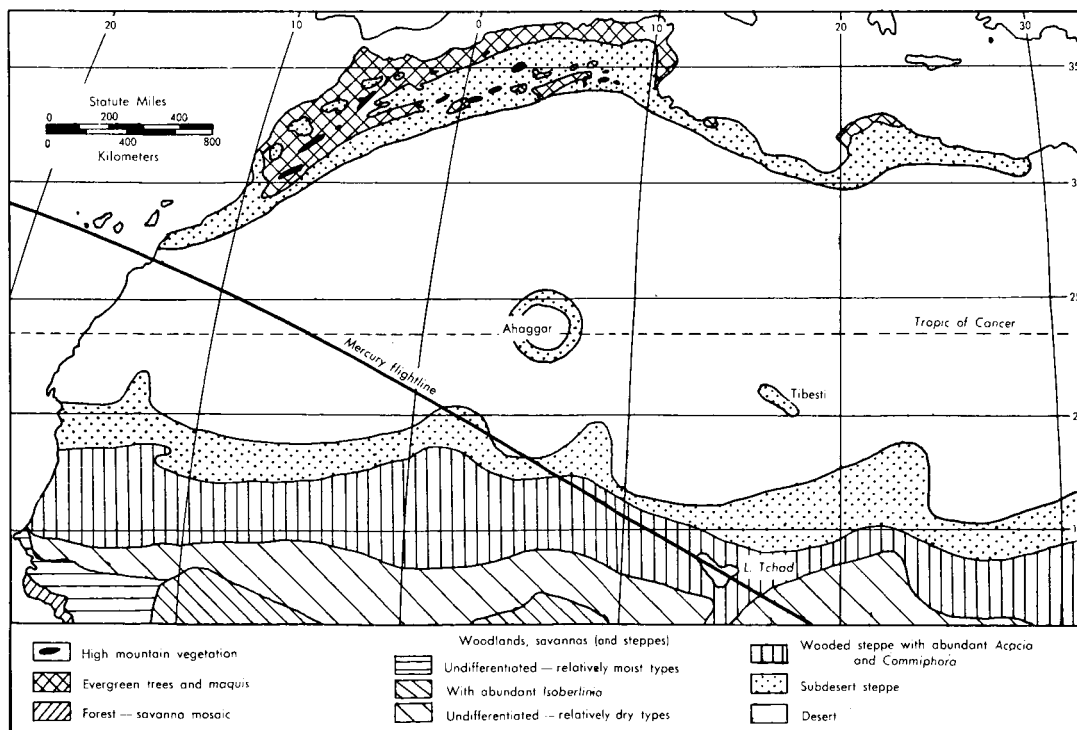


Figure 4. Vegetation of northwestern Africa (after Keay (ref. 55) and others).

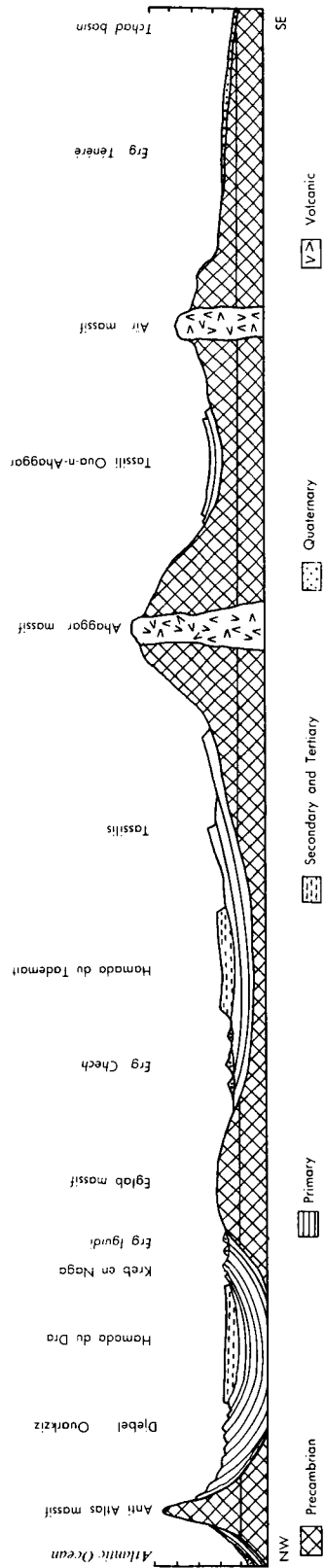


Figure 6. Schematic geological cross-section across northwestern Africa.
 Line of section is shown in figure 5.

plants and annuals including grasses flourishing for a few weeks after the rain; then to wooded steppe (257) which has a more nearly continuous cover of still short grasses after the rains, and where drought-resistant shrubs and low trees, usually thorny and deciduous, become abundant; and finally to true savanna (268) with a continuous cover of relatively tall grasses and scattered trees.

On its northern edge the desert also gives way first to sub-desert steppe. North of this appear the vegetation types peculiar to the Mediterranean type of climate, shrubby woodland on the lowlands, and forests of oak, pine and cedar on the mountains (187) (ref. 18).

Geological structure and related landform types

The Sahara has a basement of ancient altered crystalline rocks, which have long been relatively stable. It was last intensely folded by the Saharan movements (Precambrian), which produced north-south folds (230). Within the Sahara proper the Caledonian and Hercynian movements of the Primary era (230) and the Atlasic (Alpine) movements of the Tertiary era (239) caused only minor folding (ref. 19). The northwest corner of the basement, including the Anti Atlas, has been affected by two phases of Hercynian movements, the earlier with a northwest-southeast trend, the later with a southwest-northeast trend, and also by the Atlasic movements, with a west southwest - east northeast trend (ref. 30, pp. 75-76). The Saharan basement is bounded on the north by a major fault zone trending east northeast, the Sub-Atlasic line (fig. 5) or Agadir Fault (ref. 28, p. 529). North of this the Atlas Mountains were formed by the Atlasic folding in the Tertiary (ref. 19). Another folded belt bounds the basement on the west, with trends between north-south and northeast - southwest (ref. 27). Faults associated with this constitute the Zemmour fault zone (ref. 28, p. 530).

Because of its comparative stability since the Precambrian, it is easy to give a generalised description of the structure and landform types of the Sahara, as illustrated in the map and generalised cross-section, figures 5 and 6. We may visualize the Precambrian basement together with any overlying sediments as having been upwarped in a number of places into domes separated by broad basins. The sedimentary rocks, which are mainly of Primary and Secondary age in the area photographed from the spacecraft, either were never deposited over the domes, or have since been removed, so that the rocks exposed in the dome areas are mainly Precambrian. Consolidated sedimentary rocks appear at the surface mainly on the slopes of the domes, the Primary sediments usually gently folded and tilted, the Secondary and Tertiary rocks more nearly horizontal. In the basins the older rocks have been concealed under a cover of young, often Quaternary, deposits (ref. 19, pp. 38-41, 43).

This three-fold structural division into domes, slopes, and basins forms a convenient framework for the description of the main landform types found in the area.

The Precambrian rocks exposed in the dome areas form elevated rugged mountainous areas termed massifs by the French. The three principal massifs in the center of the Sahara are Yetti-Eglab, (202), the Ahaggar (230) and Tibesti (250), while the Anti Atlas area (187) may be regarded as a massif on the edge of the Sahara. In many cases Tertiary or Quaternary volcanic outpourings have occurred in the massif areas, adding an element of variety in the form of lava plateaus and volcanos to the topography developed on the Precambrian rocks (239).

The type of landform developed on the Primary and Secondary rocks of the slopes of the domes depends on how much they have been folded and tilted. Where they dip fairly steeply, erosion has left the more resistant beds up-standing as escarpments separated by vales developed on softer rocks. Such areas of parallel asymmetric ridges and valleys are known as djebels (187-195). Where the rocks are fairly horizontal a tableland, perhaps somewhat sloping, is more likely to develop, which may be bounded by escarpments on several sides. Such tablelands are known as tassilis when formed of Primary rocks where they are usually sandstone (216-230), and as hamadas where they are developed on Secondary or younger rocks which are often limestones (190-195).

In the structural basins of the Sahara occur several quite diverse types of surface material, and corresponding landforms. Areas of bare rock of almost any age may be found, but the surface is usually covered by shattered fragments of rock of gravel size, a surface type known as reg. Another type of reg, or gravel desert, is due to deposition of pebbles transported from the surrounding higher areas by torrents during periods of the Quaternary when rainfall was considerably greater than it is today (216, 223, 239). These stream beds, now dry except after the occasional rainstorms, are known as wadis (223-239). Where the material deposited by the wadis was mainly sandy, ergs or sandy deserts are found today. Usually the sand has been fashioned by the wind into one of several possible patterns of sand-dunes. The two most distinctive are longitudinal dunes developed parallel to the direction of the dominant wind (198, 206), and transverse dunes, which seem to be most frequent near the southern edge of the Sahara (247-257). In those parts of the depressions which were occupied by lakes during the wetter periods of the Quaternary, lagoon deposits such as clays, muds and lacustrine limestones cover the surface (261, 257, 243, 216, 187). Relatively small areas of this type are da'as (192). Finally in the lowest parts of the depressions, where the salts carried into such lakes became concentrated, the surface is occupied by sebkras, that is salt flats (206, 261, 195) (refs. 20, 21).

Denudation processes and related landform types

A variety of processes has contributed to the wearing away of the up-warped areas of the Sahara and the deposition of the derived material in the basins. However, it is probable that the Sahara has been an arid area during much of geological time and hence its surface often bears the imprint of the arid denudation processes. The general effect of these processes is that the

higher areas are gradually eaten away by erosion proceeding from the initially lower areas. This results in the isolation of the initially higher areas into massifs, bounded by escarpments, at the base of which are gently-sloping rock-cut surfaces known as pediments (239-243), and beyond these areas of deposition in the lowest areas. If erosion proceeds long enough the pediments may become sufficiently extensive to be termed pediplains (216, 230) or pediplains. Sometimes erosion fails to remove a small area of the higher ground, perhaps because it is made of more resistant rock, and it is left standing above the pediment or pediplain as an inselberg (239, 243).

Sources of information

The sources used are listed in the selected bibliography and acknowledged in the text.

Literature on the whole flightline. Probably the most readable and informative general books on the Sahara are those by Gautier (ref. 22) and Bernard (ref. 21). The standard geographical text on the Sahara is Capot-Rey (ref. 23). Perret's general account of Saharan relief (ref. 20) is more than adequate for most areas shown in the photos. Lelubre's article (ref. 24) is more recent but is difficult to obtain in North America. Alimen (ref. 25) deals with the Quaternary history. Smith (ref. 26) has summarised knowledge of the dune forms. Menchikoff (ref. 19) has recently outlined the geology and structure. Knowledge of the vegetation of areas south of the Tropic of Cancer has been summarised by Keay (ref. 17).

Literature on small areas. Of the numerous articles and field reports on the landforms of small areas of the Sahara (refs. 27 to 45), those found most useful were mainly published before World War II. This may be because at that period field workers wrote with a perspective similar to that of the space photograph, covering a fairly large area and emphasizing visually striking features. More recent articles have tended to deal with smaller areas in more detail.

Thematic maps. Within the last decade, geological maps on a scale of 1:2,000,000 (refs. 46-48) have become available for the entire area shown by the photographs. Certain areas have also appeared on larger scales (refs. 49-51), though maps on scales larger than 1:500,000 were not used in this study. A general picture of the geology of the entire flightline is given by two sheets of the 1:5,000,000 geological map of Africa (ref. 52). Landforms of the Sahara have been mapped in different ways by Raisz (ref. 53) and by Van Lopik and Kolb (ref. 54), and vegetation by Keay (ref. 55).

Topographic and general maps. The area is completely covered by at least two sets of topographic maps on a scale of 1:1,000,000, the French military maps (ref. 56) and the World Aeronautical Charts (ref. 57). It proved useful to compare both series with the photos, since they tend to be complementary in style and information content. Maps on a scale of 1:2,000,000 were also found convenient (ref. 58). Recent general maps of

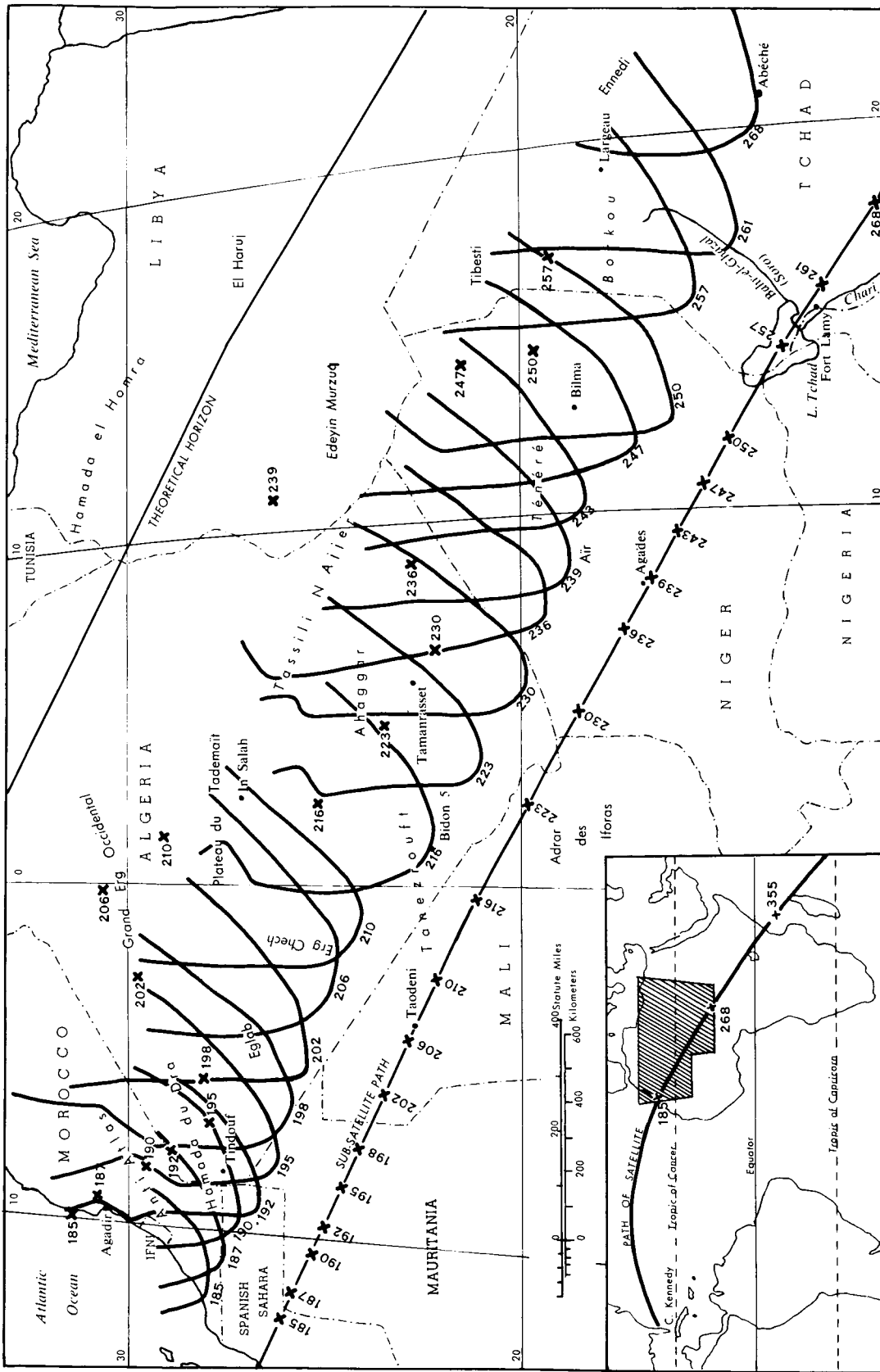


Figure 7. Map showing area covered by each of the selected interpreted photographs.

North Africa are those in the Times Atlas (ref. 59) and the National Geographic Atlas (ref. 60).

Aerial photographs. The entire area shown in these Mercury photographs is covered by vertical aerial photography, mostly taken during the last ten years, which is filed at the Institut Géographique National in Paris, and by older U.S.A.F. trimetrogon photography. Neither series was used in compiling this report.

INTRODUCTION TO THE SELECTED INTERPRETED PHOTOGRAPHS

The area covered by each of the selected interpreted photographs is shown in figure 7.

In selecting the twenty photographs reproduced in this report, the aim has been to include every part of the flightline possessing a recognizable pattern, so that for most purposes it should be unnecessary to refer to the complete film. Where a recognizable pattern appears in the foreground, photographs only two frames apart have sometimes been selected, even though they overlap considerably in the middle distance and background. Where the foreground is featureless, photographs selected may be as many as seven frames apart. Frames were preferred which show a complete feature, such as an area of dunes, a geological structure, or a vegetation boundary.

The photographs appearing in this report were derived from the film recovered from the spacecraft through the following stages. The second and third generations were contact color diapositives made so as to copy the colors of the original as closely as possible. The fourth generation was a black-and-white contact negative. The fifth generation was a black-and-white positive print on medium soft glossy paper, 3.51 times the linear dimensions of the original. Comparison with the second generation showed that surprisingly little detail was lost between second and fifth generations. The reproductions in this report were made from the fifth generation prints through the normal intermediate stages of the photo-lithographic process.

An indication of the colors on the original is given by the frontispiece. Color rendering in general is discussed on pages 100-101. The photographs are explained in two ways: by commentaries, and by overlays superimposed on duplicate photographs.

In the commentaries, features appearing on several frames are generally explained in relation to the photo in which they are best shown. Underlined numbers refer to photographs. The following abbreviations are used:

l.	left	bg.	background
c.	center	md.	middle distance
r.	right	fg.	foreground
N.	north	E.	east
S.	south	W.	west

For most photographs two overlays are provided, one showing place names, the other geology.

The place name overlays are intended to allow easy comparison of the photos with general maps (e. g. refs. 59, 60).

The second set of overlays shows geology, rather than some other distribution, because the variations of tone correspond more closely to variations of rock than to any other single mappable factor. This is because the area is a desert. The same would not usually be true of humid areas.

The geological overlays are essentially the 1:2,000,000 geological maps (refs. 46-48) transformed to the perspective of the photos. They show explicitly only the information these maps show, namely the stratigraphy of sedimentary rocks, and the rock-type and age of igneous and metamorphic rocks. The rock-type of sedimentary rocks is only shown in so far as rock-type units can be equated with stratigraphic units. The locations of major folds, basins and domes can be inferred from the stratigraphy, but the 1:2,000,000 maps mark few major faults or fractures. Structural lineaments visible on the photos have been marked on the place-name overlays.

The meaning of the symbols used on the geological overlays is given in table 3.

TABLE 3. SYMBOLS USED ON GEOLOGICAL OVERLAYS

Sedimentary Rocks

D	Recent dunes. A discontinuous covering of dunes is indicated by a fractional code. Thus: D/c means dunes partially covering Cretaceous.
qs	Salt flat.
q	Quaternary, undifferentiated.
T	Tertiary continental, undifferentiated, including Villafranchian continental: mainly hamada formation.
e	Eocene
c	Cretaceous, marine, undifferentiated.
cn	Nubian sandstone (Cretaceous continental)
ci	Continental intercalaire (Cretaceous continental)
h	Carboniferous, undifferentiated.

h ₂	Middle Carboniferous
h ₁	Lower Carboniferous
h _{1b}	Lower Carboniferous (Upper)
h _{1a}	Lower Carboniferous (Lower)
d	Devonian, undifferentiated
d ₃	Upper Devonian
d ₂	Middle Devonian
d ₁	Lower Devonian
s	Ordovician and Silurian, undifferentiated
s ₂	Silurian
s ₁	Ordovician
k	Cambrian
k ₂	Middle Cambrian
k ₁	Lower Cambrian
px	Cambrian or late Precambrian sediments or meta-sediments undifferentiated

Metamorphic and Igneous Rocks

x	Precambrian metamorphic rocks, undifferentiated
x ₃	Precambrian III schists, sericite schists, quartzites
λ x ₃	Precambrian III volcanic complexes (rhyolitic, andesitic, or basaltic)
x ₂	Precambrian II (Pharusian) phyllites, quartzites
x ₁	Precambrian I (Suggarian) gneisses, micaschists
ε	Crystalline schists, undifferentiated
γ	Granites, microgranites, granodiorites, syenites, undifferentiated
γ ₃	Younger granites
γ ₂	Pharusian granites
γ ₁	Suggarian granites
ργ	Transition from younger granites to rhyolites - microgranites
ρ	Rhyolites and other ancient volcanic rocks (Precambrian), undifferentiated
β	Young basalts and other volcanics
δ	Diabases (dolerites), diorites, gabbros, serpentines

+ The plus sign indicates the combination of units, e. g.
 k+s means Cambrian and Ordovician;
 ds+s means Middle and Upper Devonian

Four types of line are used on the geological overlays. This is because the boundaries on the geological maps do not everywhere agree with those apparent on the photos, and because on both maps and photos boundaries may be either definite or uncertain. The exact meanings of the lines are given in figure 8, but broadly speaking a continuous line means map and photo are both definite, a dotted line means map and photo are both uncertain, a broken line means the map gives information the photo does not, while a chain line means the photo gives information the map does not give.

Line	Geological Map	Photo
-----	Definite	Absent
—————		Vague Definite
.....	Uncertain, inferred or indefinite	Absent Vague
-----		Definite
-----	Absent	Vague Definite

Figure 8. Lines used on geological overlays

In the last few photos (257, 261, 268) variation of tone is more closely related to variation of vegetation than geology, so that geology overlays are not given and vegetation boundaries have been added to the place name overlays.

It would have been possible to include overlays showing other factors. Landform overlays would be relevant, but in most cases the landform regions are described in the commentaries, and their location is shown on either the place name or geology overlays. Overlays showing land-use, types of farming, or other economic distributions would not be useful here, since they would be mainly blank. In other areas, where human activities have visibly affected the landscape, such overlays would be very relevant.

SELECTED INTERPRETED PHOTOGRAPHS

Photograph 185

During its eighteen minute crossing of the North Atlantic the Mercury spacecraft camera photographed little other than sea and cloud. Photograph 185 is the first which shows an appreciable area of land.

The area photographed is the Moroccan coast. Many coastal landmarks can be identified. The most distant bay visible is that from which open the Straits of Gibraltar, though the Straits themselves cannot be seen. Beyond it the coast of Spain is just visible.

The darker area of ocean is free of cloud; the whitish area represents a layer of stratus and strato-cumulus over the ocean. The striking correspondence between the edge of this cloud and the coastline suggests that the cloud is due to cooling of the air immediately above the sea by the cool ocean water. Along this coast the sea is cooler than the land practically throughout the year. It is not certain whether the boundary between the cloud-covered ocean and the cloud-free ocean corresponds to a change in the temperature of the surface water mass, or to a change in the characteristics of the air mass which lay over it at the time the photograph was taken.

Other clouds are induced by the several ranges of the Atlas Mountains which rise in the case of the Haut Atlas to almost 14,000 feet (4600 m.). The most distant line of clouds visible probably lies over the Sierra Nevada, almost a thousand miles (1600 km.) distant, in Spain, and beyond the theoretical horizon.

On the land the most conspicuous patterns are geological. This might not be so if the area had a dense vegetation cover, but in fact the only areas of forest within the photograph lie on the mountains, which are obscured by cloud. The foreground is a desert or semi-desert. However, narrow strips of vegetation can be seen following the beds of some of the wadis flowing to the coast, the Chebika, Dra, Massa and Sous.

Comments on the complex geological structures of the right foreground will be made under 187. The light-colored area near the coast (left foreground) is an area of Cretaceous limestone, a small example of an hamada. The dark area near the coast between the mouths of the Dra and the Chebika probably represents a surface layer of Villafranchian (early Quaternary) coastal sand dunes and marine deposits. The one or two lines paralleling the coast in the extreme left foreground probably mark coastal terraces formed by the sea at some stage of the Quaternary when it stood at a higher level than at present (refs. 46, 49, 50).



Figure 9 (a) Photo 185

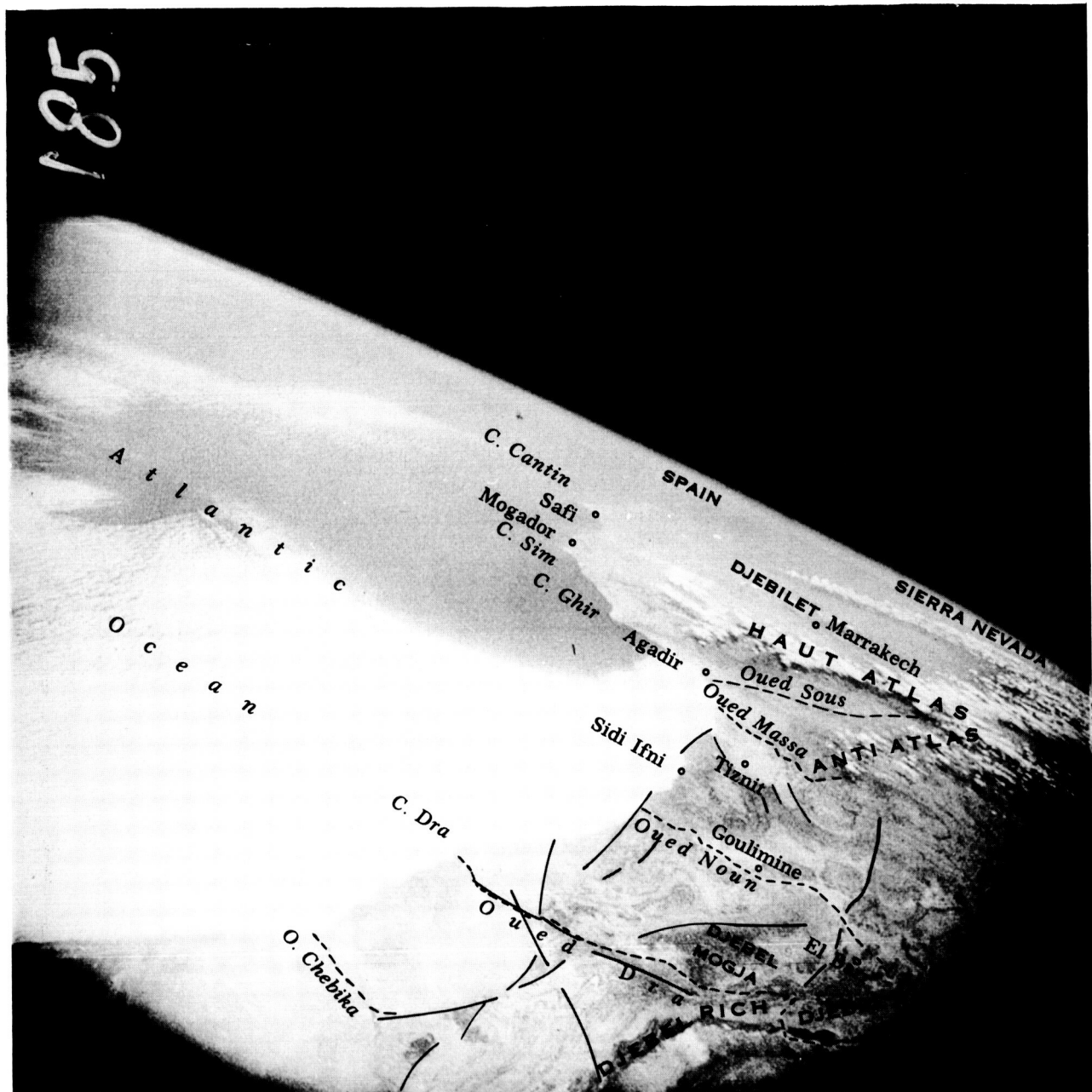


Figure 9 (b) Photo 185 with place name overlay

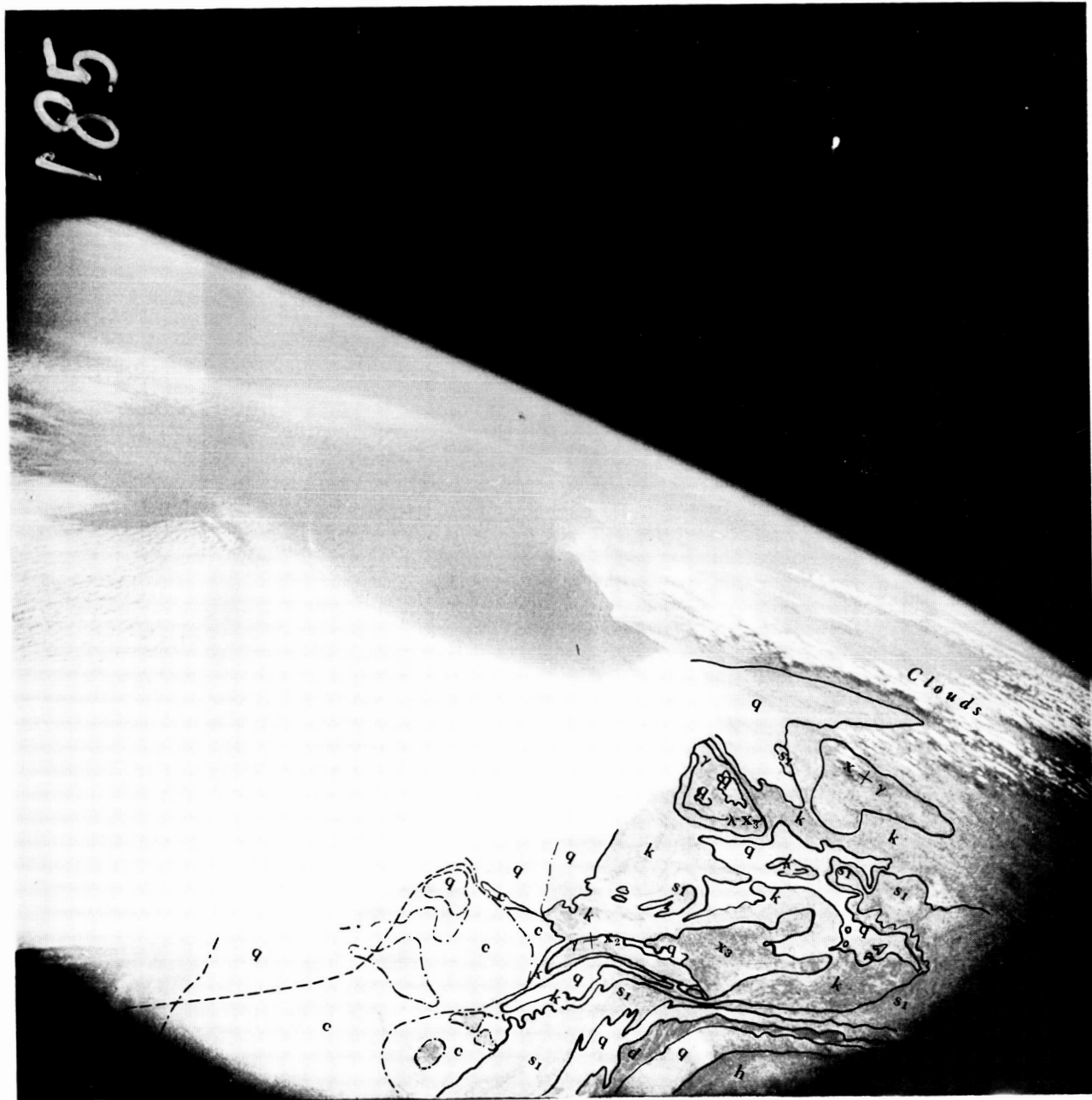


Figure 9 (c) Photo 185 with geological overlay

Photograph 187

The complicated pattern which occupies most of this photograph represents the outcrops of numerous beds of Primary rock which have been tilted towards the SSE and then planed off by erosion. The narrow bands representing the outcrops of individual beds run generally from WSW to ENE. A zigzag shape has been given to some of these otherwise straight outcrops by small folds with axes roughly SW to NE, crossing the outcrops obliquely. Interference between these folds and others trending NW-SE has produced elongated dome or basin structures in places. Structural lineaments in the left foreground show the northeasterly trend of the Zemmour fault zone (ref. 28, p. 530), and in the right foreground a northwesterly trend.

The rocks involved are of all ages from the oldest Cambrian in the NW to the middle Carboniferous in the SE, as shown in the cross-section (fig. 11) and include a variety of sedimentary rocks. The different degrees of resistance of these rock-types means that, although the area appears flat in the photographs, in fact certain outcrops notably of sandstone stand up as long narrow ridges extending from WSW to ENE, whereas others, mainly schists and shales, form the intervening depressions. The highest ridge, the Djebel Ouarkiz, developed on a hard Carboniferous limestone, rises perhaps 700 ft (200 m.) above its surroundings. The Djebel Bani is developed on an Ordovician quartzitic sandstone. Where the structure forms a basin or dome circular ridges and depressions exist. The area exemplifies the djebel type of landform.

The depressions owe their origin to the softness of the Primary rocks which underlie them, but in fact the light tones between the ridges on this photograph are not the Primary rocks themselves but a thin covering of Quaternary deposits. These include spreads of sand, gravel terraces, and a widespread lacustrine limestone. Wadis follow the depressions, generally from E to W, and in places break through the ridges in narrow gorges (foum).

Beyond the djebel area rise the Anti Atlas mountains. The direction of the range corresponds with the trend of the Atlasic folding but the rocks exposed are Precambrian, part of the basement which underlies the whole Sahara. In this area of older, brittle rocks faults are frequent, and the Tiznit basin (l. md.) for example, is surrounded by fault-line scarps. (refs. 46; 50; 36, pp. 130-134, 171, 228; 32, p. 69 and map; 33, map; 21, p. 384; 30, p. 76; 12).



Figure 10 (a) Photo 187

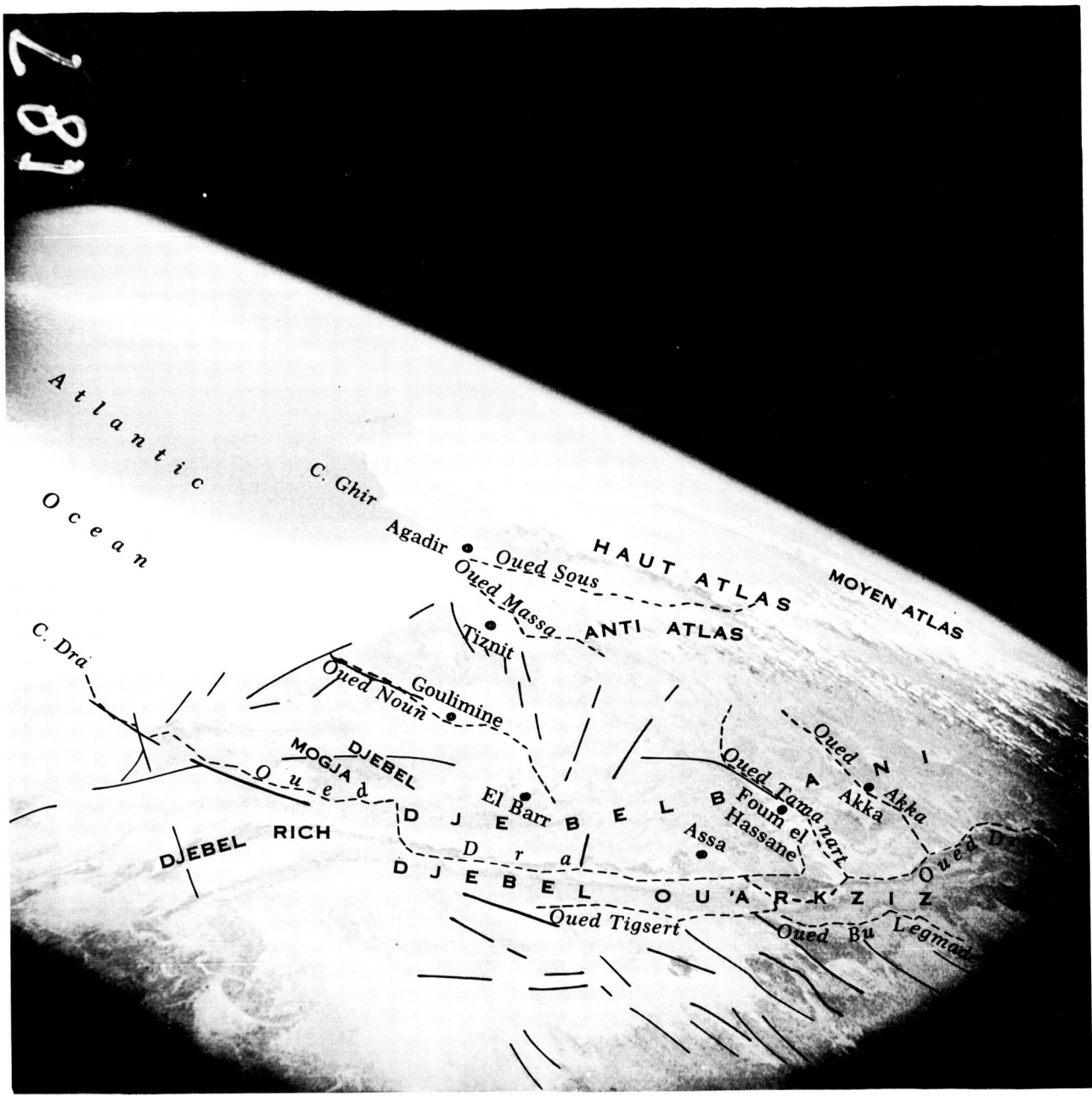


Figure 10 (b) Photo 187 with place name overlay

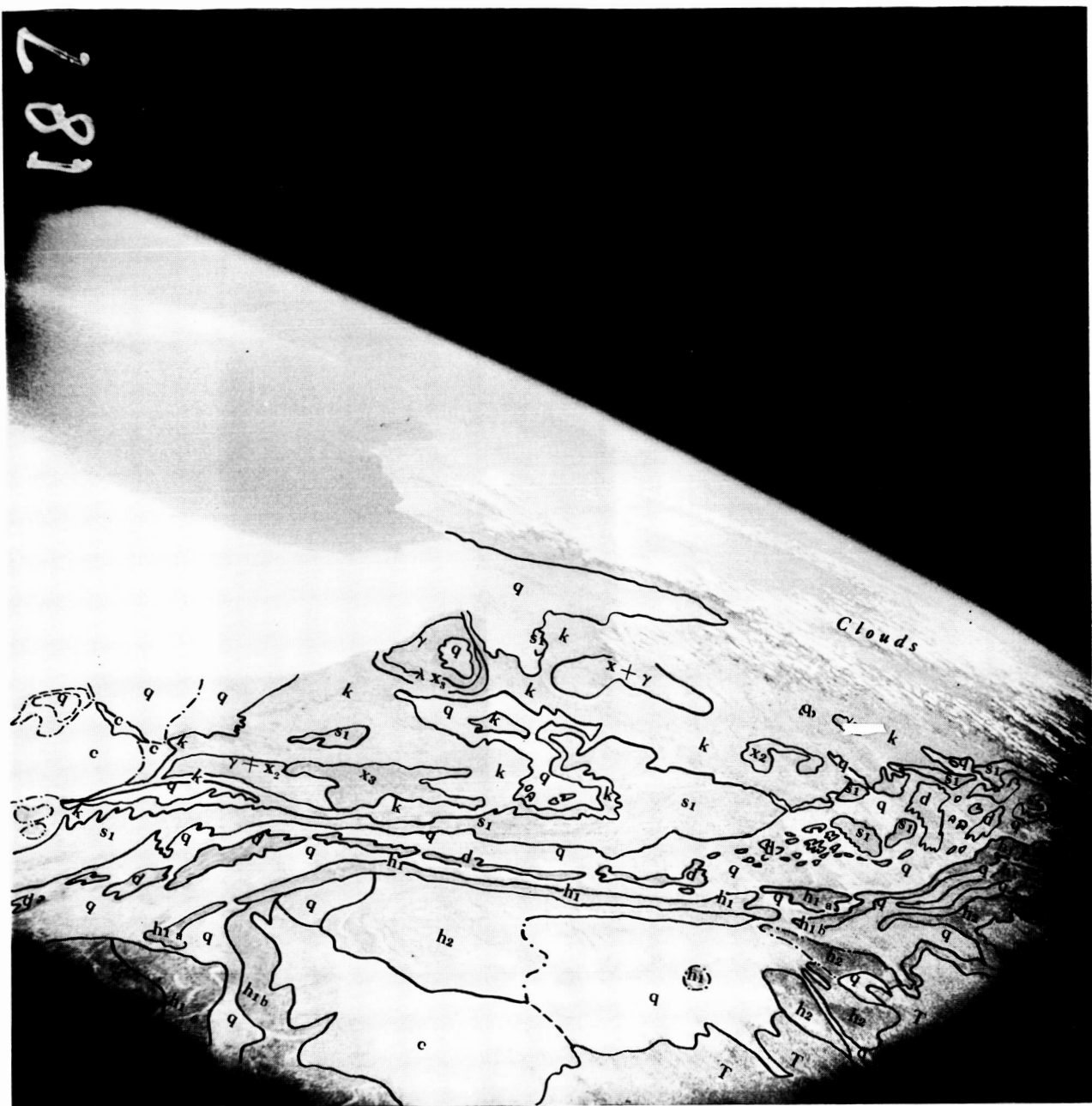


Figure 10 (c) Photo 187 with geological overlay

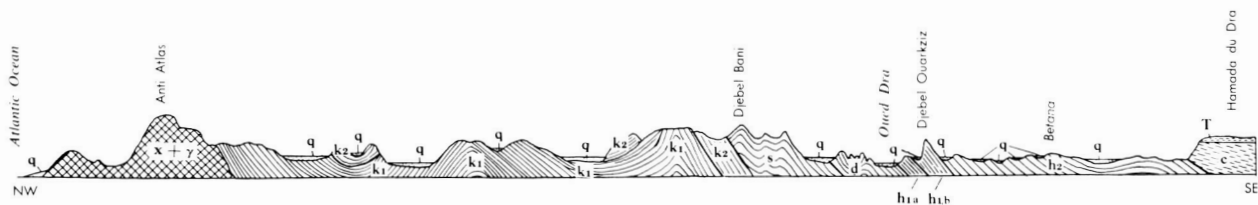


Figure 11 Typical geological section across the area shown in Photo 187

Photograph 190

SE of the djebel area in the middle distance lies the Hamada du Dra (fg.), to be described under 192. In the left foreground parallel lines appear on the hamada surface, running NE-SW, and representing low ridges and furrows on the ground. Individual ridges are continuous for such long distances that it is unlikely the orientation is determined by the dominant wind (ref. 26, p. 11). More likely, erosion has picked out lines of structural weakness, probably bedding. Since the surface rock is mainly limestone, perhaps solution has been important. Water action must have been effective at least in transportation, since sinuous wadis can be seen. The photo in fact reveals the ridges only over part of the area where they occur (ref. 50), perhaps because those appearing are closest to the camera, and because erosion has cut most deeply in the western part of the hamada (ref. 29, p. 218). The ridges may be most pronounced here because of more powerful erosion by the Dra and Saguia el Hamra systems, which have the ocean for their base level, and which have eaten into the edges of the hamada. Differences in past or present climate, surface rock, dip, or massiveness of bedding could also explain this.

Where erosion has eaten into the northern edge of the hamada middle Carboniferous rocks are exposed, the youngest Primary rocks of the Dra depression. The most easterly of such areas (r. md.) is called the Betana, and the name is sometimes applied to similar areas further west. Generally schists and shales predominate over sandstones, so that these areas form lowlands, veneered with Quaternary deposits, and crossed by low parallel ridges. Close to the edge of the hamada, the Primary rocks are often covered by material which has fallen from the cliff behind. Some suggestion of these conditions can be seen in the left middle distance (ref. 36, pp. 228-229).

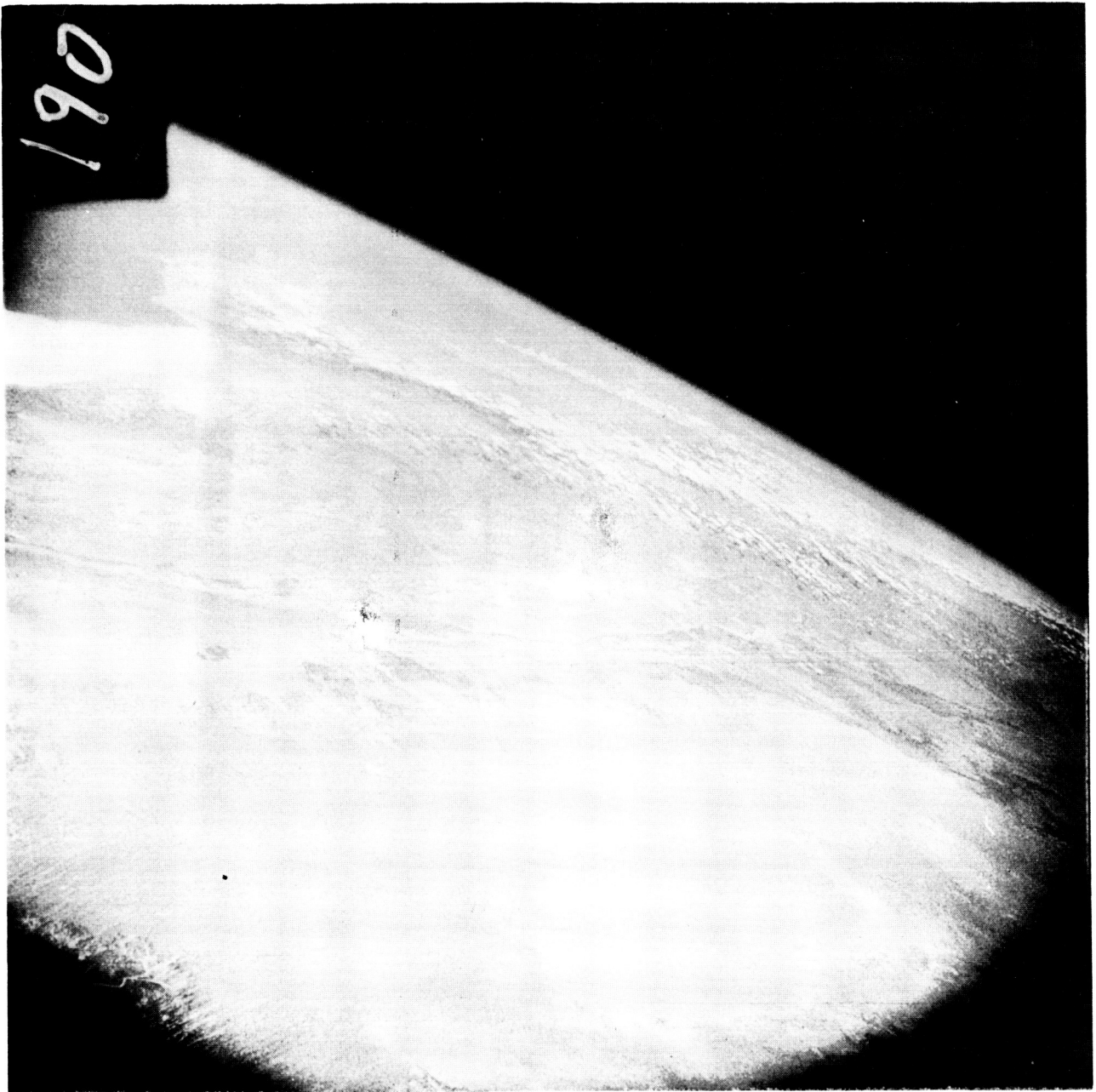


Figure 12 (a) Photo 190

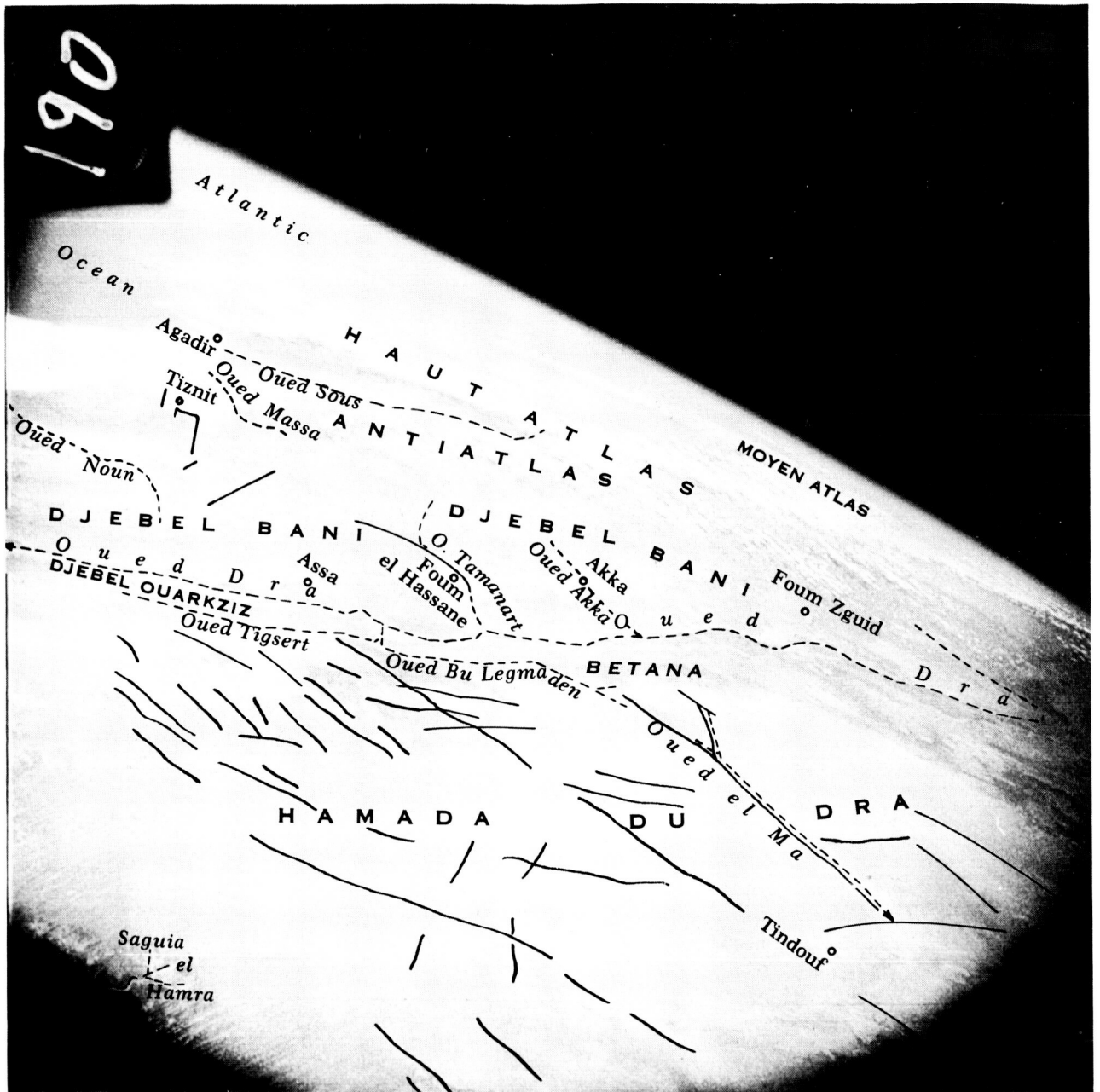


Figure 12 (b) Photo 190 with place name overlay

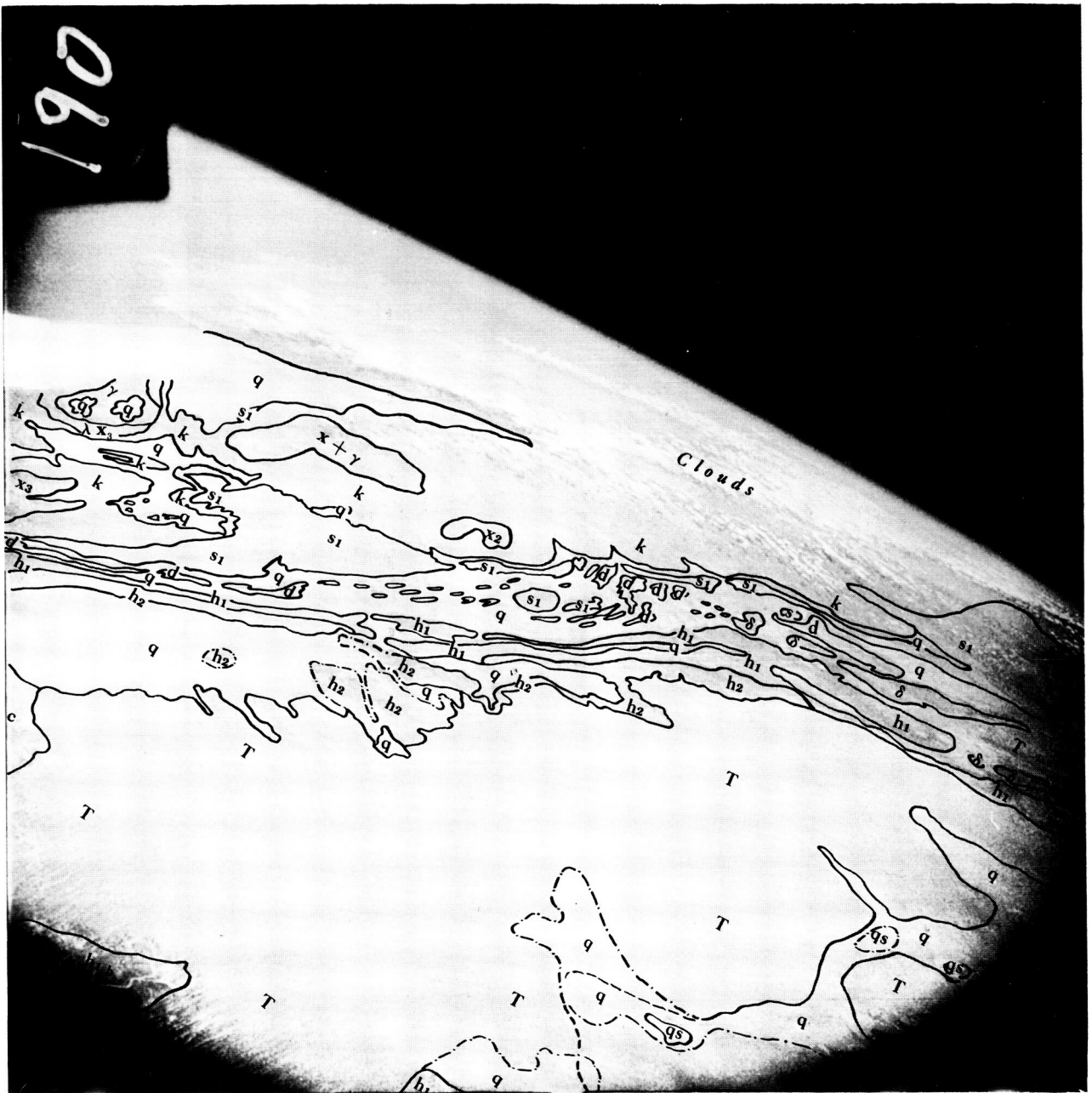


Figure 12 (c) Photo 190 with geological overlay

Photograph 192

The entire width of the Hamada du Dra is visible in this photograph. A hamada is typically a tabular desert area developed on nearly horizontally-bedded limestones of Cretaceous to Pliocene age. A hamada is bounded on most sides by an escarpment, beyond which the underlying folded or tilted rocks are exposed, as in this case. These immense surfaces are usually covered by angular fragments of rock, broken by weathering in place, and often polished by wind action. On the ground, the effects of wind erosion are everywhere easily seen, though this is not visible on the photograph. If the hamada is composed of limestone, features formed by solution of the rock and its subsequent precipitation are also widespread, and it is on the northern, that is the humid, edge of the hamadas that thick calcareous crusts are to be found. The rocks making up the Hamada du Dra are mainly calcareous sandstones and gypseous marls, everywhere capped by a layer of siliceous limestone. The surface rocks at least are of Pliocene or Early Quaternary age. The present topographic surface was probably developed by later erosion. (ref. 36, pp. 173, 221; 20, pp. 248, 249, 253; 34, pp. 59, 62; 29, pp. 71-72, 130, 350-353).

Hamadas have a distinctive hydrography. The courses of the few major wadis such as the Oued el Ma are engraved indistinctly. The da'las are the main hydrographic element. These are shallow closed basins, some fed by small wadis, covered with clayey soil. Vegetation is usually more abundant in them. The da'las grade on the one hand into sebkas (salt flats), such as the Sebkra de Tindouf (md.) and on the other hand into small sink-holes. Around the entrance to these may be a little loess (wind-borne silt), but no plants except after a storm (ref. 20, p. 253; 36, p. 222).

The Hamada du Dra is a very favorable area for distinguishing structural lineaments, since it has a surface of uniform rock-type and low relief. The lineaments apparent on 190, 192 and 195 may be grouped into five families. One family, trending NW, runs straight across the hamada and the Primary and Precambrian rocks to the south. This family seems to be regularly spaced about 50 km. apart. The direction is that of the Early Hercynian earth movements which folded the Ougarta mountains (206, l.bg.). A second group of frequent but less-persistent lineaments runs perpendicular to the last. The third family which runs ESE, the fourth which trends ENE, and the fifth which curves round from NW to W, run parallel to the strike of the Primary rocks along the S, NW, and NE edges of the hamada respectively. They may well be causally related (ref. 35, pp. 451-453.).



Figure 13 (a) Photo 192

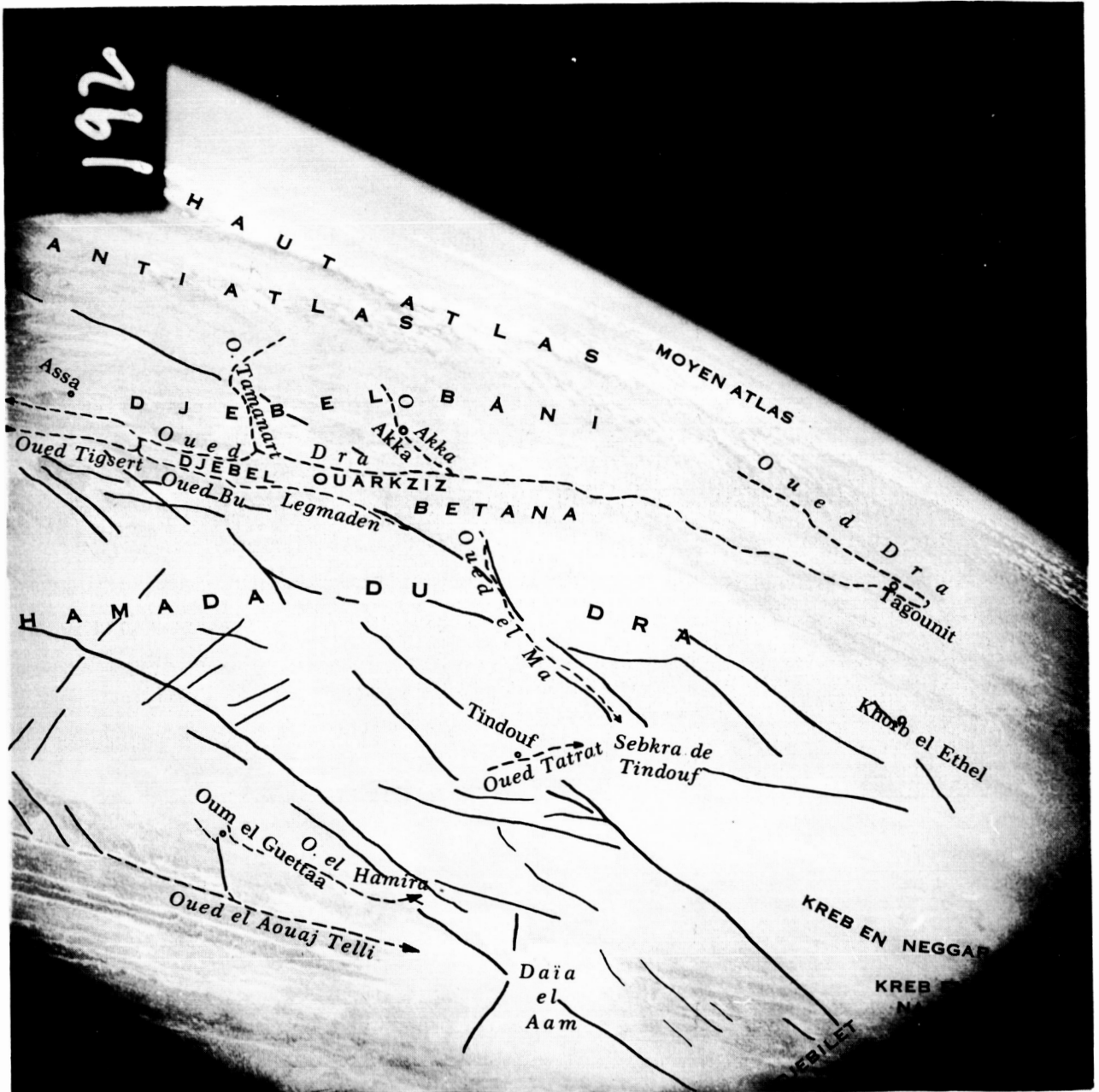


Figure 13 (b) Photo 192 with place name overlay

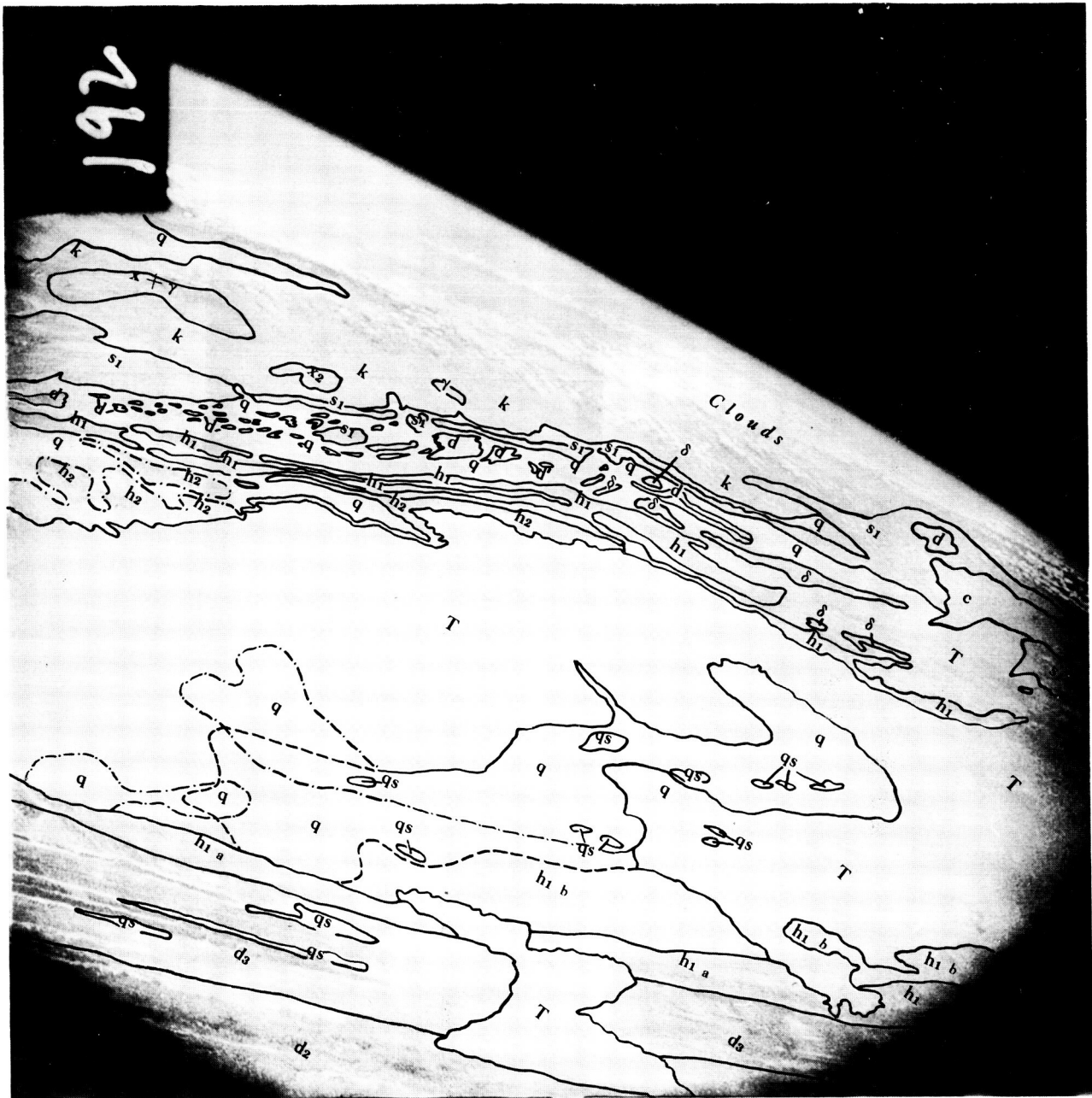


Figure 13 (c) Photo 192 with geological overlay

Photograph 195

This photograph shows clearly three of the main divisions of Saharan relief, as illustrated in the cross section (fig. 15). The mottled area (r.fg.) is part of the Yetti-Eglab massif, an area of low relief developed on Pre-cambrian rocks. The striped area (md.) is a djebel, made up of escarpments developed on northward-dipping Primary rocks. The light area (md.) is a hamada of almost flat-lying Tertiary or younger rocks. Beyond these can be seen another djebel area, that already described along the Oued Dra, and another massif, the Anti-Atlas, partly covered by cloud (ref. 20, p. 242).

The djebel area (md.) is similar to that along the Oued Dra (bg.), but the escarpments are straighter since the rocks dip more uniformly. The scarps are developed on limestones and sandstones varying in age from Ordovician to Carboniferous, while the intervening valleys are developed on schists. Sebkras (salt flats) are found at the foot of many of these scarps (r.md.) (ref. 20, p. 242). The scarps, known locally as kerbs or krebs, are here less than 100 ft. (30 m.) in height, but further west they are higher, e.g. in the foreground of 192 (ref. 36, p. 226).

The almost perfect horizontality of the hamadas contrasts with the marked relief of the djebel areas. This contrast is accentuated by the dark, almost black colors of the polished Primary rocks of the djebels, which cut into the white hamada areas. Not all hamadas are the same color as this however. The Hamada el Homra (236, bg.) means literally 'red hamada'. On the Plateau du Tademaït (216, l.bg.) the color of the pebbles covering the hamada varies between yellowish-grey and inky black according to the division of the Cretaceous rocks which outcrops at the surface. In fact the whiteness of the Hamada du Dra seems to be a peculiarity of the Plio-Pleistocene hamadas (ref. 20, p. 253; 21, p. 384).



Figure 14 (a) Photo 195

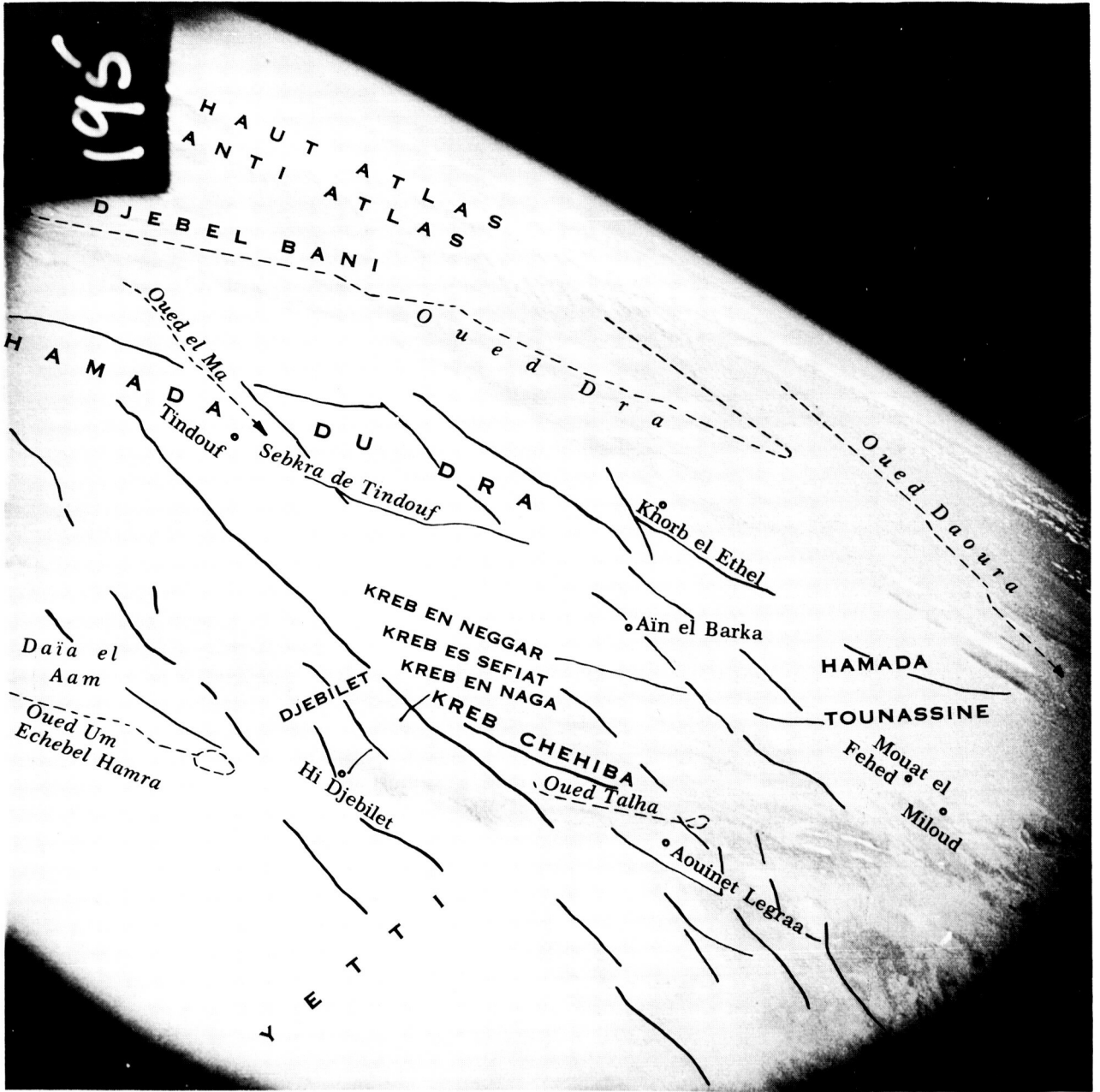


Figure 14 (b) Photo 195 with place name overlay

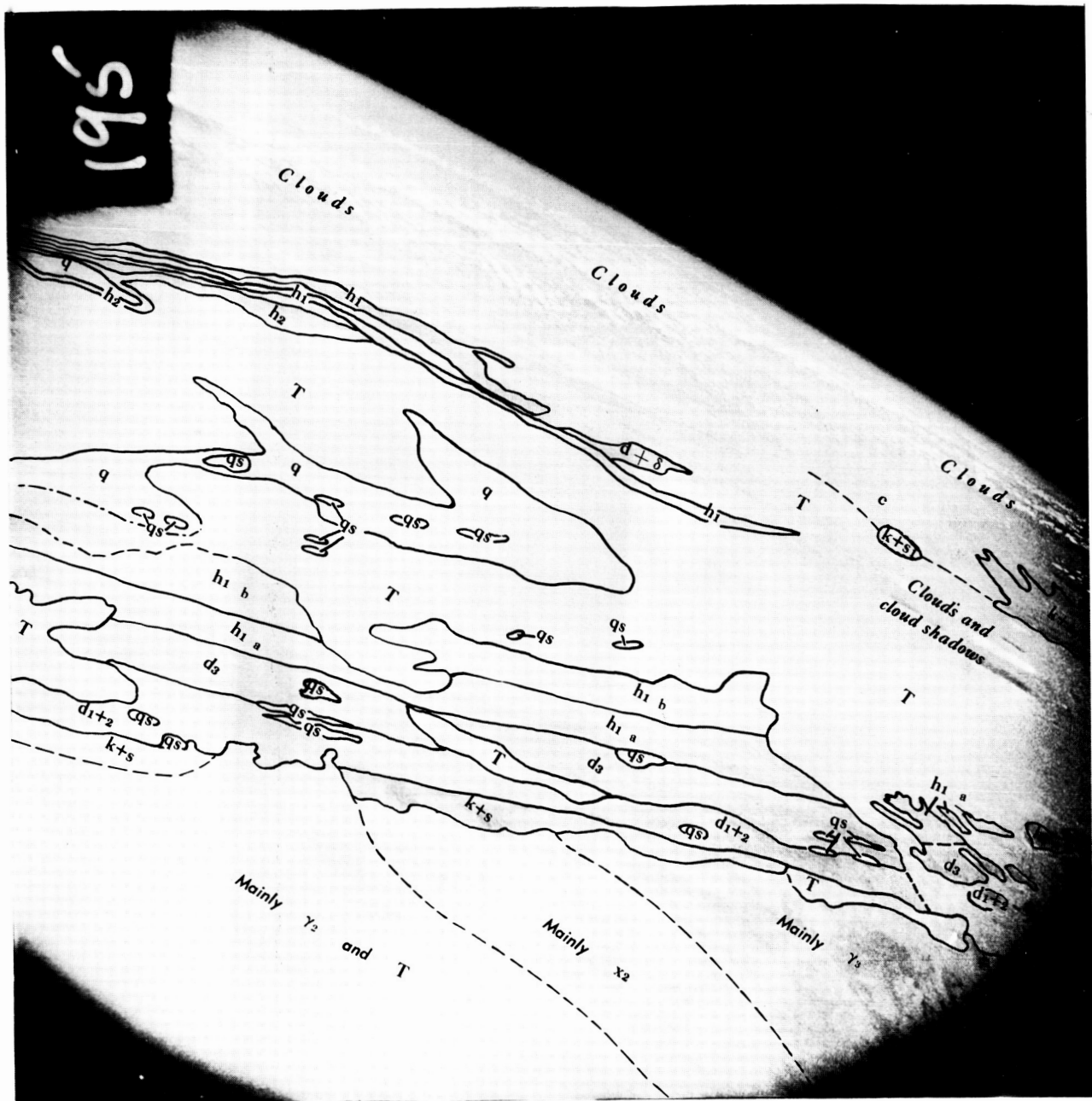


Figure 14 (c) Photo 195 with geological overlay

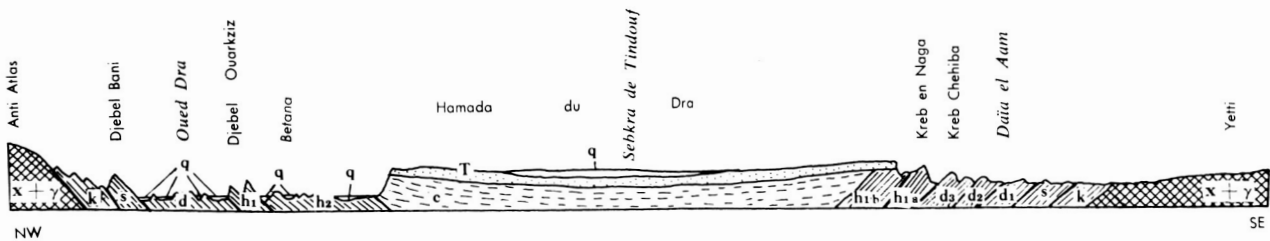


Figure 15 Typical geological section across the area shown in Photo 195

Photograph 198

This photograph shows the first erg seen by the camera in the spacecraft. An erg is a sand-covered area, normally in a structural basin where sand was deposited by wadis during the Quaternary when runoff was greater. In the case of the Erg Iguidi, seen here, the sand was brought by the Oued Daoura and deposited in the shallow depression between the Eglab massif (r. fg.) and the djebel (l. md.). Usually the wind has sculptured the sand spreads of the Quaternary wadis into one of several possible patterns of dunes. In this case, the dunes are longitudinal, that is they are long sand ridges parallel to the direction of the dominant wind, the northeast trades, which formed them. The dunes are close together in the deposition area of the Oued Daoura in the middle distance but unravel farther to the SW (fg.) into a less and less close mesh, between the strands of which the underlying rock becomes more and more visible (ref. 20, pp. 241, 386).

The major dune-chains, trending NE are reddish on the original color photograph, whereas the minor dunes, branching SE from them, are almost white. The red color is thought to be characteristic of dunes formed before the second pluvial period i. e. in the early Quaternary, whereas the paler dunes are younger (ref. 25, p. 138). Apparently there have been changes in the dominant wind.

In the foreground of this photo and 195 there is difficulty in relating the geological map to the tones of the photo, apart from the dunes themselves. If the map is correct, then there is wide variation in the tone of rock-types X_2 and γ_3 from place to place within 195 to 202.



Figure 16 (a) Photo 198

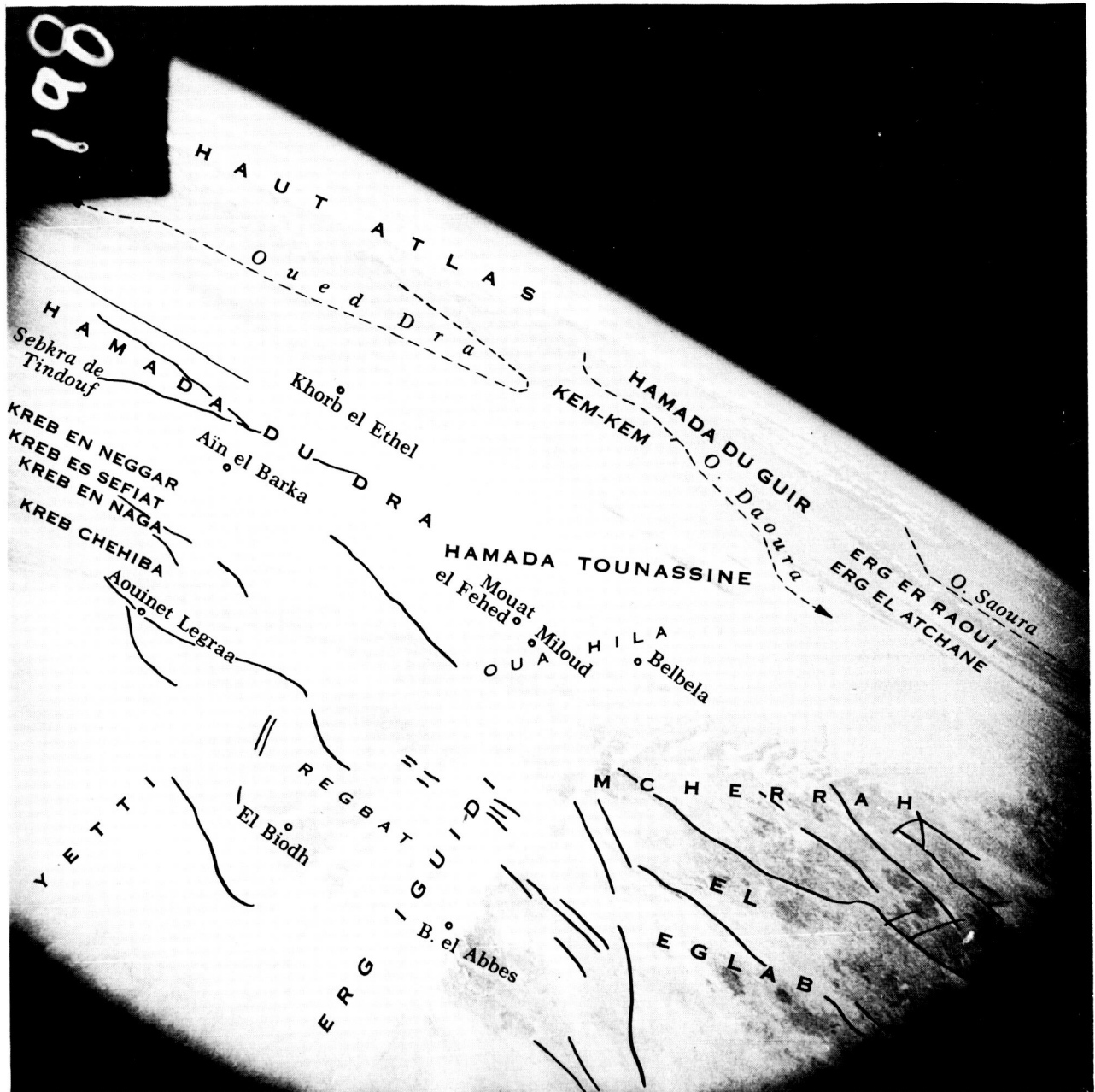


Figure 16 (b) Photo 198 with place name overlay

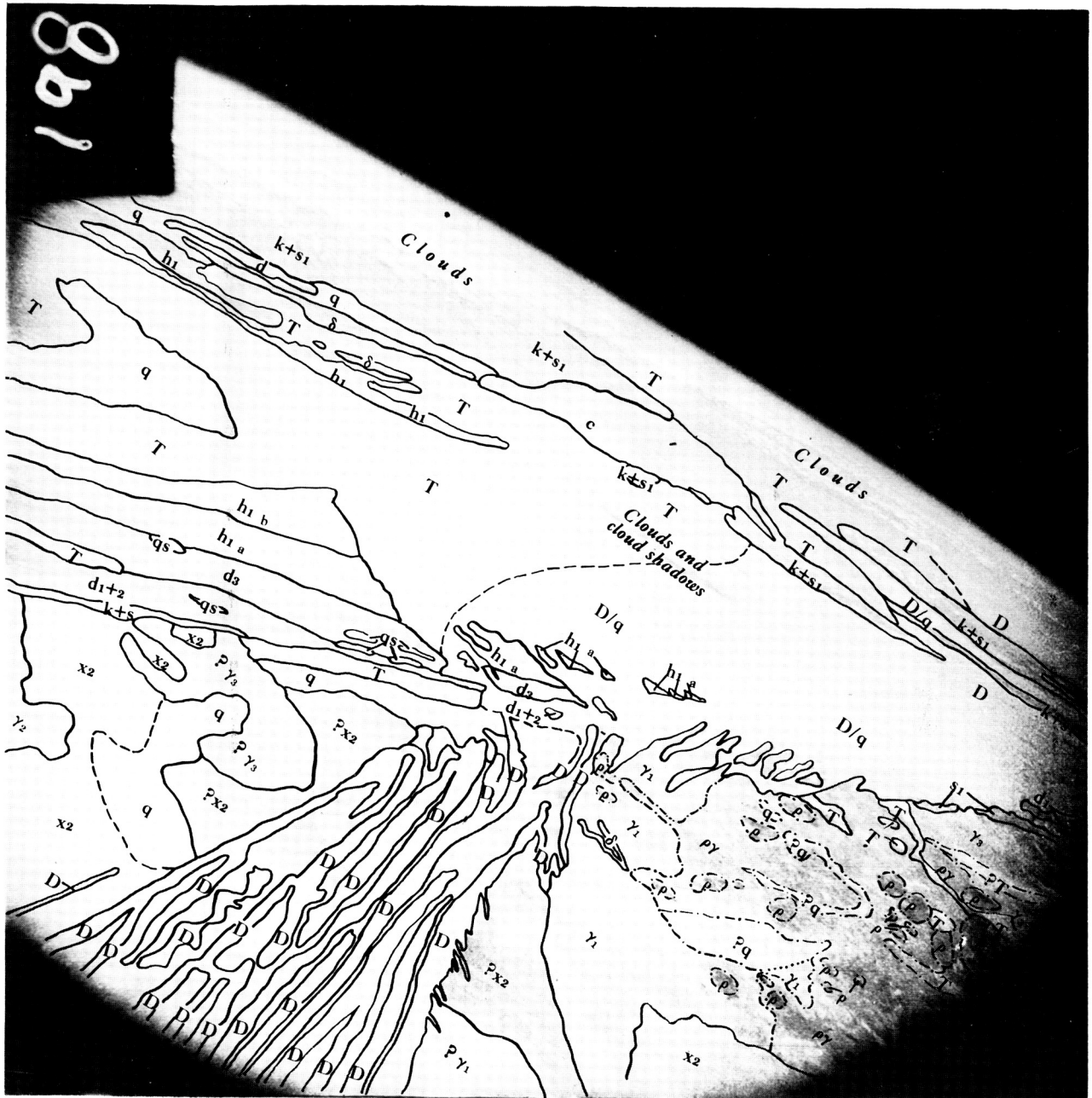


Figure 16 (c) Photo 198 with geological overlay

Photograph 202

This photograph shows the Eglab, the westernmost of the central Saharan massifs, and by far the lowest, since heights reach only 1600 ft. (500 m.) above sea level. The area is mainly composed of Precambrian crystalline rocks especially granite. Earth movements since the Precambrian have been limited to broad folding parallel to the Atlas and the formation of the slight syncline in which the Erg Iguidi was deposited (ref. 20, p. 241).

On the photo one can distinguish rhyolitic intrusions (almost black), from the surrounding microgranite aureoles (dark grey), and the granite country rock (medium grey), though these units are difficult to define on the ground because of intergrading (ref. 37, p. 104). On the 1:2,000,000 map rhyolites are not distinguished from microgranites.

The light-toned strips which form a dendritic pattern like huge wadi-beds are labelled on the 1:2,000,000 geological map as hamada formation. They do not in general correspond to present day wadi beds. Whether or not they are fragments of a formerly extensive cover is not clear, but it has been assumed that they follow structural weaknesses in the basement rocks, and they have been plotted as lineaments.

In addition to the well-marked NW structural trend, 198, 202 and 206 show E and NE trends.

In placing the exact outline of D, and in separating it from T, the red color of D on the original was useful. The area D/?h does not fit the 1:2,000,000 map.

The mountain chains of Tabelbala and Ougarta, (bg.) which are respectively W and E of the Erg er Raoui, are composed of Primary sandstones limestones and schists in a dome-and-basin structure, so that a series of curved escarpments exist. They are continued to the W by the djebels N and S of the Hamada du Dra, and to the SE by the tassilis of the Ahenet area (ref. 20, p. 243; 36, pp. 117-119, 148, 171).

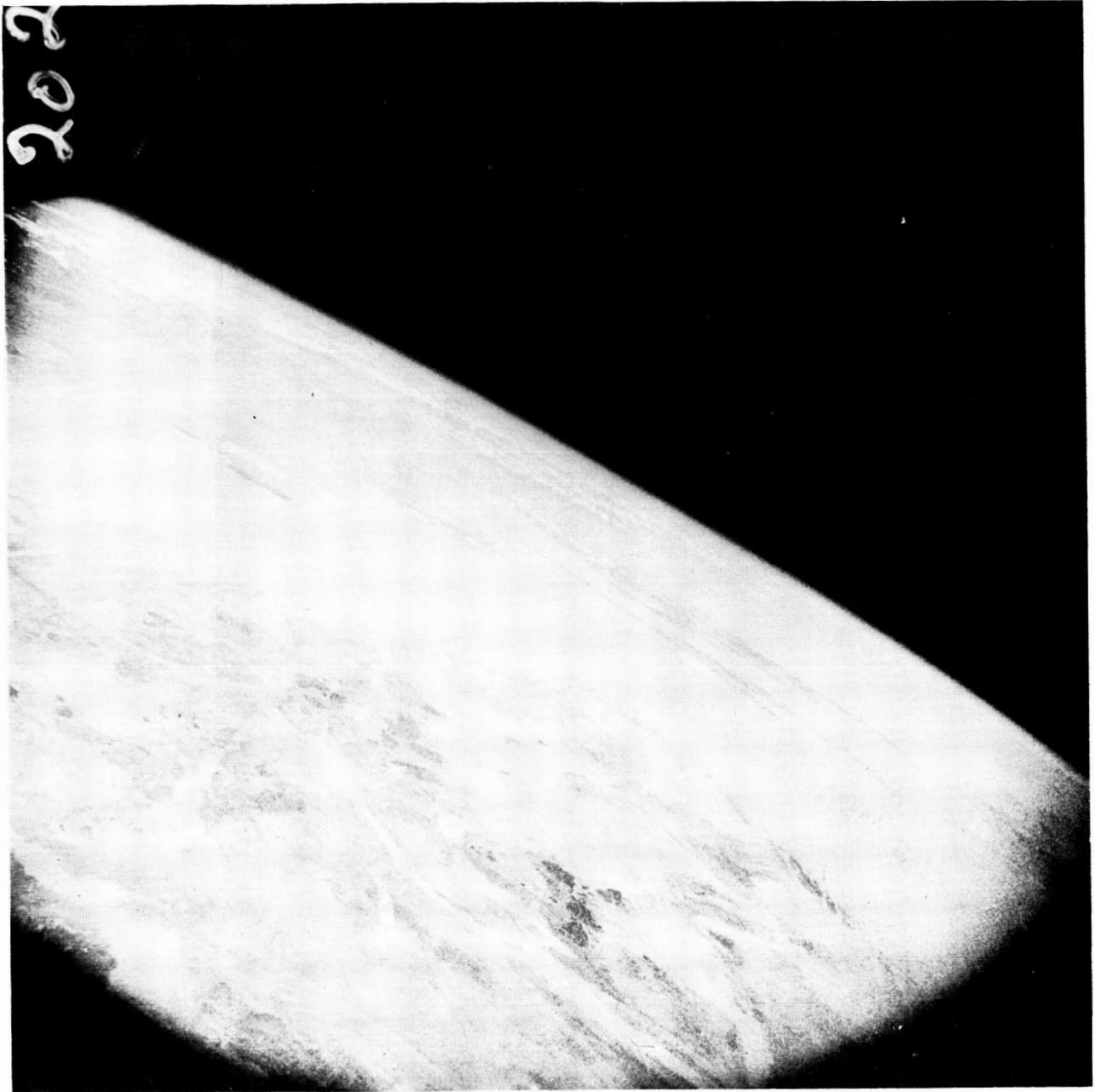


Figure 17 (a) Photo 202

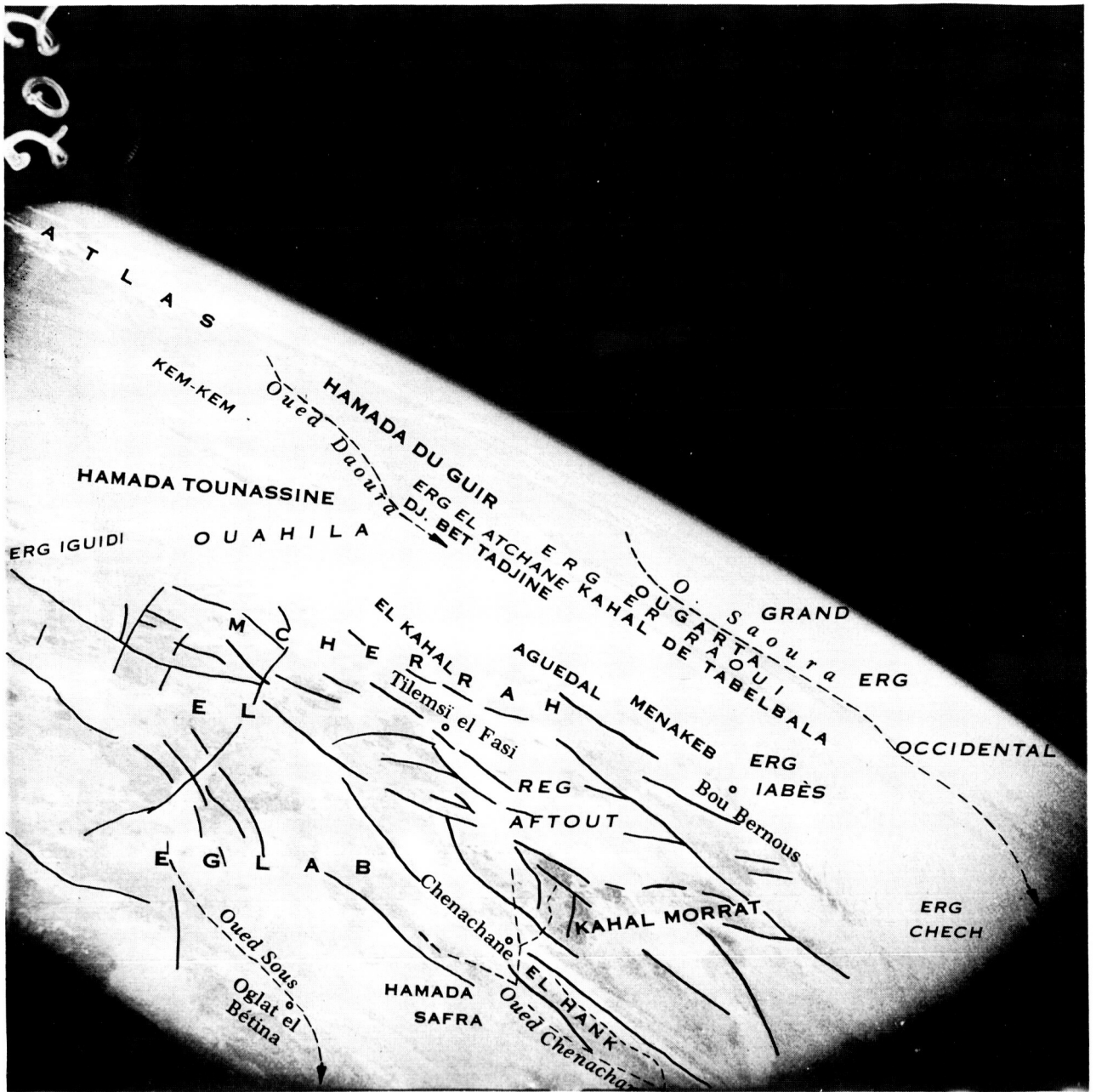


Figure 17 (b) Photo 202 with place name overlay

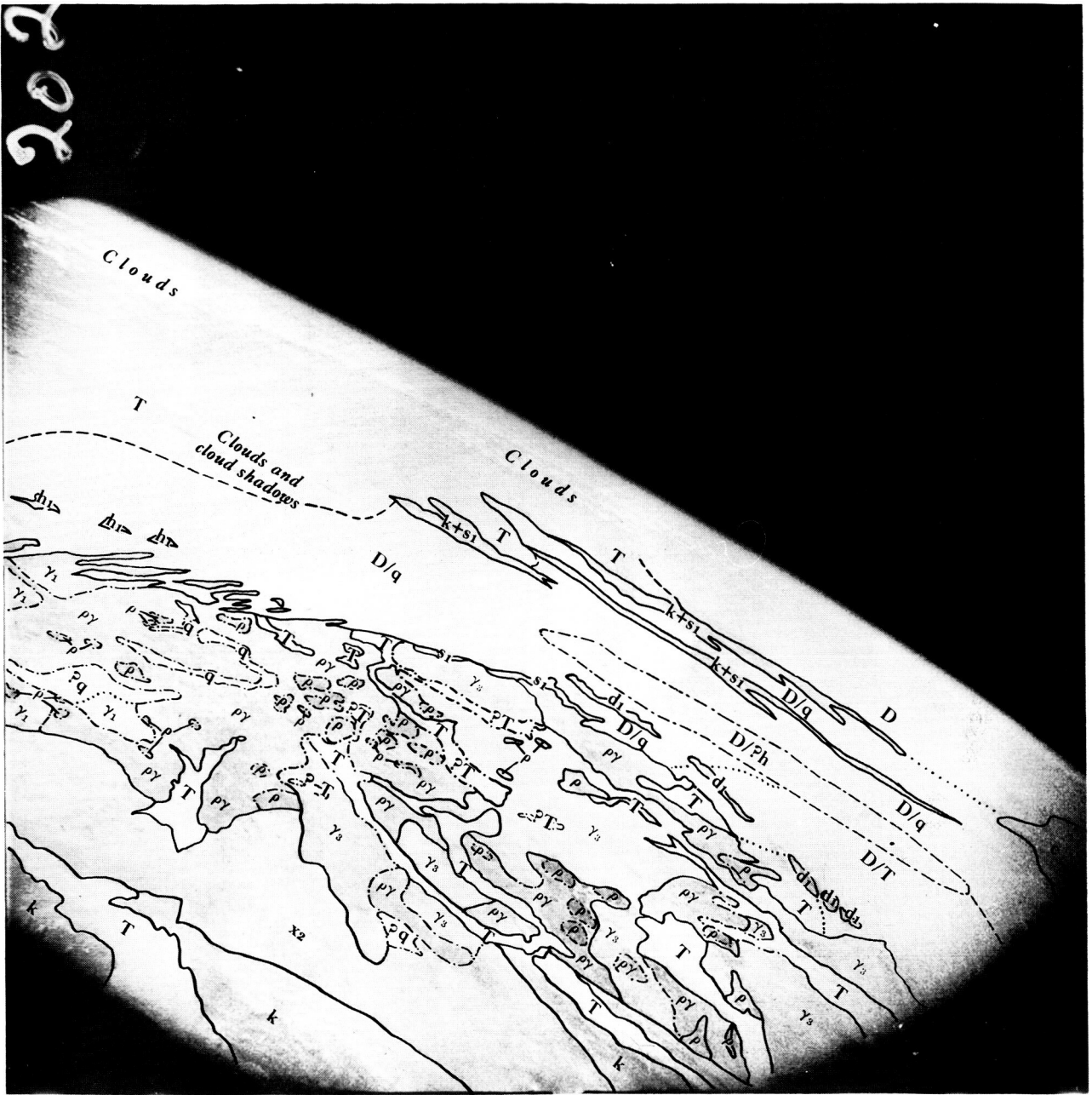


Figure 17 (c) Photo 202 with geological overlay

Photograph 206

The best example of a longitudinal dune area seen by the Mercury space-craft camera was the Erg Chech, seen here (fig.). The erg consists of endless chains of dunes perhaps 300 mi. (500 kms.) long and a mile or two in width (zemoul), separated by bare areas which here, in the N of the erg, are about 7 miles (10 km.) wide (feidj). The width of the corridors everywhere exceeds that of the dune chains. Often the sand rests directly on rock, not gravel. The dune chains parallel the dominant winds, almost always the Trade Winds. However, the curvature of the dunes towards the N (md.) suggests that some other wind, perhaps the westerly winds which blow in winter, have some effect at the latitude. Although small dunes sometimes move appreciably, the big ergs are practically fixed during a human lifetime, probably because moisture is held within them. The dunes in this photograph appear to be unchanged since they were surveyed for a French map in the 1930s.

The Erg Chech occupies the northern end of the huge Taoudenni basin, which is of structural origin. The sand was laid down by the Oued Saoura during the Quaternary, when it had sufficient flow to reach this far. At the same time this wadi system hollowed out the Gourara basin, which is not of tectonic origin, and which is now filled by the drift of the Grand Erg Occidental (c.bg.) (ref. 20, pp. 372, 380, 383, 384, 386).

Not all ergs are equally dry. The Erg er Raoui (bg.) and the Erg Iguidi are close to the points of disappearance of wadis flowing from the mountains to the N, so that their underground water supplies are regularly replenished, and wells and areas of camel pasture are abundant. The Erg Chech on the other hand is a very dry erg. (ref. 22, pp. 99, 102).

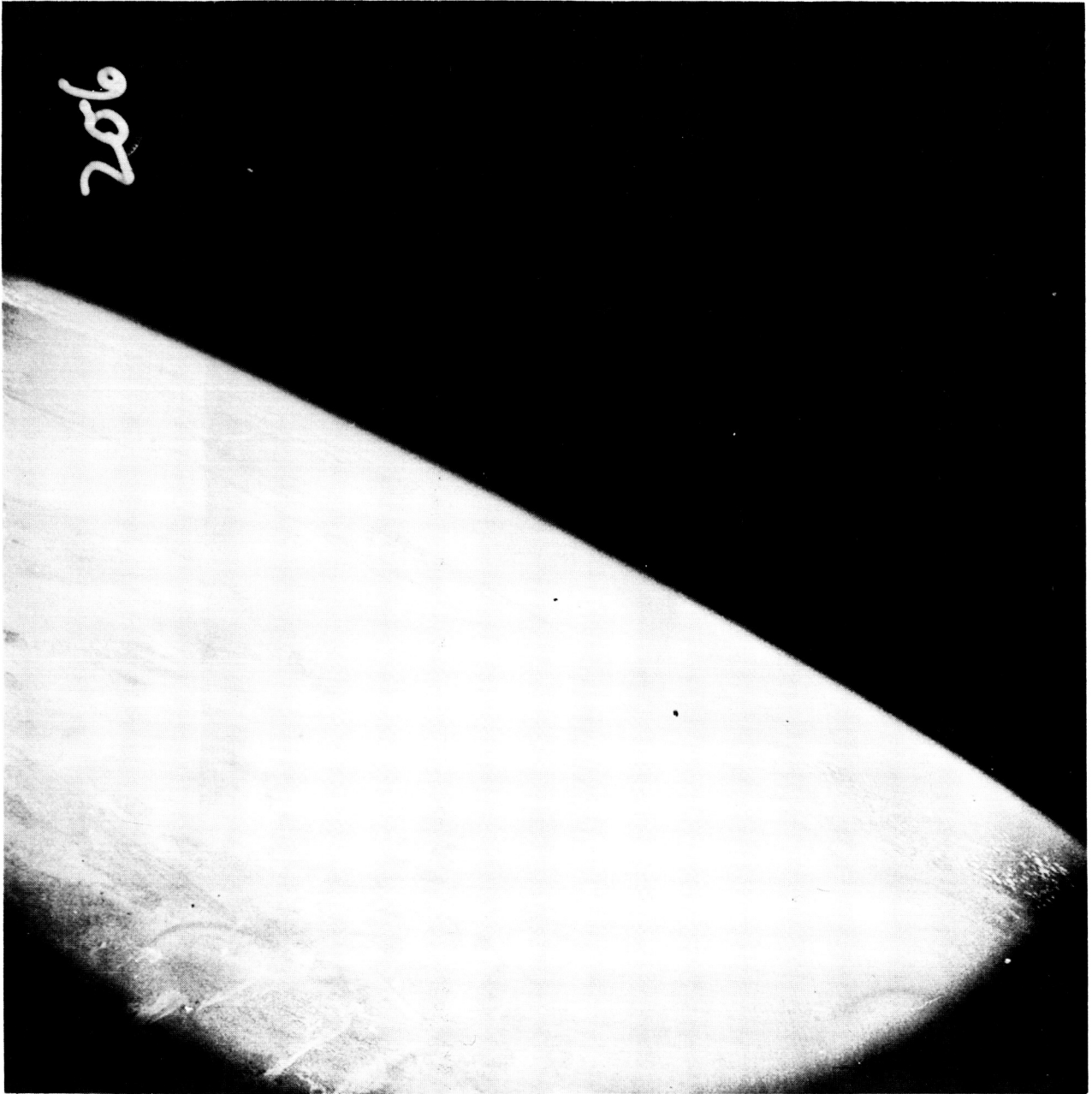


Figure 18 (a) Photo 206

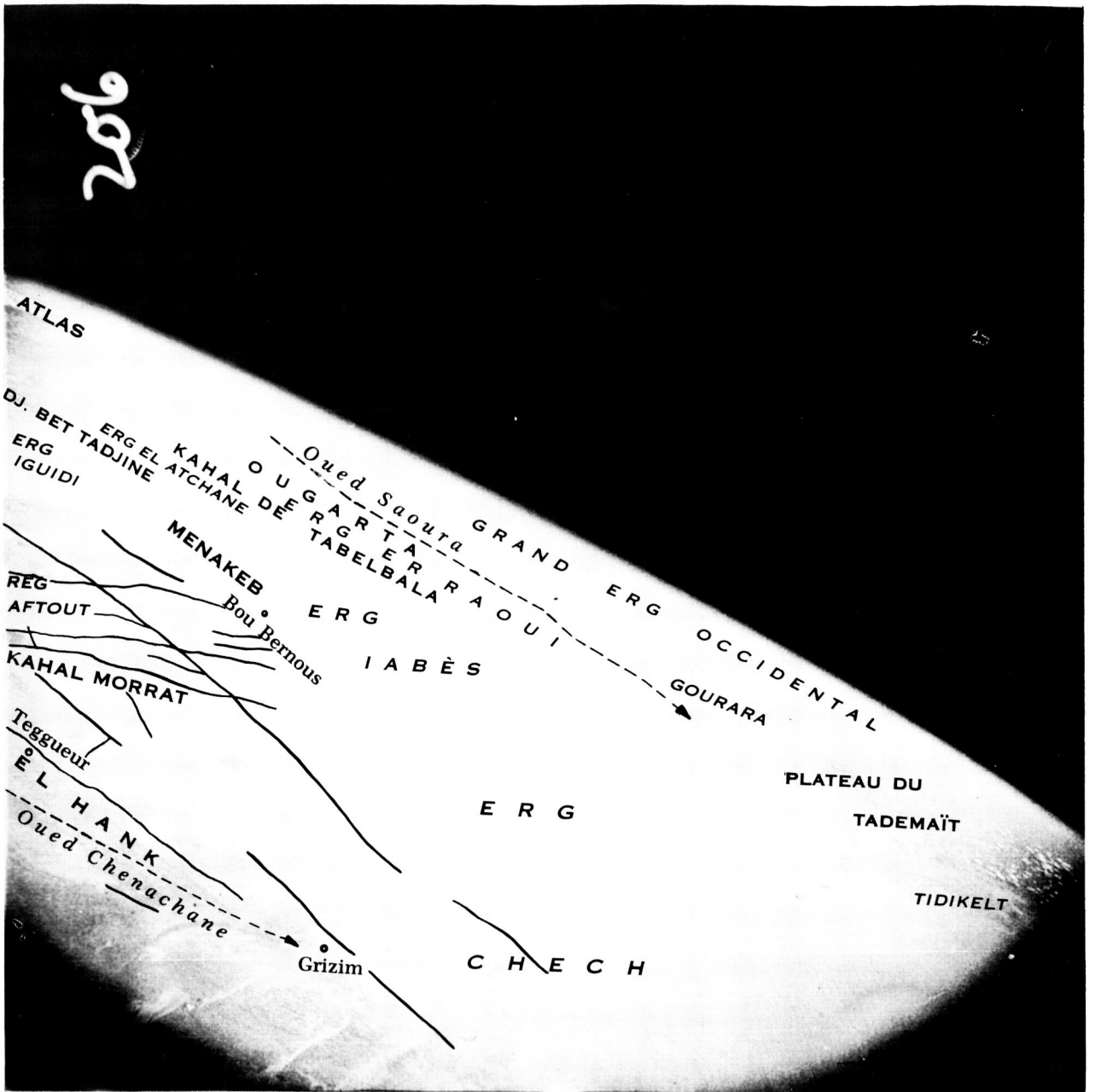


Figure 18 (b) Photo 206 with place name overlay

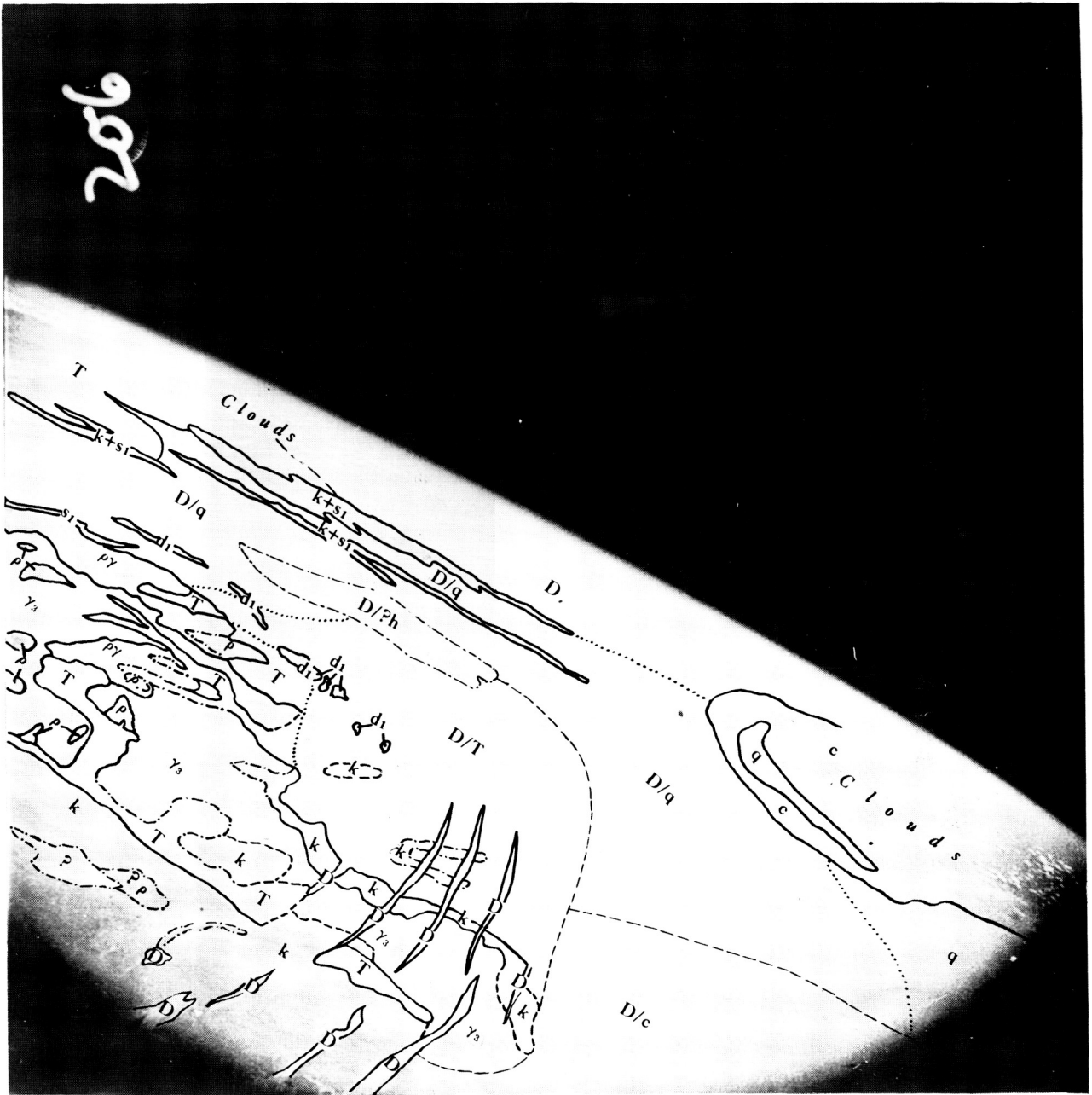


Figure 18 (c) Photo 206 with geological overlay

Photograph 210

This is the first photograph in the series which shows clearly a large area of reg, or gravel desert (r. fg.). It appears as a featureless light and medium grey area. Part of the gravel has been brought down from the Ahaggar massif (off the photo, r.) and hence the thickness of the reg gets less and less as one advances westwards. The reg is also partly formed by the breaking up in place of the underlying rocks, which are mainly Pre-cambrian crystalline rocks, and Ordovician and Cretaceous sedimentary rocks. The gravelly surface of such a reg is very easily motorable and indeed one of the main trans-Saharan motor-routes runs across the area of the Tanezrouft shown in this photograph (ref. 20, pp. 373, 376, 377; 21, p. 364).

The light-toned area in the right middle distance is the plain of Tidikelt. This long narrow depression is very variable in width because, although the northern edge along the Tademaft escarpment is fairly straight, in the S the plain extends up the various bays of the pretassilian area of folded Primary rocks to be described under 216. The lowest parts are occupied by salt flats, the remnants of once more extensive lagoons, the deposits of which conceal the Primary rocks over much of the plain (ref. 20, p. 369).

North of Tidikelt rises the Plateau du Tademaft (c. bg.), a typical hamada formed of Cretaceous limestone. It is continued to the E by the Plateau du Tinrhert (216, r. bg.). Unlike the Plio-Pleistocene hamadas such as the Hamada du Dra, the upper surfaces of these Cretaceous hamadas are black, while the lower slopes are grey. The foot of the Tademaft escarpment is followed by a line of oases supplied with water by springs from the limestone, the most southerly of which is In Salah (ref. 22, p. 192; 20, p. 253).

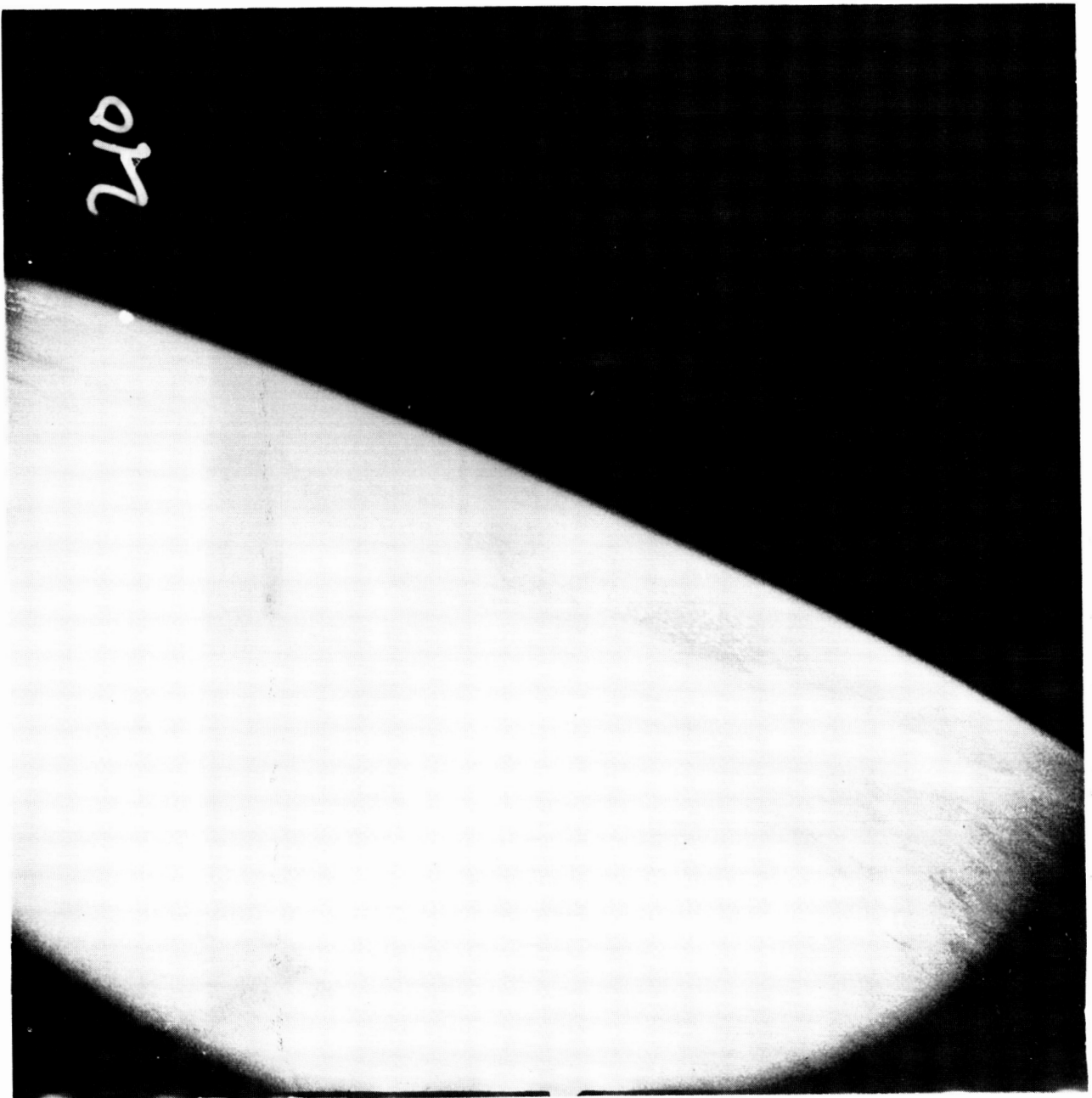


Figure 19 (a) Photo 210

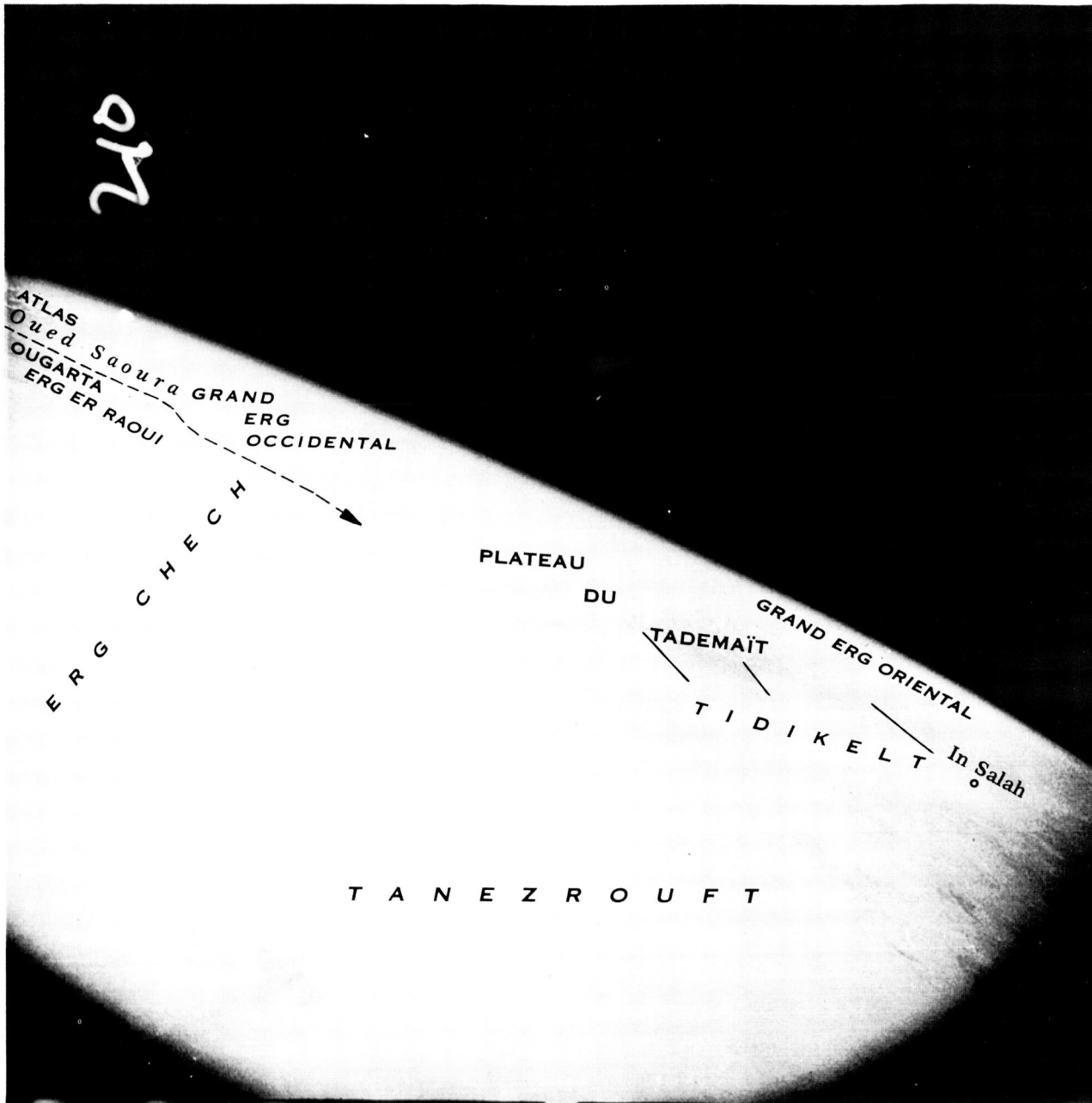


Figure 19 (b) Photo 210 with place name overlay

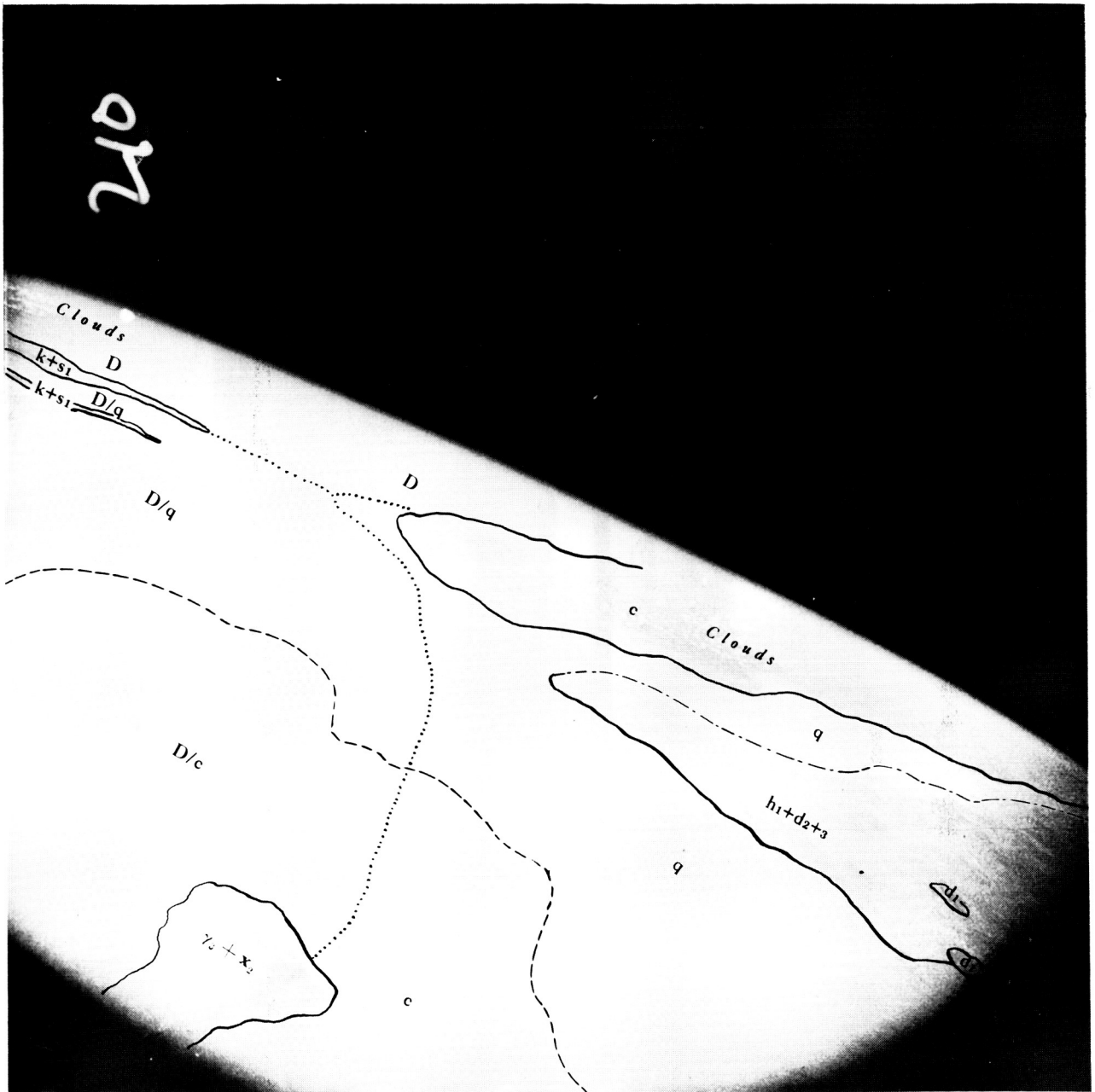


Figure 19 (c) Photo 210 with geological overlay

Photograph 216

The dark areas in the middle distance of this photograph represent mountains, part of the belt of tassilis that almost encircles the Ahaggar, the central massif of the Sahara. Typically a tassili is a slightly tilted plateau of Primary rocks bounded on most sides by escarpments. It is therefore very similar to a djebel, except that the rocks do not dip so steeply. The tassilis are in fact two separate lines of plateaus, the inner and the outer tassilis, separated by the intra-tassilian furrow, and succeeded to the N by the pre-tassilian depression. For example, in this photograph the Adrar Taohenna is part of the inner tassili, while the Adrar Tikkadouine is part of the outer tassili. This distinction can be traced from here round the northern end of the Ahaggar as far as In Ezzane (c.bg. of 236). The age of the rocks making up the tassilis can be seen from the cross-section (fig. 21). Broadly speaking the inner and outer tassilis are made up of sandstones, while the intra-tassilian furrow and the depression north of the tassilis are underlain by shales and schists.

In this area of the tassilis there is superimposed on the gentle northward dip of the rocks a series of flexures with axes N-S, probably caused by movements along N-S fractures in the basement rocks. These are reflected in the outline of the northern edge of the tassilis as an alternation of promontaires and bays (ref. 20, p. 244). The only lineaments plotted on 210 and 216 are those resulting from this structure.

Three main mountain groups are included in this western area of tassilis. The Asedjrad in the W is the lowest and driest. The Ahenet (c.md.) rises 1000 ft. (300 m.) above its surroundings to a height of 2500 ft. (800 m.) above sea level. Though there are wells, it is a poor dry region, even for stock. The Mouydir (r.md.) reaches a height of 5100 ft. (1680 m.) above sea level, water and pasture are more abundant, and there are a few small spots of cultivation (ref. 21, p. 362; 41).

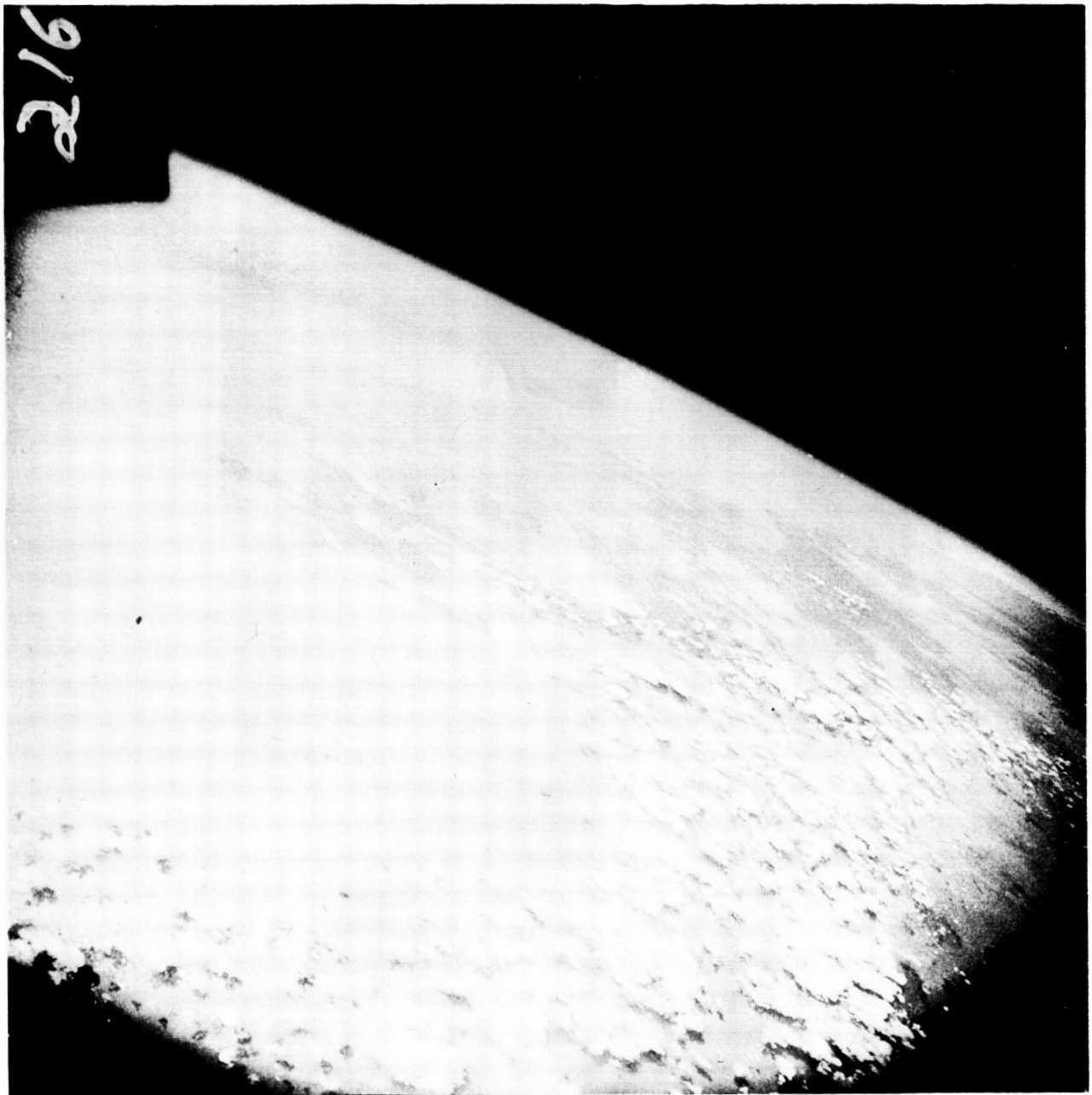


Figure 20 (a) Photo 216

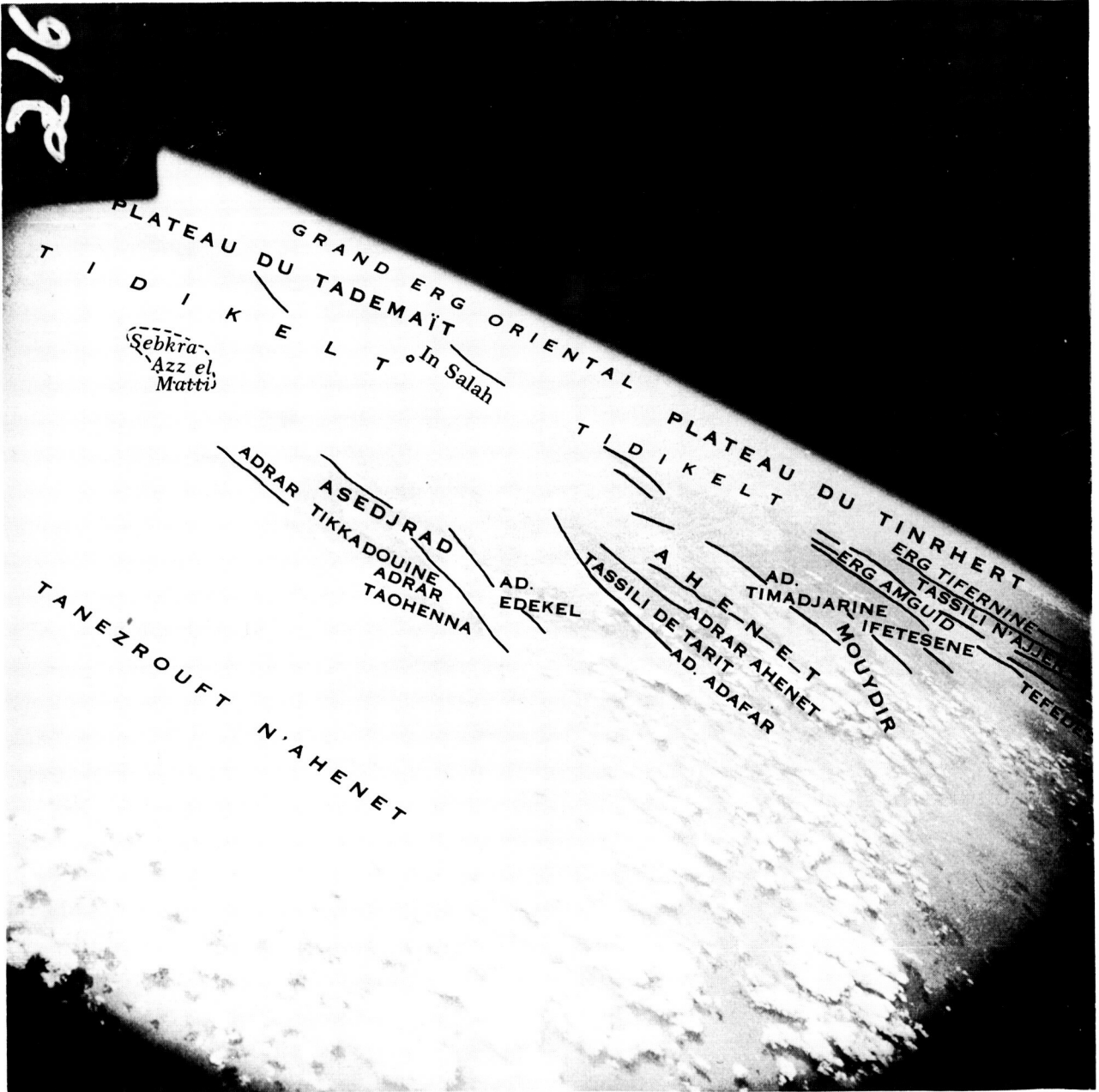


Figure 20 (b) Photo 216 with place name overlay

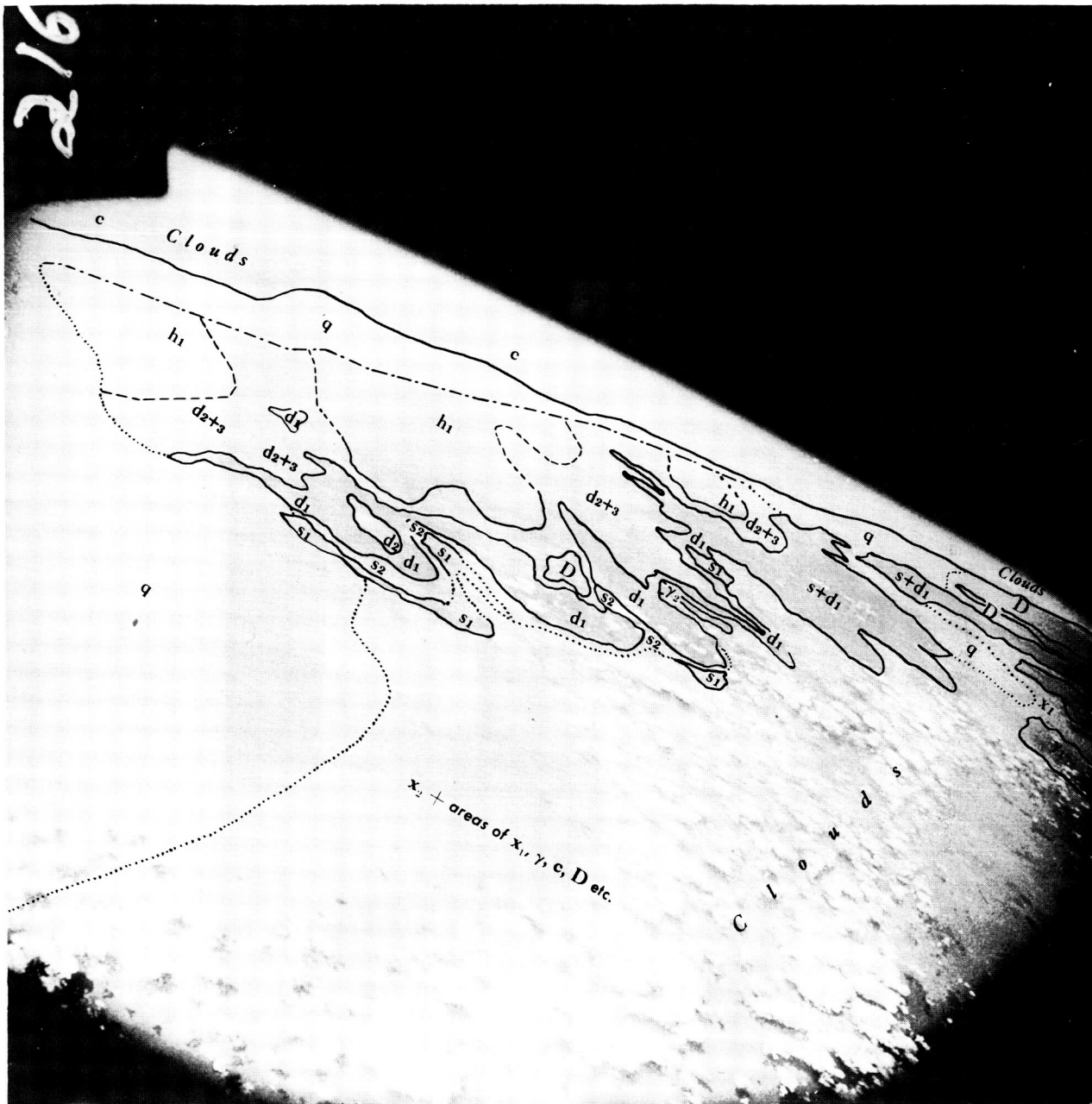


Figure 20 (c) Photo 216 with geological overlay

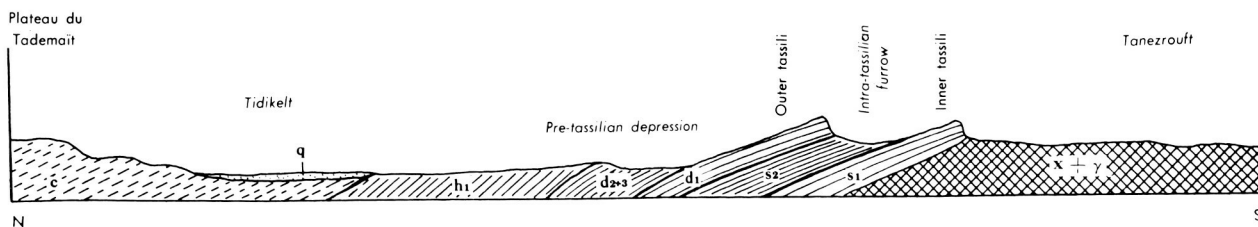


Figure 21 Typical geological section across the area shown in Photo 216

Photograph 223

The belt of tassilis seen on 216 is not continuous round the southern side of the Ahaggar massif (r.md.). In many places the gravel desert of the Tanezrouft (md.) reaches to the foot of the Ahaggar. Only fragments of Primary rocks remain forming miniature tassilis, such as the Tassili n'Adrar (fg.). These are on the whole horizontal plateaus, but are varied by slight tilting, folding, or faulting. At their edges they break up into isolated columns, a few hundred feet in height. Perhaps some of these are visible in the foreground (ref. 20, pp. 245-246; 22, p. 111).

The marked change in tone in the right foreground appears to represent a low escarpment, facing W, very likely developed along a fault. The beds of wadis crossing it appear dark, probably because of moisture and vegetation, but perhaps because material from the area of dark volcanic rocks (r.md.) has been carried down by them. The scarp does not appear on the 1:2,000,000 maps either as a fault or as a continuous rock-type boundary, though in places it corresponds to a boundary between Precambrian granite to the E and Precambrian schist and gneiss to the W.

The northern belt of tassilis, the Tassili n'Ajjer, is also visible, in the right background, though it is better shown on 230. It continues the characteristics of the western tassilis. The intra-tassilian furrow can be distinguished, separating the inner and outer tassilis, while the Erg Tifernine and Erg Issaouane occupy two bays along the northern edge, separated by a long promontory.

Between the northern tassilis and the Ahaggar lies a series of depressions. These include the plains of Amador (r.md.) and Admer (230, r.bg.). The several plains are separated by low sills which seem to correspond to areas of young volcanic rocks, such as the Edjere (c.bg.) and Adrar des Ajjers (230, c.bg.). These may perhaps have been poured out along weaknesses trending N-S, that is at right-angles to the general direction of the depressions. Some of the plains have become occupied by ergs, such as the Erg Amguid (c.bg.), and the Erg d'Admer (230, r.bg.). The material for these has been brought down by wadis radiating from the Ahaggar (ref. 20, pp. 237, 238, 240, 243; 21, p. 359).

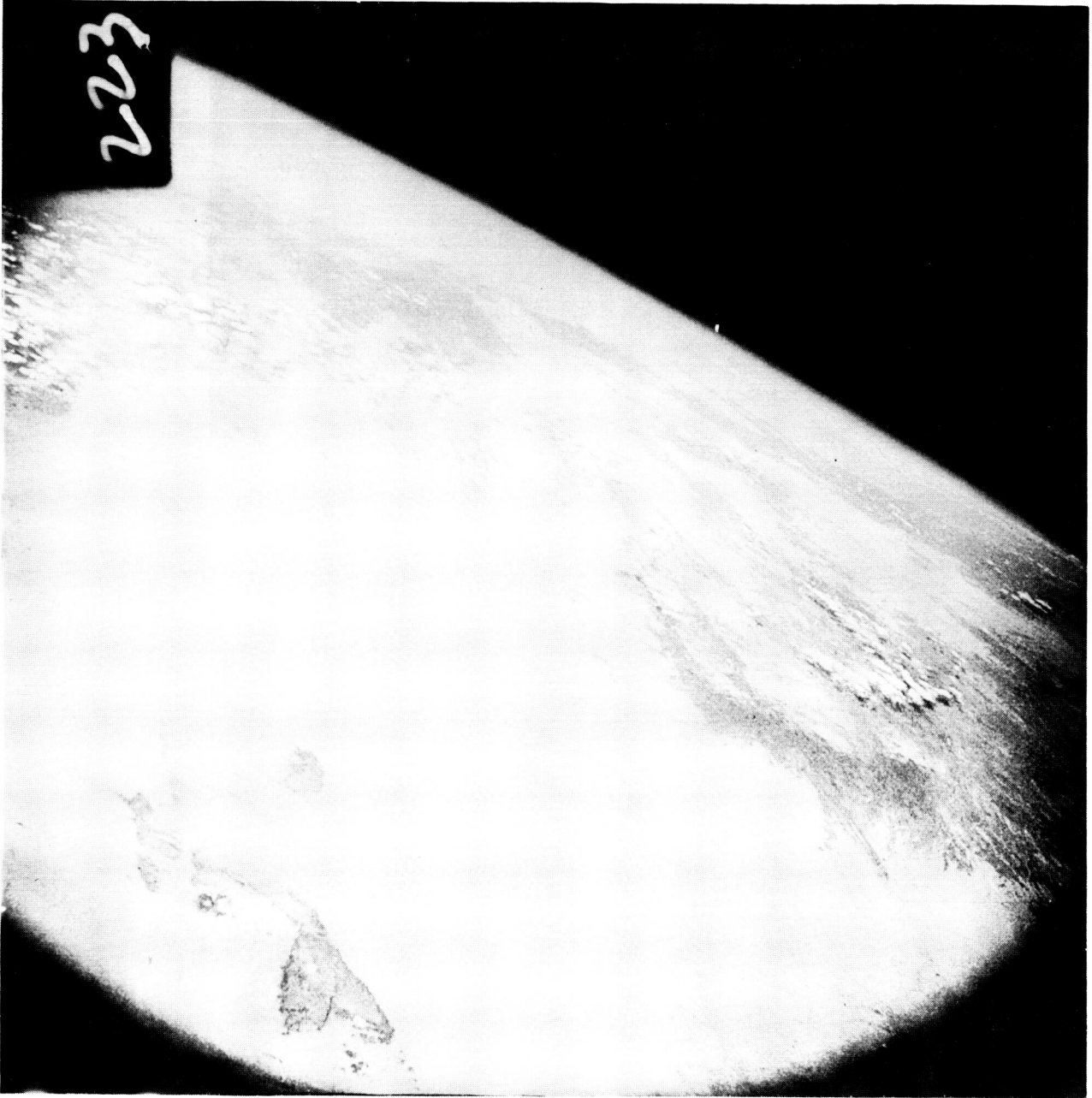


Figure 22 (a) Photo 223

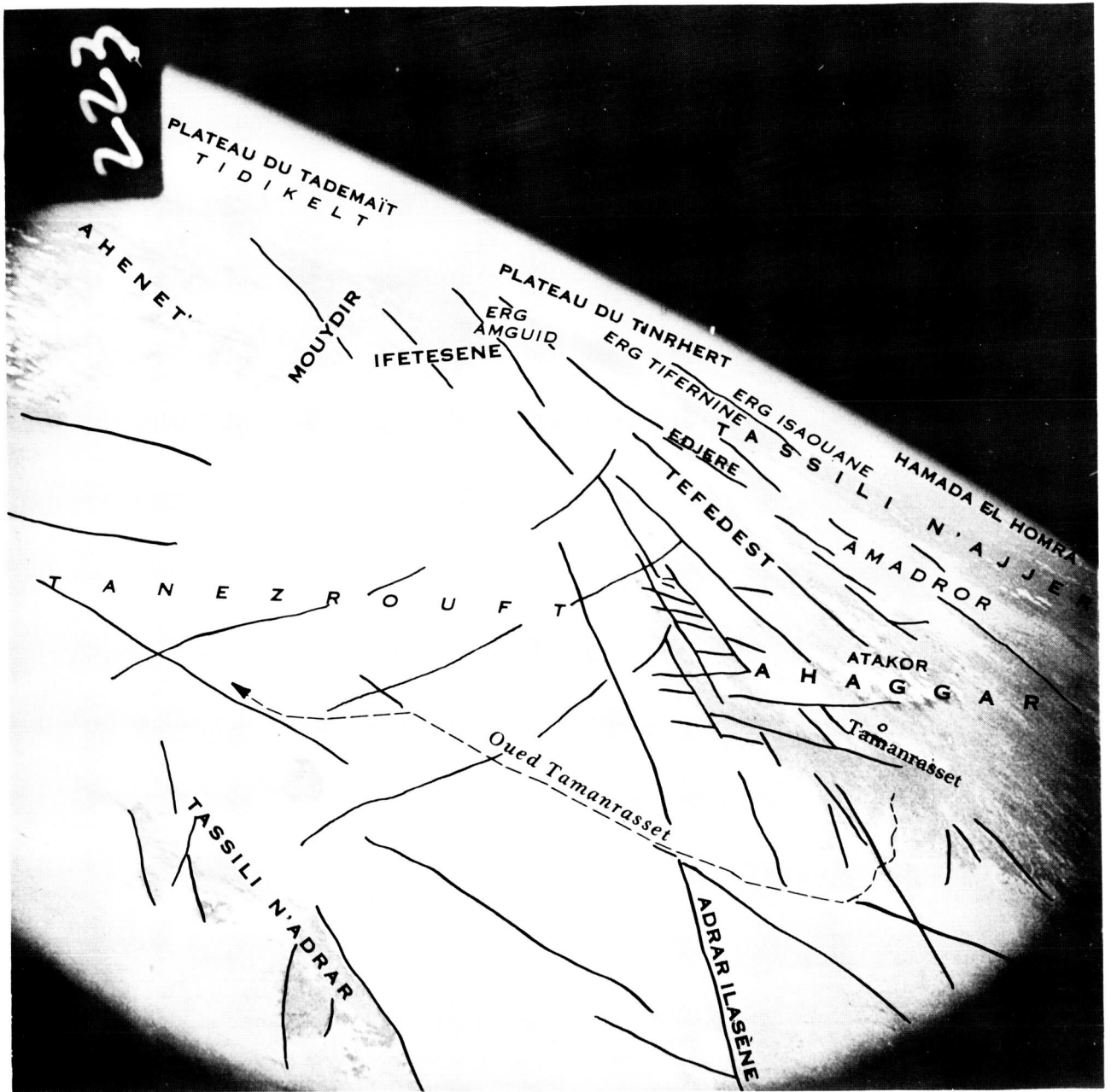


Figure 22 (b) Photo 223 with place name overlay

Photograph 230

In the middle distance of this photograph appears almost the whole of the Ahaggar massif. Though not so high as the Tibesti area further E, this is the true central massif of the Sahara because of its central position and large area. Its average altitude is about 3000 ft. (1000 m.) but the higher ranges often exceed 6000 ft. (2000 m.). The central dome, the Atakor (l. md.) reaches 8000 ft. (2500 m.), and this in turn is surmounted by volcanic peaks, of which the highest, Tahat, reaches 9900 ft. (3003 m.).

The massif is mainly composed of metamorphosed Precambrian sediments that were strongly folded by the Saharan earth movements, which took place before the Ordovician. The Saharan structures have a N-S trend which is clearly visible in 223 and 230. Later the area has been dissected and levelled several times by desert, semi-desert and normal erosion processes. It now resembles an imperfect peneplain with the most resistant rocks still sticking out. These include Precambrian volcanic rocks and quartzites with their outcrops aligned N-S, parallel to the ancient folds; old intrusive rocks such as the granite which makes up the Tefedest area which rises to 7650 ft. (2330 m.) to the north of the Ahaggar; Quaternary volcanic rocks such as those forming the Tahat; and other rocks raised along folds and faults of Late Hercynian or Atlasic trend, that is generally NE-SW and E-W. Because of the criss-cross nature of these several structural trends, the Ahaggar has been likened to an area of uneven paving stones. The aptness of this simile is illustrated by the photograph. An additional lineament direction occurring in the Tanezrouft in 223 is WNW and NW, perhaps the Early Hercynian trend.

South of the Ahaggar the Primary sandstones reappear forming tassilis such as the Tassili Oua-n-Ahaggar (fg.), but in many areas they have been removed, so that over much of the lowland in the fg. are exposed the same crystalline basement rocks which make up most of the Ahaggar highlands (ref. 21, p. 364). In the left foreground appears a linear pattern similar to that reported by Grove from the area NW of Tibesti (ref. 42, fig. 1 caption). He suggests that it is due to the picking out of joints in the rock by wind of a generally parallel direction, and the filling of the joints by sand. In this case the direction is approximately ENE, and the rocks are Precambrian gneisses and schists probably having a strongly-marked foliation, so that this explanation appears likely.



Figure 23 (a) Photo 230

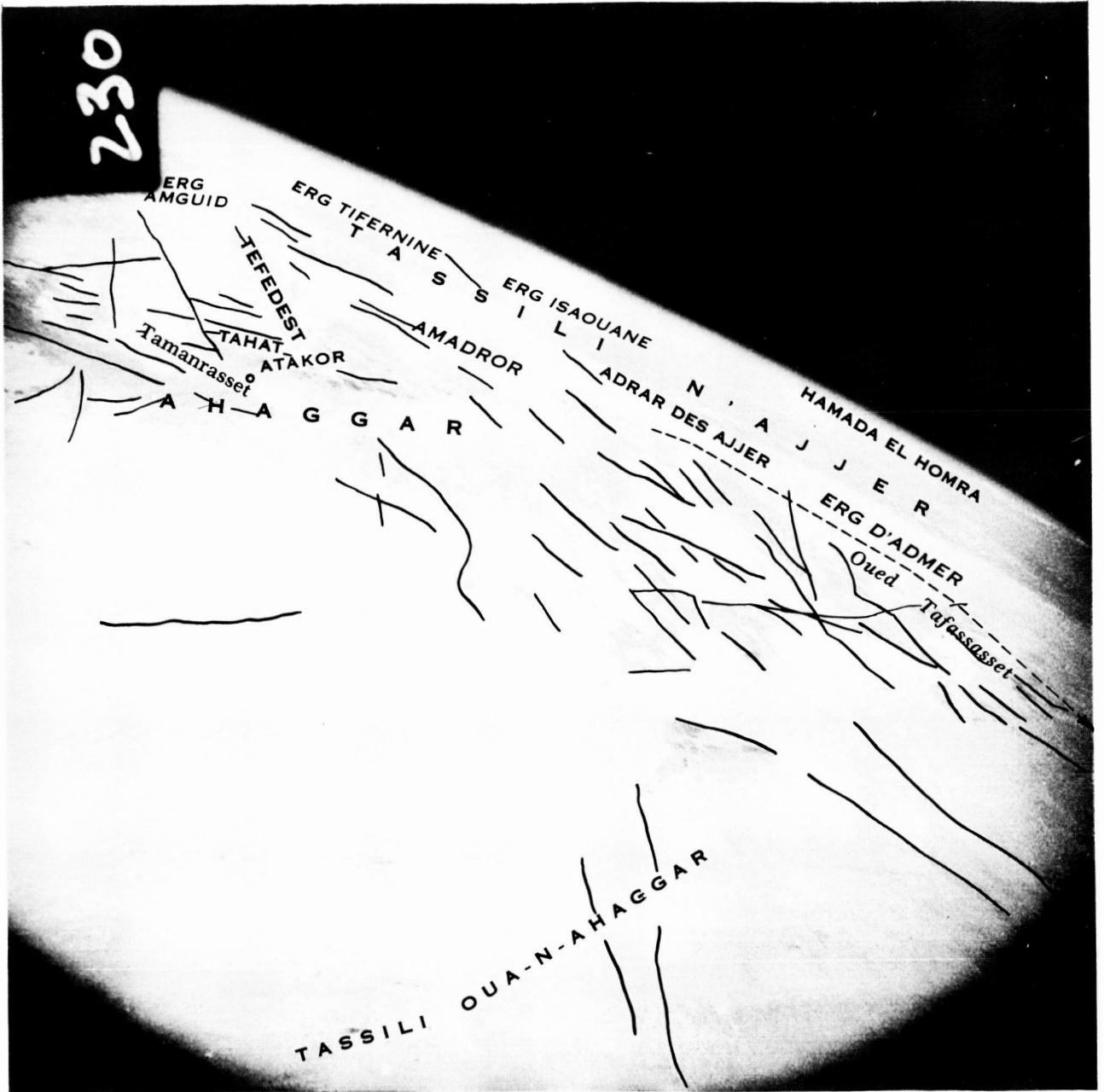


Figure 23 (b) Photo 230 with place name overlay



Figure 23 (c) Photo 230 with geological overlay

Photograph 236

Photograph 236 shows the northern end of the Aïr mountains (fg.). These may be regarded as an isolated fragment of the Ahaggar massif, composed of Precambrian basement rocks. These include parallel bands of mica-schists, quartzites, and other Precambrian metamorphic rocks, the quartzites forming the highest areas. The E-W structural trend visible in the Aïr in 236 and 239 seems to be in conflict with Perret's statement that the alternation of more resistant and less resistant bands is due to N-S folds. The main part of the mountains are a dissected plateau of mean elevation 2500 ft. (800 m.), above which rise the remnants of ancient volcanos to form the highest areas. The highest point, Mont Tamgak, of height 5900 ft. (1800 m.) is visible on 239. The lavas are mainly basaltic (ref. 20, p. 234).

The main wadi beds are broad, sand-filled, and with a gentle slope, but the minor tributaries have cut short, deep gorges. The majority of the wadis of Aïr flow SW where they lose themselves in the plain of Talak (l. fg.), which is consequently rich in water and pasture (ref. 21, p. 366; 38, p. 351).

So far, the areas shown in the spacecraft's photographs have been so dry that the vegetation has not been worthy of mention. However, the Aïr is close enough to the belt of equatorial rains and sufficiently high in altitude to enjoy some rain in almost every year. The resulting vegetation is confined to the valleys, which are often covered with grass and bushes. Elsewhere the bare rock is exposed and has acquired a black desert varnish, except in sheltered rifts which retain pink and red surfaces (ref. 21, pp. 317, 319; 38, p. 351).

The area (md.) between Aïr and the Ahaggar is a tassili of Primary rocks. The photo shows parallel stripes running ENE and resembling the outcrops of a series of beds striking in that direction, but the 1:2,000,000 maps do not show such a simple outcrop pattern. The stripes on 236 grade into the fine lines on 230, which have been ascribed to wind action, but they are much larger. Smith (ref. 26, p. 11) states that the wind can erode solid rock into knobs and ridges elongated in a direction independent of the strike, but these stripes are so wide and continuous that it is difficult to believe they were formed in this way. Perhaps the correlation of geological units has been complicated by the boundary between Algeria and Niger.

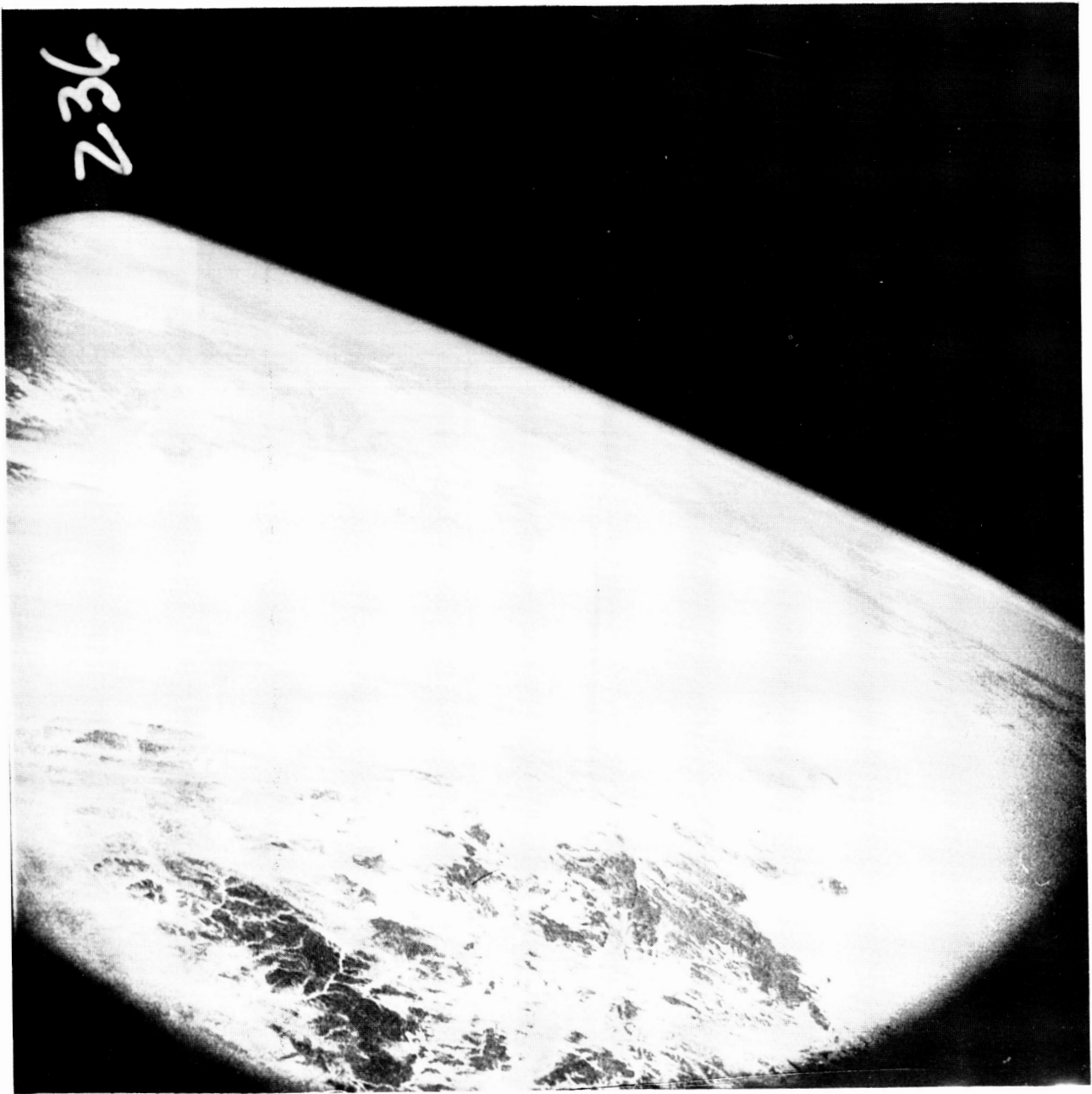


Figure 24 (a) Photo 236

236

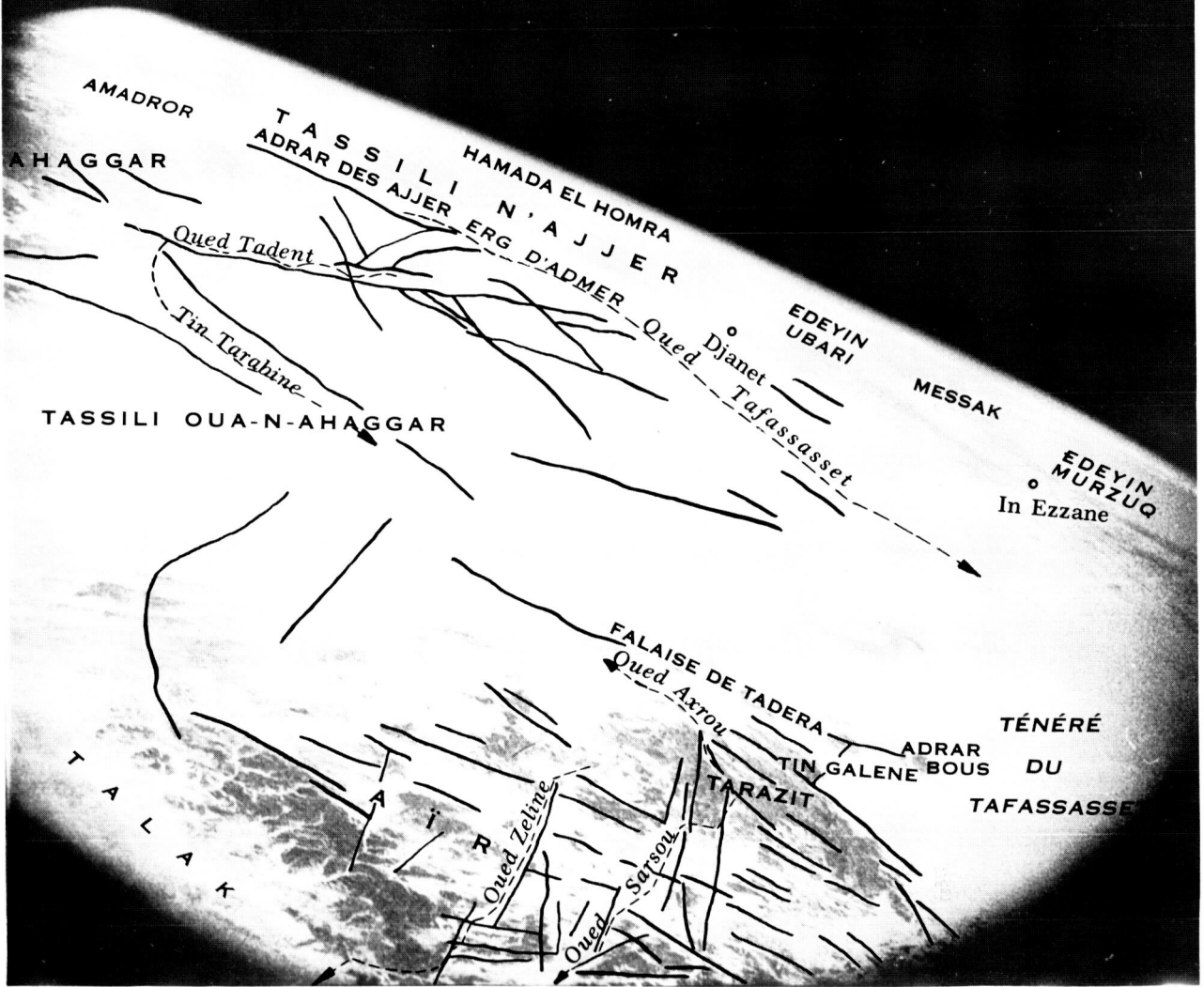


Figure 24 (b) Photo 236 with place name overlay

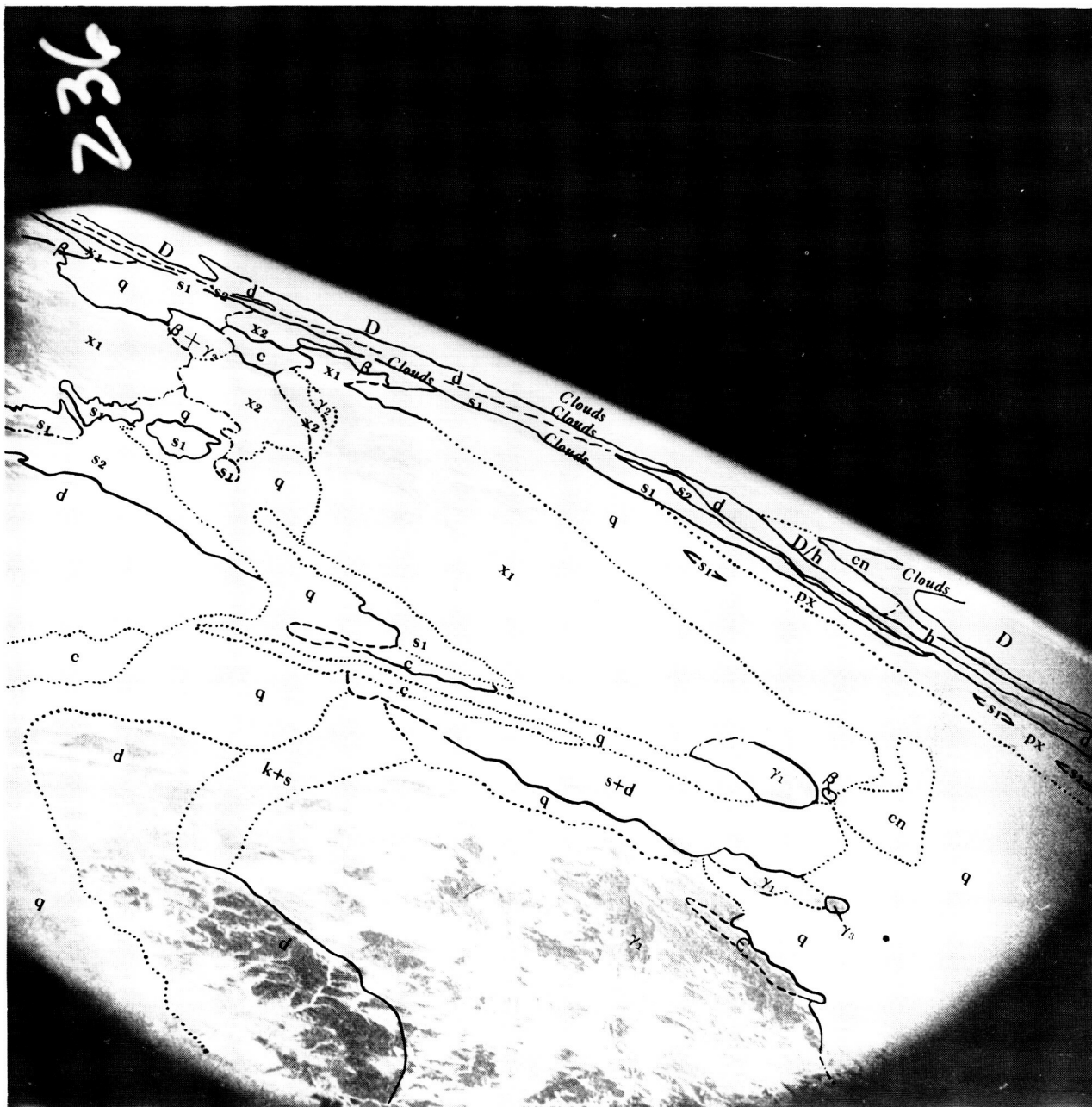


Figure 24 (c) Photo 236 with geological overlay

Photograph 239

In this photograph can be seen (fg.) Mont Tamgak (5900 ft., 1800 m.) the highest point of the Aïr.

In the right foreground, NE of the dark mass of mountains, is an area of uneven grey tone. The exposed rocks are the same as those making up the mountains but they have been worn down by erosion so that they are now practically at the same level as the basin to the northeast. From this area rise residual mountains such as Mont Sirret and Adrar Bous, both of which probably owe their preservation to local areas of the younger granite which has resisted erosion. The area is crossed by the courses of the few wadis which descend from the Aïr to the E but the main part of their deposition has taken place further NE. This area may be regarded as a pediment.

Beyond this stretches an enormous area of extreme desert similar to the Tanezrouft, known here as the Ténéré. In the NW this includes areas of bare rock and regs composed of rounded pebbles (l.md.). Further S between 19 and 17° N is a huge erg (r.md.), not here formed into marked dune patterns. Above this rise in places residual masses of sandstone, for example Adrar Madet (243, fg.) (ref. 21, pp. 364, 374; 20, p. 368).

In the background are visible the Edeyins, two huge closed basins each 200 by 450 miles (300 by 700 kms.) in extent. These are developed between the outer tassili (l.bg.) and the Cretaceous escarpments of the Hamada el Homra (bg.), so that the Edeyin depressions are structurally a continuation of the plain of Tidikelt. Their bottoms are occupied by lagoon deposits and dunes. The Messak chain (bg.), which divides them, is formed of Primary rocks flanked by some Cretaceous remnants. Its trend is exactly Atlasic, that is towards the NE. The separation of the area into two basins must be partly due to earth movements which continued until after the Cretaceous (ref. 20, p. 368).

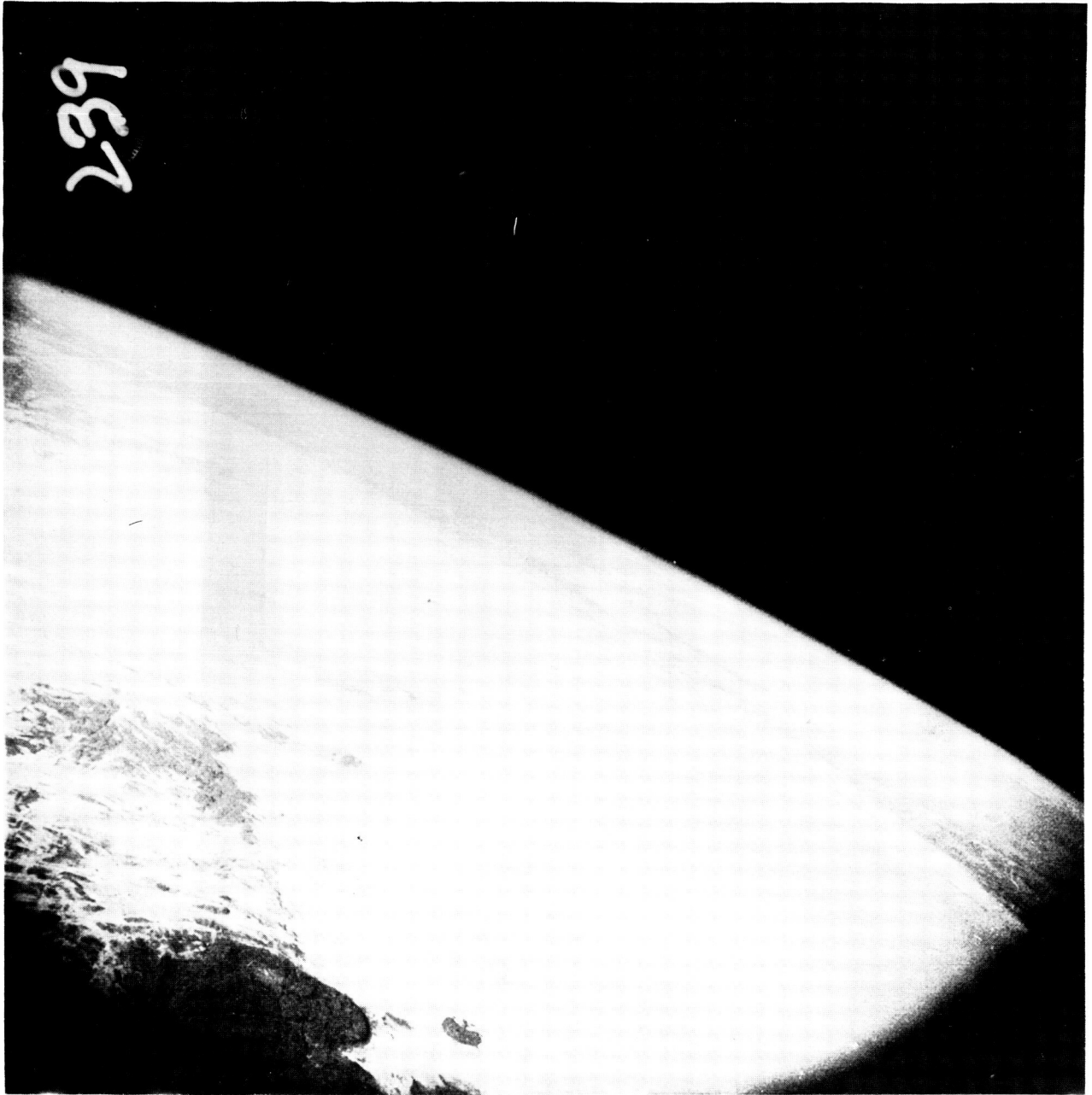


Figure 25 (a) Photo 239

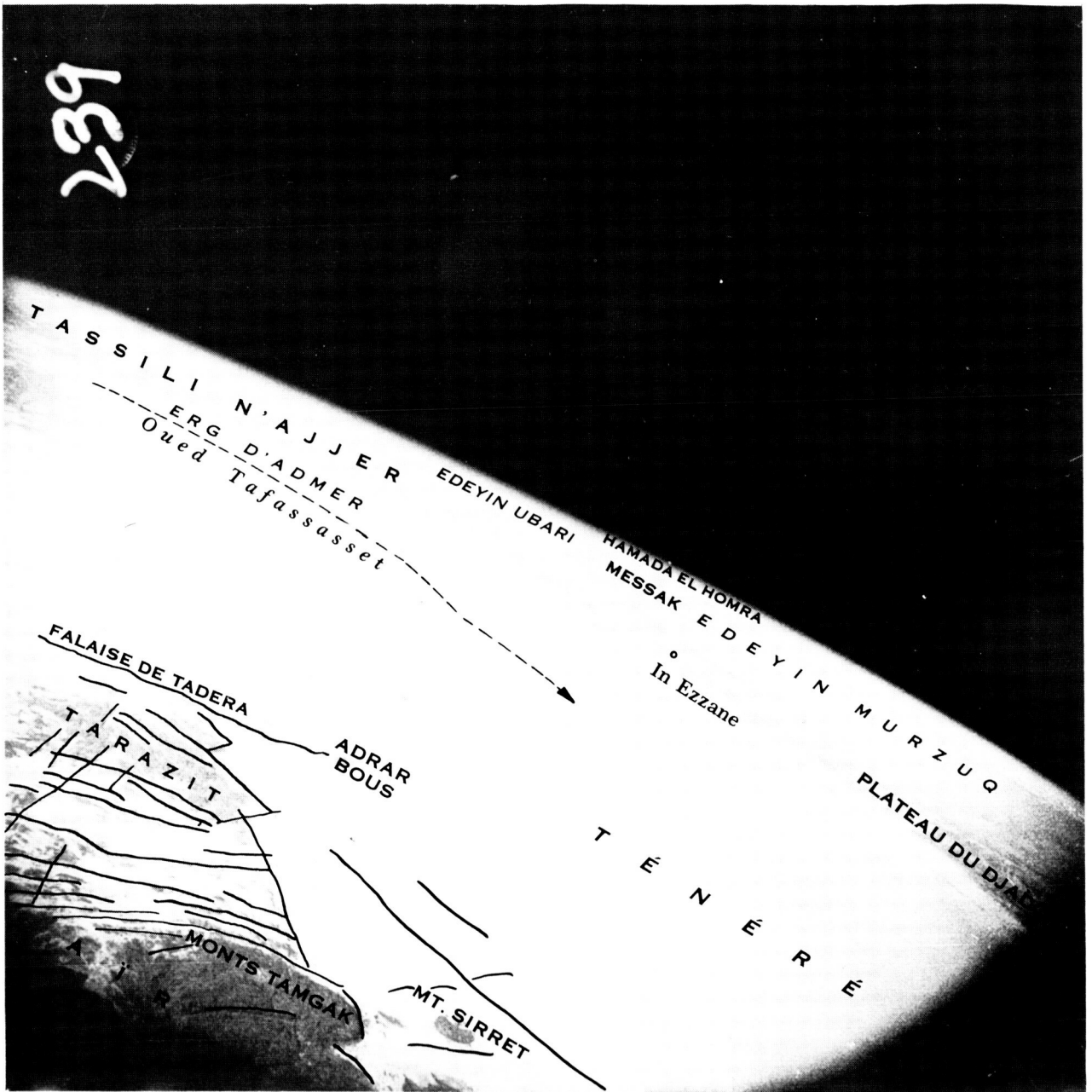


Figure 25 (b) Photo 239 with place name overlay

Photograph 243

This photograph is centered on the relatively low area between the true central massif of the Sahara, the Ahaggar, (just off the photo to the W), and the more eastern massif, the Tibesti, part of which just appears on the right of the photo. This is the Fezzan in the broad sense. The lowness of the area, (under 2300 feet, 700 m.) is due to its structure, but although it is bounded E and W by N-S faults, it is probably more a downwarp than a true rift valley. The general slope of the rock layers towards this area tends to accumulate ground water, so that the area has numerous oases. The main group of oases, the Fezzan in the strict sense, is invisible in the background of the photo, but others appear, for example in 247 (md.) (ref. 22, pp. 172-173; 20, p. 254).

In this downwarp Primary rocks have been preserved and outcrop in the Plateau du Djado (md.). This is very broken country, for the sandstones, schists, and diabases (dolerites) are almost horizontal and have been divided up by wadis into a series of tablelands separated by deep gorges. (ref. 38, p. 350).

At the foot of the escarpment of the Plateau du Djado is a belt of exposed Cambrian rocks and slightly metamorphosed schists, separating the escarpment from the area covered by Quaternary deposits. This may be regarded as a pediment.

In the foreground is Adrar Madet, a large example of an erosion residual in the middle of the Ténéré desert, composed of Cretaceous continental sandstones (ref. 47).

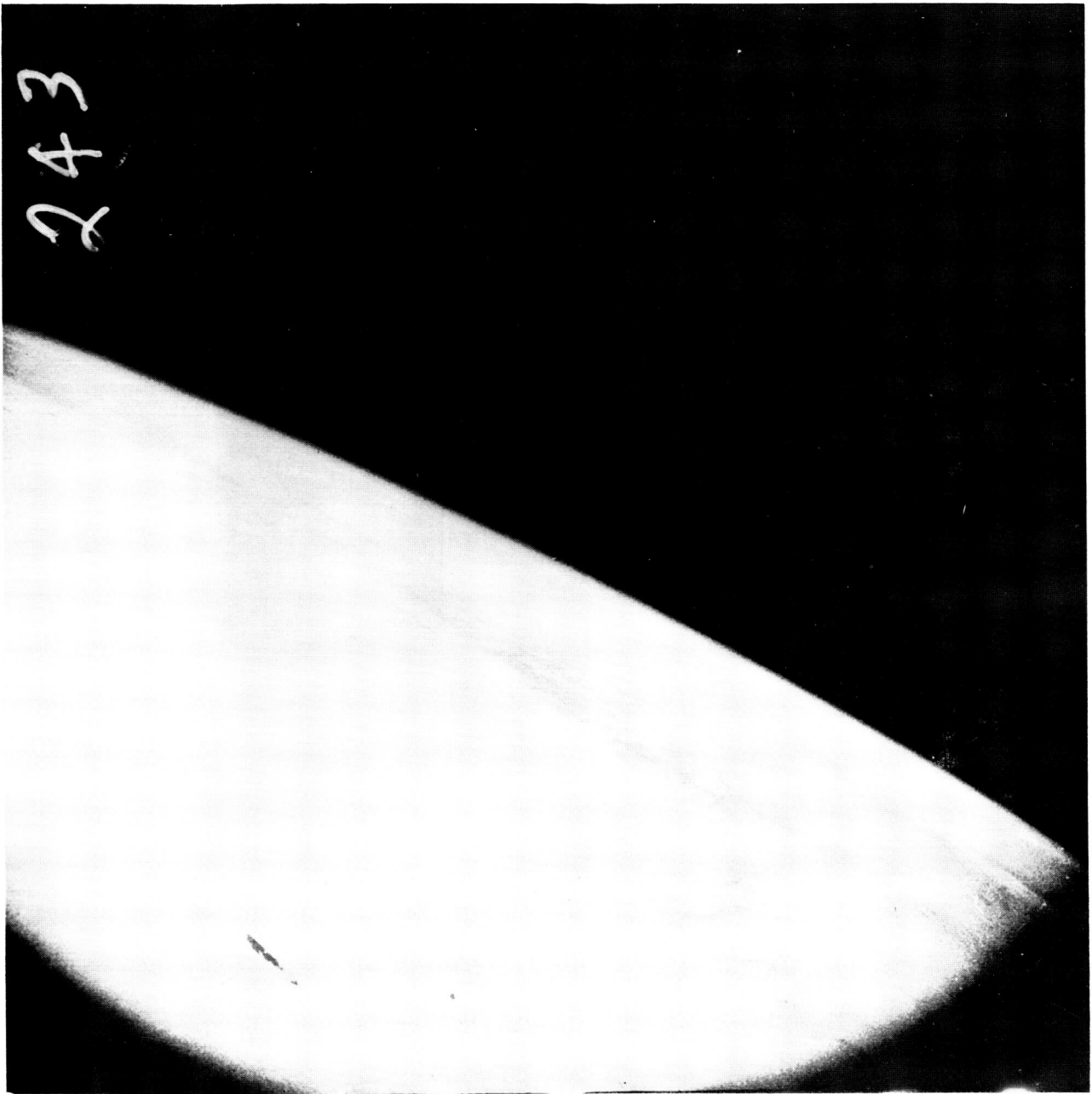


Figure 26 (a) Photo 243

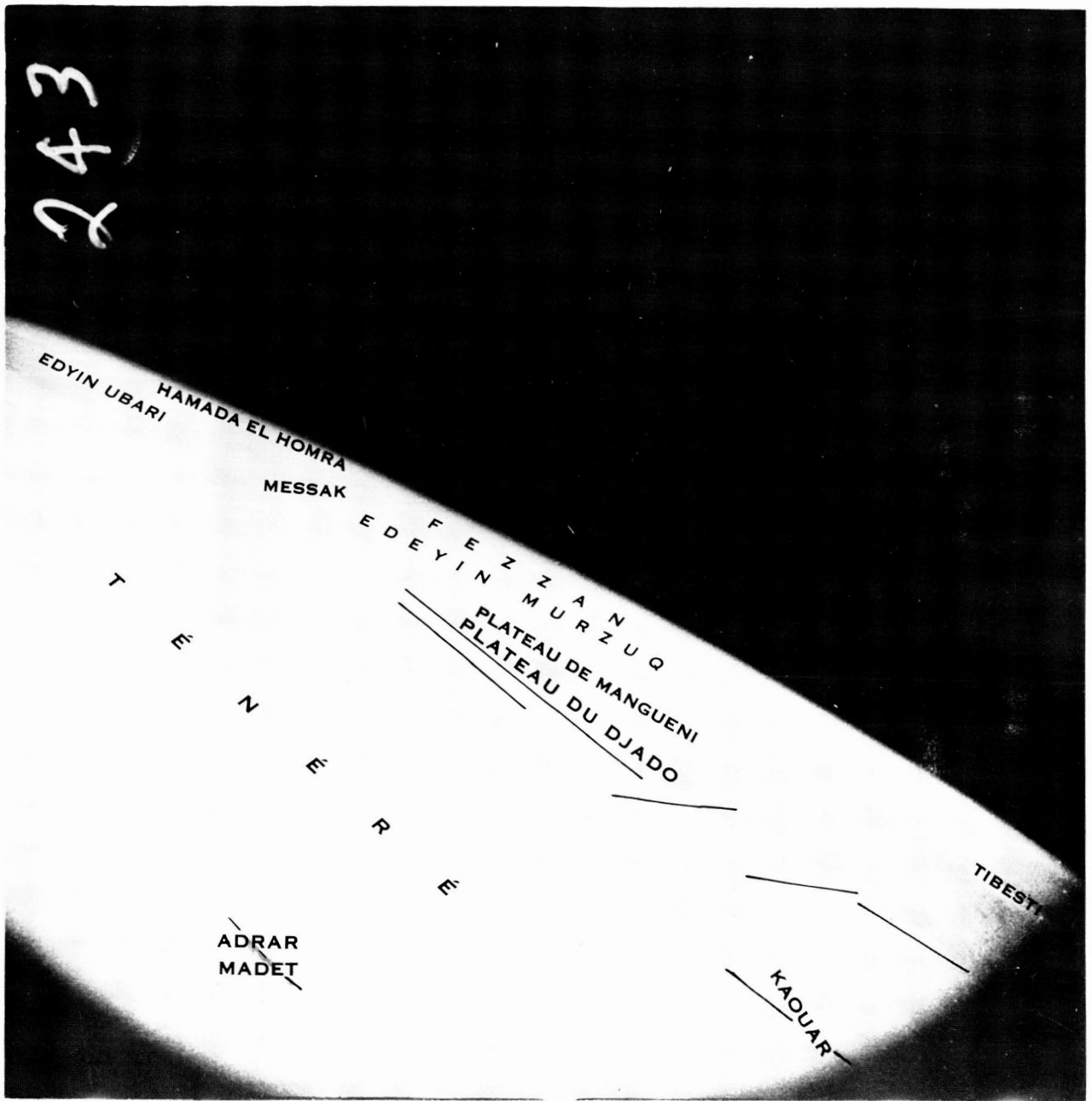


Figure 26 (b) Photo 243 with place name overlay

Photograph 247

This photograph illustrates the way that N-S faults divide the Fezzan into separate basins. The Kaouar (c. md.) and Achegour (l. md.) escarpments, both oriented N-S, mark such fractures. Ground water comes to the surface plentifully along the Kaouar scarp, supplying the oases of Kaouar and Bilma (c. md.) (ref. 20, p. 374; 22, p. 179).

The Erg du Ténéré (fg.) corresponds to the area where the Wadi Tafassasset, descending from the Ahaggar, terminated its flow at one stage in the Quaternary. The erg has been fashioned into dunes mainly from 80 to 500 ft. (25 to 150 m.) in height. The central part of the erg (fg.) is the first area of transverse sand-dunes seen by the spacecraft camera. These are oriented NW to SE, that is at right-angles to the dominant northeasterly winds, and resemble ripples on the surface of water. However, in the areas N and S of this belt longitudinal dunes with an orientation ENE to WSW are found again. Those to the N are visible on this photograph, but since they are exactly parallel to the direction of movement of the film in the camera they appear like scratches on the film. Those to the S can be seen on photo 250 (l. fg.) (ref. 20, pp. 374, 387; 40, p. 44).



Figure 27 (a) Photo 247



Figure 27 (b) Photo 247 with place name overlay



Figure 27 (c) Photo 247 with geological overlay

Photograph 250

The foreground shows the southern part of the Erg du Ténéré and the northern part of the Erg du Manga which continues it southwards. It can be seen that there is here an alternation and even an overlapping of transverse and longitudinal dunes.

This complicated pattern suggests that some influence is at work which is not present in the central Saharan areas of longitudinal dunes like the Erg Chech. No doubt this influence is, directly or indirectly, the Southwest Monsoon, which penetrates to this area for a short time each year, bringing some rain that supports a slightly denser vegetation. Whereas the northern part of this photograph is true desert virtually devoid of vegetation except occasionally for widely scattered solitary plants, the foreground is covered by sub-desert steppe. This area has low perennial plants widely spaced, while annuals including grasses flourish for a few weeks each year after the rains. Stunted trees become increasingly more frequent towards the S. The presence of this vegetation probably helps to keep the dunes fixed in position. (ref. 20, pp. 387-388; 44, pp. 506-515; 21, p. 393; 17, p. 10).

The dark area in the right background is Tibesti, easternmost of the three central Saharan massifs. It is shown better on 257. This is a mountainous area, roughly triangular in shape, with sides 250-300 miles (400-500 km.) long. It rises abruptly to over 11,000 feet (3300m.) from the three surrounding depressions, which are only a few hundred feet in altitude - Borkou, to the SW (r. md.), the Fezzan, to the NW (c. bg.), and the Libyan desert, to the NE (257 r. bg.). It is mainly covered by volcanic rocks that have burst through the crystalline basement rocks and through great thicknesses of overlying horizontal sedimentary layers. An area occupied by the latter can be seen in the centre background, in this case mainly sandstones of Ordovician to Carboniferous age (ref. 22, p. 161).

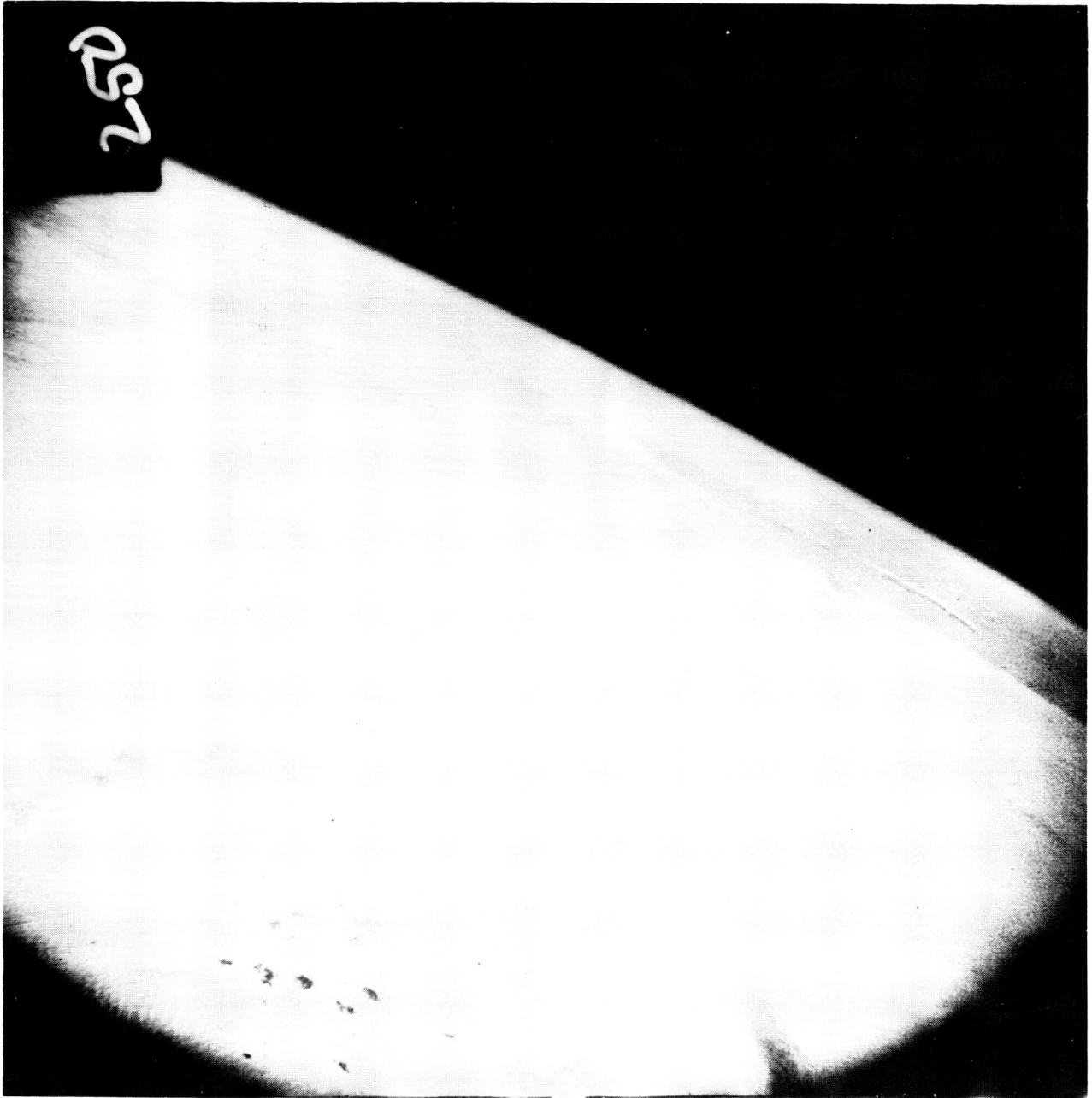


Figure 28 (a) Photo 250

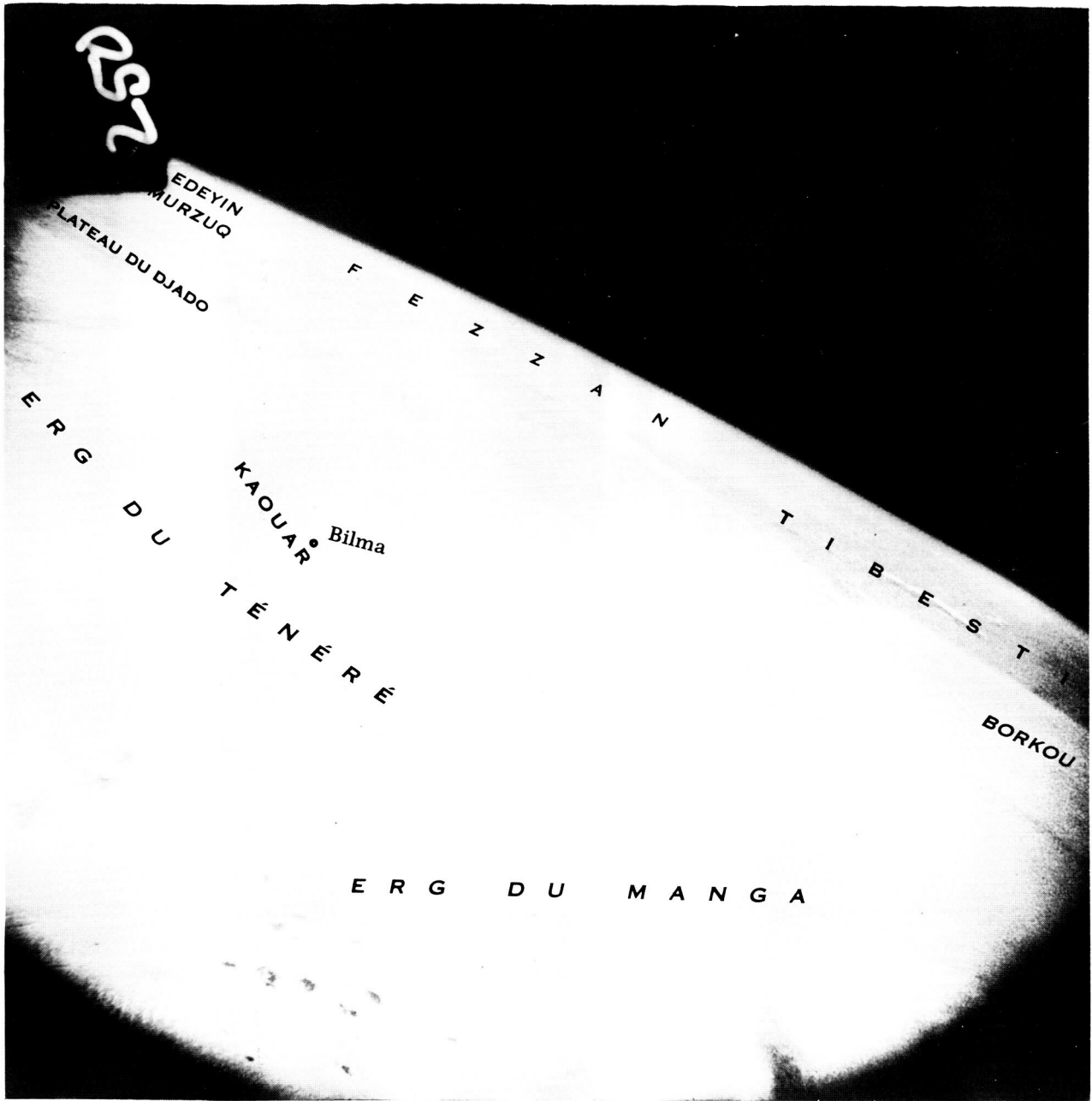


Figure 28 (b) Photo 250 with place name overlay

Photograph 257

When this photograph was taken the spacecraft, which for 2000 miles had been crossing areas where no sign of vegetation could be seen, was rapidly traversing zones of successively denser vegetation, as the belt of heavy tropical rainfall was approached. The distinct darkening in tone between the middle distance and the foreground probably represents the transition from the sub-desert steppe mentioned under 250 to wooded steppe. This type of vegetation includes drought-resistant shrubs and low trees, usually thorny and shedding their leaves in the dry season. In the rainy season, which would have just ended when this photograph was taken, there are also numerous grasses less than 3 ft. (1 m.) high, but not a continuous carpet. Trees may be grouped in clumps, and moreover the area is scattered with semi-permanent pools surrounded by rings of dense forest in the wet season, but occupied only by cracked mud in the dry season. These latter characteristics may account for the somewhat granular pattern of the vegetation in the foreground (ref. 17, p. 10; 39, pp. 102-106).

This pattern is to be distinguished from the grain of the photograph, which is much finer, and also from the linear pattern of fixed dunes. These are the northern part of the Kanem dunes, which are the continuation of the Erg du Manga on the NE side of Lake Chad. This area differs from the Erg du Manga mainly as it has been relatively recently flooded by a larger Lake Chad, so that the hollows between the dunes are quite extensively filled with clayey or clay and sandy deposits. The hollows are referred to as wadis. (ref. 21, p. 393; 20, pp. 387, 388).

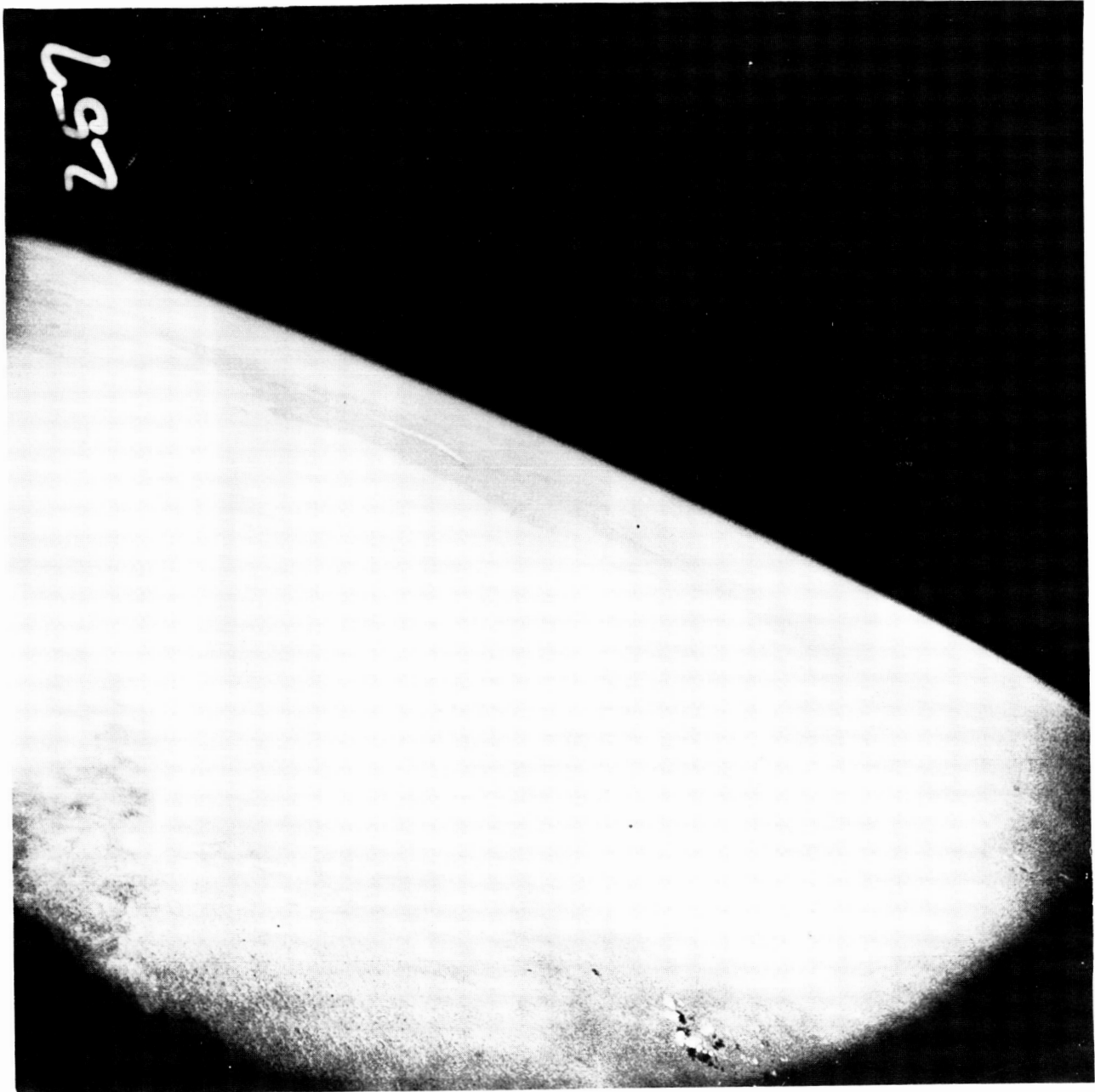


Figure 29 (a) Photo 257

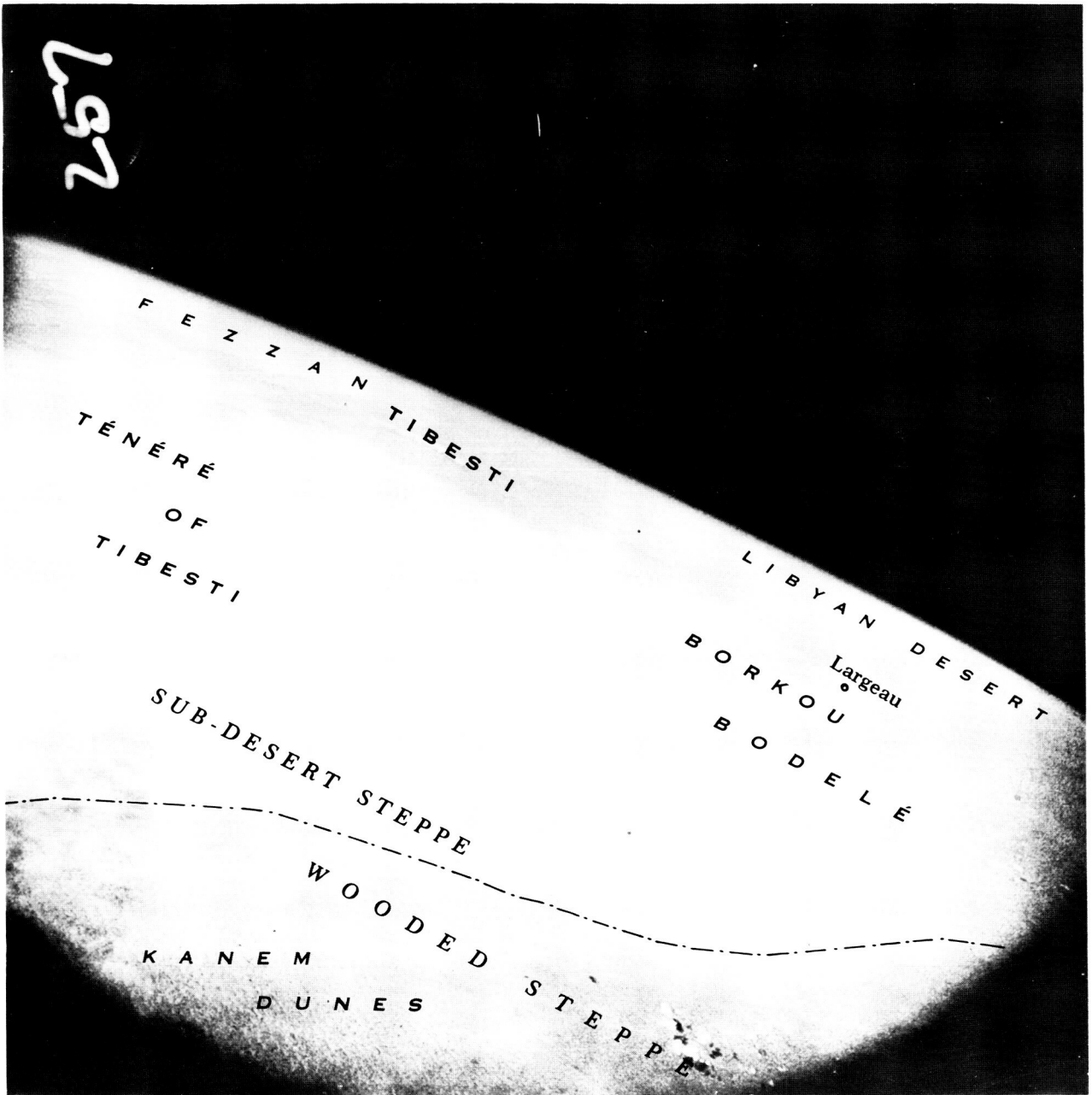


Figure 29 (b) Photo 257 with place name overlay

Photograph 261

Lake Chad itself does not appear on any of the photographs in this series though it must be close to the near edge of this photo. In the left middle distance lies Borkou, the vast basin which extends from Lake Chad to the Tibesti highlands (l.bg.). The basin is floored with alluvium, lacustrine limestones and diatomites; the deposits of an immense lake which during the Quaternary must have extended from the NE of Nigeria as far as the edge of the Tibesti (ref. 48; 43; 45, pp. 465-467).

More recently this lake must have shrunk, and divided into two parts. One occupied the Bodelé and Eguéfi areas (md.), the lowest part of Borkou, sometimes termed the 'Chad Netherlands', and was fed by the overflow of water from the other lake, which was on the site of the present Lake Chad. Traces of the channel which carried this overflow, the Bahr-el-Ghazal or Soro, can be seen in the foreground. It is now reduced to a chain of pools and marshes (ref. 20, p. 375).

Today the level of Lake Chad is about 150 ft. (50 m.) above the bottom of the Chad Netherlands. The fact that the waters of Lake Chad remain fresh suggests that it has still an outflow, and it is probable that ground water seeps from it through the fairly permeable sandy earth into the lowlands of Bodelé and Eguéfi, where it sometimes rises high enough to form swamps or temporary lakes (ref. 22, p. 166).

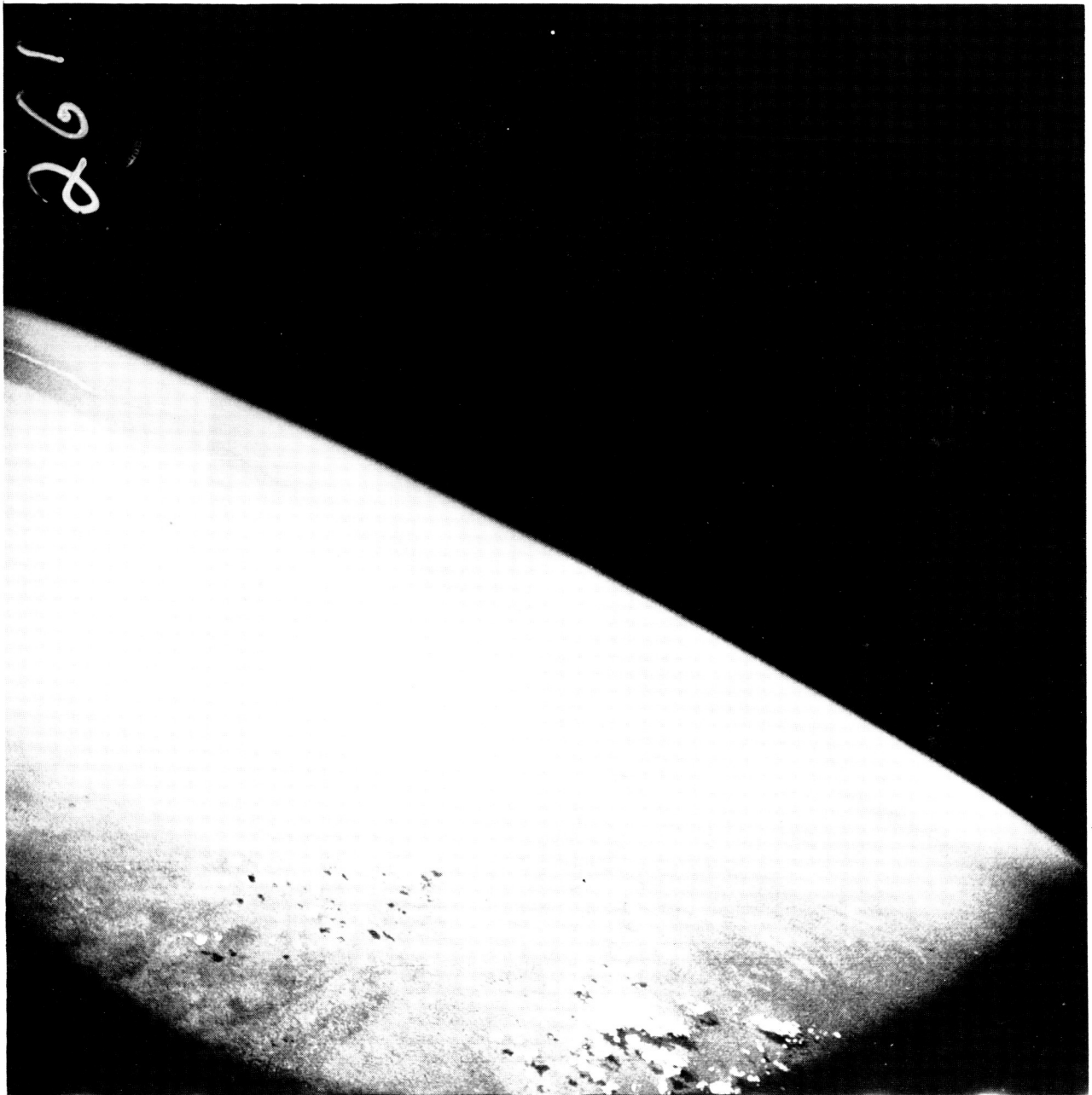


Figure 30 (a) Photo 261

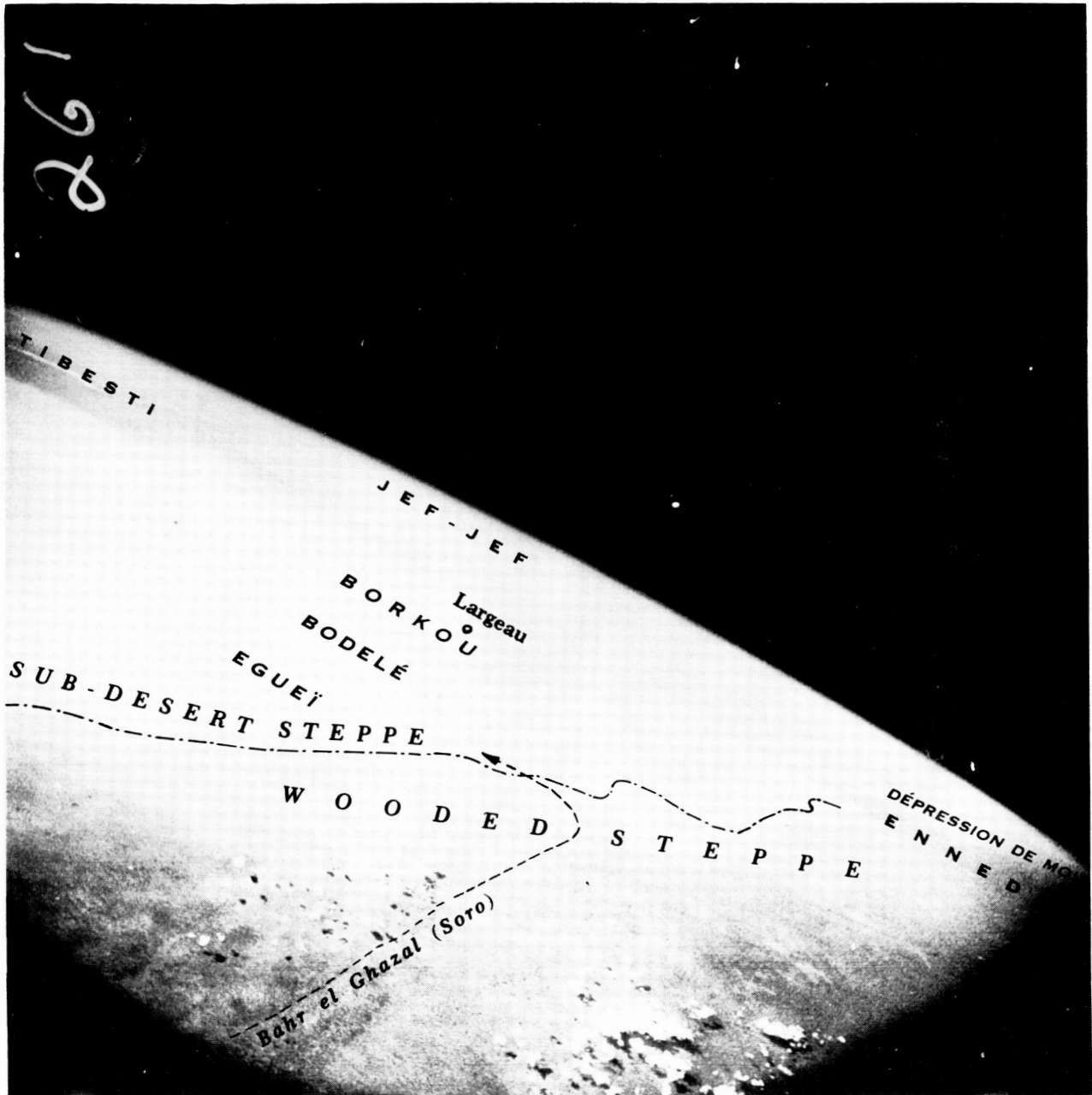


Figure 30 (b) Photo 261 with place name overlay

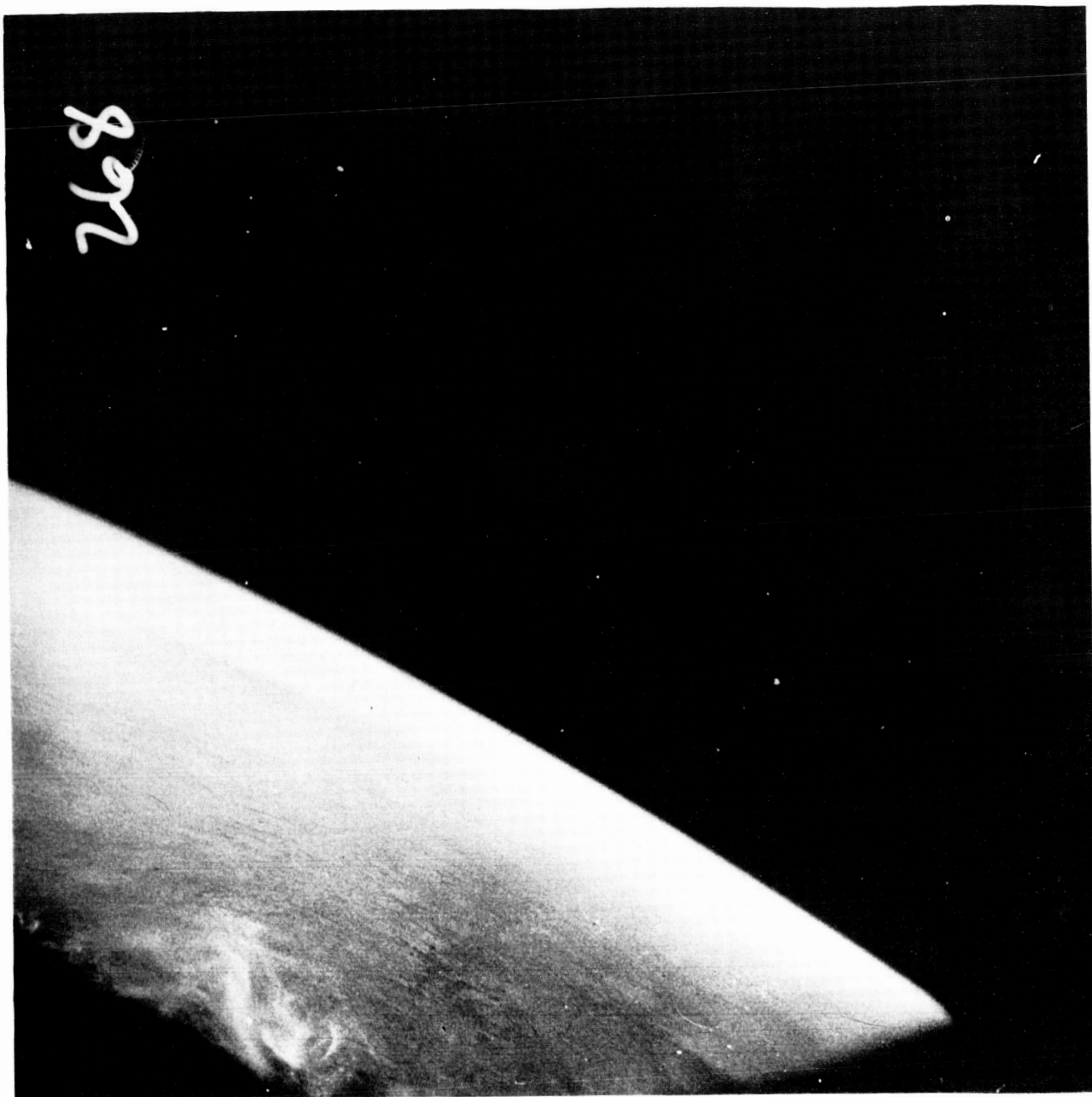


Figure 31 (a) Photo 268

Photograph 268 The most interesting feature on this photograph is the increasing darkness in tone, corresponding to the increasing density of the vegetation. This probably represents a transition from the wooded steppe already described to true savanna. In this zone man has influenced the vegetation sufficiently by burning and cultivation so that man-induced plant communities predominate. This may account for some of the patchwork pattern in the middle distance. Usually there is continuous grassland 3 to 5 feet (1-1.5 m.) high with scattered trees 10 to 50 feet (3-15 m.) high. There is a marked winter dry season, during which the leaves are shed, grasses dry

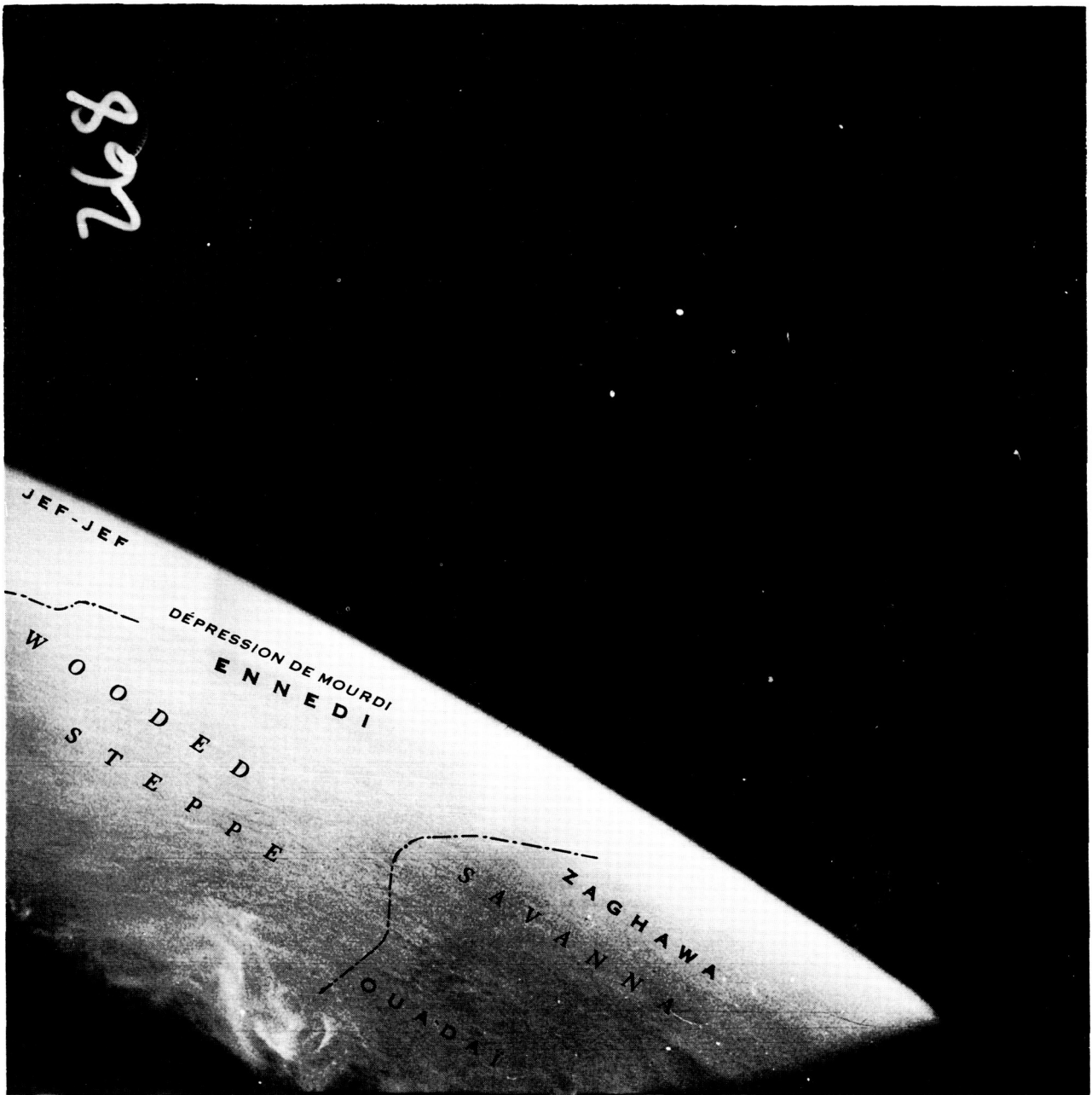


Figure 31 (b) Photo 268 with place name overlay

up, and in which burning occurs (ref. 17, p. 9; 39, p. 100). The wisp of cloud in the foreground is the edge of a more or less continuous cover of cloud which at the time of the Mercury flight extended from here as far as the East African coast. At the same time the spacecraft was crossing areas where darkness was approaching. Although some ground detail can be seen, for example round Lake Rudolph, it was not considered profitable to attempt to study the photographs beyond this point.

COLORS

Manned Spacecraft Center has issued copies of Mercury photos in three color versions: 'true color rendering', 'high color contrast', and 'general interest'. The following statements are based on examination of second generation color diapositives of 'true color rendering' type. When the fifth generation black-and-white enlarged positive prints are compared with the second generation color diapositives, it is clear that the usual reduction in contrast between diapositives and prints has occurred. However, the prints were made on a medium soft paper so that little detail was completely lost. The information which was lost was in areas of fine detail at low contrast in the original. For example, the transverse dune field in 247 appears more extensive in the diapositive.

The color diapositives were almost entirely in shades of blue. This is because of the superimposition over the whole picture of blue light scattered from particles in the atmosphere, making in total a quantity large compared with the amount of light reflected from the ground. However, they are not much bluer than a high altitude aerial photo would be if taken without filters. This is understandable, since an aircraft at 36,000 feet is already above 75% of the mass of the atmosphere.

Almost the only yellowish or greenish hues in the photos occur in a narrow curved strip along the foreground edge of the field of view. Because of the shape and location of this strip it could only be caused by accidental reflection into the camera of tungsten light originating inside the spacecraft. Greenish vegetation would certainly be present at the southeastern end of the flightline when the photos were taken. The absence of greenish hues must therefore be due to the relatively poor ability of yellow, green (or blue) light reflected from the ground to penetrate the atmosphere, so that the color representing such areas on the photos is predominantly that of blue light reflected from the atmospheric particles.

In two areas dark blue bedrock outcrops do have a slightly greenish tinge. The rocks of the Ahr (236) and some of the outcrops in 187 show this. The only slightly greenish tinges appear in the foreground of 236 and 187, photos which point downwards more steeply than the average, so that the mass of air to be penetrated is less.

Usually the only color visible other than blue is red, always very faint. Red light, with its longer wavelength, would penetrate in larger quantities than yellow or green. Areas which appear reddish are mainly areas of Quaternary continental deposits. These are, in order of redness, the dunes of the Erg Iguidi (198), the other northern longitudinal dune areas (206, 230), sand and gravel spreads near the Wadi Dra (185), and southern transverse dune areas (239, 251). The possible connection between color and age in dunes has been referred to under 198. In addition some rock outcrops have a reddish tinge. The best example is in 185, where the red appearance of the Cambrian rocks southeast of Tiznit clearly distinguishes them from the adjacent Precambrian and granitic rocks. These rocks are described as

purplish schists and red formations (ref. 31, p. 33). In the same frame (185) background areas north of the Haut Atlas appear distinctly pink despite the length of the passage of the rays through the atmosphere. The hamada deposits have the most complete lack of red.

In those color diapositives where the red color is present, it is usually easier to separate geological or landform units, since a color difference may be visible in addition to the tone difference present on a black-and-white print. However, only two small cases occurred where a boundary was visible on the color photos which had been overlooked on the black-and-white prints. One was in 198 where the reddish color of the dunes allowed them to be more accurately distinguished from elongated areas of bluish hamada deposits. The other was in 239 and 243 where the pediments round the inselbergs Mt. Sirret and Adrar Madet could be distinguished from surrounding depositional areas by the slightly warmer color of the latter. In addition, because of the generalisations established above, color assists in the identification of the areas separated.

RESOLUTION

Evidence of the resolution of the photographic system is by chance given by the image of a series of longitudinal dunes in the left foreground of photo 246 (not reproduced in this report). The image of these dunes must be close to the limit of resolution because between the second generation color diapositive and the fifth generation enlarged print used, part of the image became indistinguishable but part survived. At the point where the image becomes indistinguishable, it consists of parallel dark lines of density about 1.1, separated by spaces of density about 0.2 i. e. the density scale is about $1.1 - 0.2 = 0.9$ (contrast 8 to 1). Three measurements of the distance apart of the lines in different parts of the image averaged 1.44 lines/mm.

From this we can estimate that the resolution of the original diapositive may be about 7 lines/mm for a density scale of 1.2 (contrast of 16 to 1), taking into account that (1) the print was 7.25 inches square, the diapositive 2.25 inches square; (2) there would be loss of resolution between first and fifth generations, but examination of the second generation suggests this was less than might have been expected; (3) diapositives are capable of a greater range of densities than prints. We can further estimate that the resolution of the system in terms of a standard test object having density scale 3.0 (contrast 1000 to 1), but consisting of lines shorter in relation to their width than those measured, might be about 13 lines/mm. An independent check on the approximate correctness of this figure is given by the size of the stereoscopic effect obtainable, as described in the next section.

Estimates, based on the above figures, of the size of objects just distinguishable on the ground must take into account the foreshortening due to the oblique view the photographs give. In 195, which has the largest foreground scale (1:2,800,000) and smallest nadir angle, it should be just possible to distinguish two lines on the ground which produce a density difference of

1.2 in the diapositive, if they are $\frac{1}{7} \times \frac{1}{2} \times 2.8 = 0.2$ km wide and 0.2 km apart, and if they run in the direction the camera is pointing. If they run perpendicular to the direction the camera is pointing they would have to be $0.2 \times 1.4 = 0.28$ km wide and 0.28 km apart, assuming that rays from the foreground reach the lens with a nadir angle of 43° . For 268, which has the smallest foreground scale, and largest nadir angle, the corresponding figures would be $\frac{1}{7} \times \frac{1}{2} \times 5.0 = 0.36$ km and $0.36 \times 2.2 = 0.79$ km.

All the above estimates of resolution may be in error by a factor of 2 or 3, but not by an order of magnitude.

Direct estimates of the ground resolution in the foreground of the photos described in the section on interpretation give figures of 200 to 800 m., depending on the contrast, shape, and orientation of the features considered, and the nadir angle of the photo. This agrees with what would be expected from a resolution of 10-15 lines/mm. It should be borne in mind that the smallest mappable units are several times the ground resolution, say about 1/2 to 3 km.

STEREOSCOPIC EFFECT

Observed

Limited stereoscopic effects can be obtained when the MA-4 photographs are examined under a hand stereoscope. It is not difficult to fuse the images of two adjacent photos, or of photos two frames apart, to form a stereo-image. In this image clouds clearly appear to float above the ground, but the existence of the third dimension in the image of the ground itself is problematical in most places.

The only area where it is easy to see the third dimension on the ground is in the middle distance of 185 to 188, east of Tiznit. Here, the curving ridge formed by the lower Cambrian rocks, (k_1) rising to about 1000 m. above sea level, or 500 m. above its surroundings, appears like a ridge about 25 m. high on 9 x 9 inch air photos taken from 20,000 ft. (6 km.) with a 6 inch lens. Nearby the Djebel Ouarzemimene and Djebel Tachilla, rising to about 400 m. above sea level or 300 m. above their surroundings, appear like embankments about 5 m. high on the same type of air photos.

The difficulty in seeing a three-dimensional image of the ground in most parts of most photographs is due to the following factors:

- (1) the small scale, i. e. great height, coupled with short focal length
- (2) the graininess of the images being fused, due to the small size of the originals
- (3) relatively small base-height ratio, due to the medium-angle lens used

- (4) oblique nature of the photographs, so that a stereo-image cannot be seen over the whole area of an overlap at one time
- (5) lack of large relief features to facilitate accurate relative placing of a pair of photos
- (6) changes in satellite height of about 0.2 km, changes in nadir angle up to several degrees, and in azimuth up to about a degree between successive exposures, so that successive photos are not exactly in the same plane.

The following may be the reasons that the only undoubted three-dimensional image of the ground occurs in the middle distance rather than the foreground despite the greater distance from the camera. (1) Near Tiznit, the local relief reaches 500 m. In the foreground, it happens always to be less than about 200 m., except in the Air; here the tone and shadows alone give such a strong impression of relief that one cannot be sure whether or not any of the relief effect seen in the stereo-image is due to stereovision. (2) Near Tiznit scattered clouds assist accurate setting of a pair of photographs, whereas the foreground is usually free of clouds. (3) In the foreground, the width of the overlap, in which must be found well-defined points to set the photographs, is at a minimum. In the middle distance, there is a wider overlap between adjacent photos, or alternatively photos two frames apart can be used, yielding twice the base/height ratio.

In theory

For comparison with the above observations, the size of the stereoscopic effect which can be expected from the MA-4 photos can be calculated as follows:

For a vertical photograph we have:

$$\frac{p}{f} = \frac{B}{H-h} ,$$

where p is stereoscopic parallax of a point at height h above a datum level, H is height of camera above the same datum level, f is focal length of lens, and B is air base. From this, it follows that:

$$\frac{\delta h}{\delta p} \approx \frac{dh}{dp} \approx \frac{H^2}{Bf}$$

so long as h is small compared with H. $\frac{\delta h}{\delta p}$ is the ratio which indicates the height difference on the ground which corresponds to a particular difference of parallax observed with the aid of some type of stereoscope. Average values for the spacecraft are H = 170 km, B = 44.5 km for successive frames, and f = 75 mm. With a single photo resolution of about 10 to 15 lines/mm we could probably see differences of parallax of about 0.05 mm, i. e. $\delta p = 0.05$, so the smallest height differences visible would be:

$$\delta h = \delta p \frac{H^2}{Bf} = 0.05 \times \frac{(170 \times 10^6)^2}{44.5 \times 10^6 \times 75} = 4.3 \times 10^5 \text{ mm.} = \underline{\underline{430 \text{ m}}}$$

In the case of an oblique photograph, one would expect an even poorer stereo-effect, but the figure would be of the same order as the observed height differences of about 300 and 500 m.

For comparison, values for a typical air photograph might be $H = 6 \text{ km}$, $B = 3.6 \text{ km}$, $f = 150 \text{ mm.}$, and the smallest δp visible about 0.01 mm. In this case, the smallest height difference discernible would be

$$\delta p \frac{H^2}{Bf} = 0.01 \times \frac{(6 \times 10^6)^2}{3.6 \times 10^6 \times 150} = 666 \text{ mm. or } \underline{\underline{0.66 \text{ m}}}$$

These figures, 430 m. against 0.66 m., are not a fair comparison of the potential ability of space photographs to reveal heights. If we compare vertical air and space photos, having the same resolution, focal length, and film size, the smallest height differences visible are directly proportional to the height of the camera. Therefore, a spacecraft at 170 km would only be $\frac{170}{6} = 28$ times poorer than an aircraft at 6 km. Putting this another way, $\frac{170}{6}$ an aerial camera in a Mercury spacecraft could reveal height differences as small as $0.66 \times 28 = \underline{\underline{18 \text{ m.}}}$

INTERPRETATION

General

The MA-4 photography of the western Sahara has been used for this study because it is the only known strip of recovered satellite photographs showing a large extent of land clear of haze or cloud. The western Sahara is not ideal because it is neither so little known that all information extracted from the satellite photos would be new knowledge, nor is it yet covered by detailed and reliable maps which can be confidently used to test the correctness of satellite photo-interpretation. Nevertheless, several conclusions can be reached from examination of the MA-4 photographs.

In general, the space photographs show the same types of distribution as would air photos of the western Sahara, namely rock-type, structure, land-forms and drainage pattern. These can be interpreted through variation in the same factors: tone, texture, pattern, and shape as seen in plan. But what would be called pattern on air photos becomes texture on the space photos, while texture on air photos disappears into tone on the space photos. Three-dimensional form is not so useful in interpretation because of the small stereoscopic effect obtainable, as mentioned above, but it is to some extent replaced by color.

As would be expected, small point and line features, which would be visible on air photos, disappear on the space photos, including in this case all man-made features. At the same time, long linear features and large areal features, too large to be noticeable on air photos, become very obvious on the space photos. Indeed, if the photos had been taken rather differently, a stereomodel of an area as large as this could have been obtained. Certainly,

subtle tone and color changes can be picked out which would be lost in a mosaic of the hundreds of air photos needed to cover the area. Moreover, they provide a uniform coverage across political boundaries (e. g. in 236, 187). In addition, distributions which are too extensive to appear completely even on one space photograph, for example the vegetation zones on 257, 261, 268, can confidently be interpreted by comparing tones on space photos some distance apart in the strip, since the whole strip is in effect photographed simultaneously under uniform camera conditions, while the illumination varies gradually and regularly due to changes in the altitude of the sun at various parts of the orbit.

In the same way that a detailed survey made from aerial photos is checked by ground work in critical areas, a wider study based on these space photographs would be checked by selective use of aerial photographs or field work.

Photographs such as these call for study by two types of specialist. Because they provide an entirely new, broad perspective, they demand study by people without preconceived ideas about the Sahara, but who are familiar with one or more of the relevant sciences - structural geology, geomorphology, plant geography, etc. In addition, if they are to be fully utilised in tying together numerous local surveys, they should be studied by specialists in the rocks, landforms, vegetation, soils, etc. of the areas photographed.

Geology

Geological patterns are usually obvious on these photos because of the absence of a vegetation or organic soil cover.

Structure is the most readily interpreted aspect of geology. The strike of bedding (192, 236) and schistosity (239), the axes of folds (195), pitching folds (223), and elongated basin structures (187) can often be picked out. However, the direction of dip of the beds involved may not be obvious because the detailed three-dimensional form of the outcrops and the drainage pattern developed on them may not be visible. Consequently, some background information on landforms, rocks, or structures from existing maps or reports may be needed to establish whether structures are anticlines or synclines, domes or basins.

Most interesting of all, it is possible to map structural lineaments which extend for hundreds of kilometers, passing across rocks of all ages from Precambrian to early Quaternary, and therefore probably representing deep-seated fractures in the basement rocks. These are manifest in different places as lines of solution hollows, long, narrow salt flats, elongated volcanic outbursts, drainage lines, changes of rock type, and so forth. Their continuity may be obvious on the space photos, but might not be noticed on the numerous air photos needed to cover the same area (compare ref. 61).

Structural lineaments visible on the photos have been indicated on the place name overlays. Following the definition of Lattman (ref. 62), these

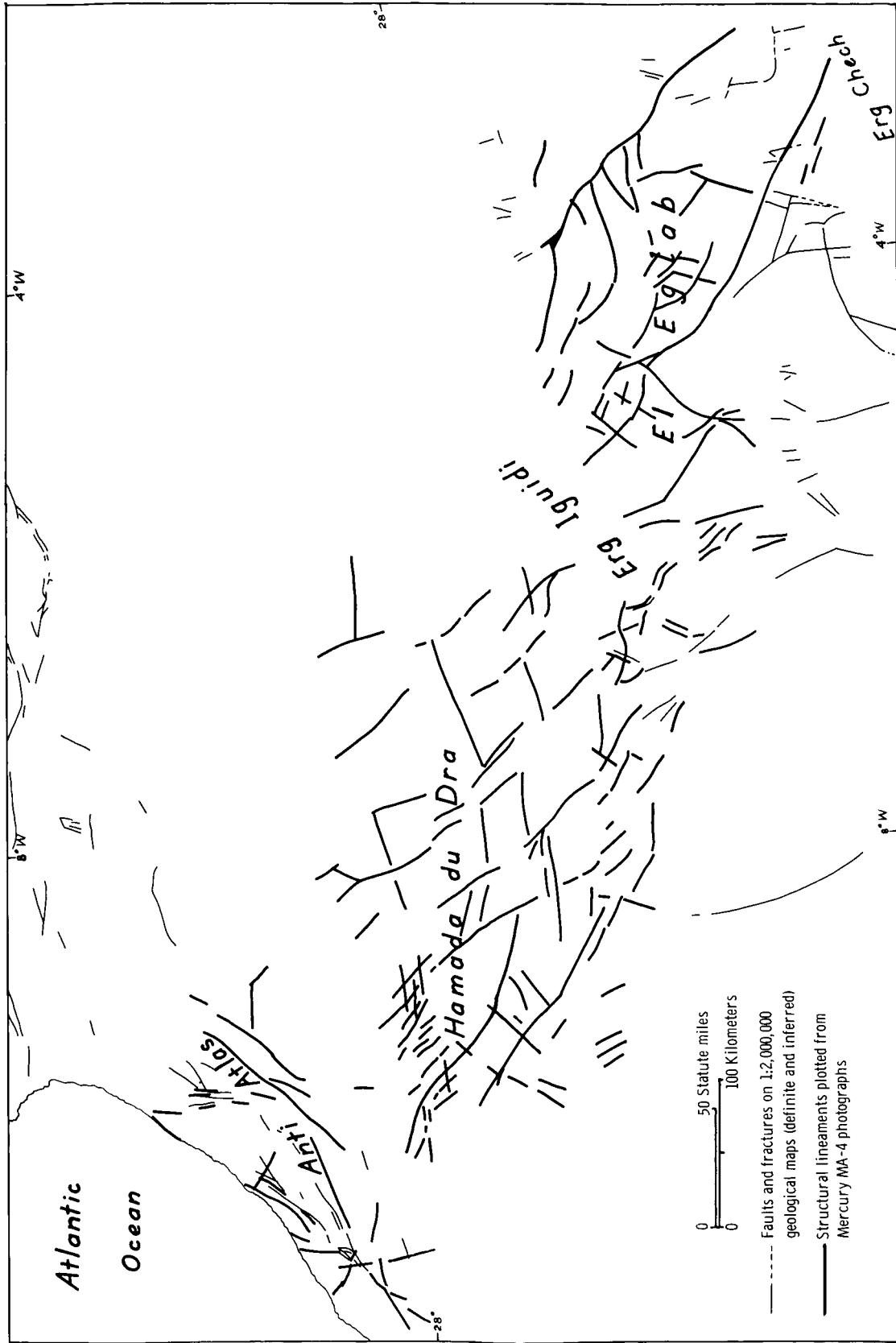


Figure 32. Structural lineaments of the northwestern Sahara.

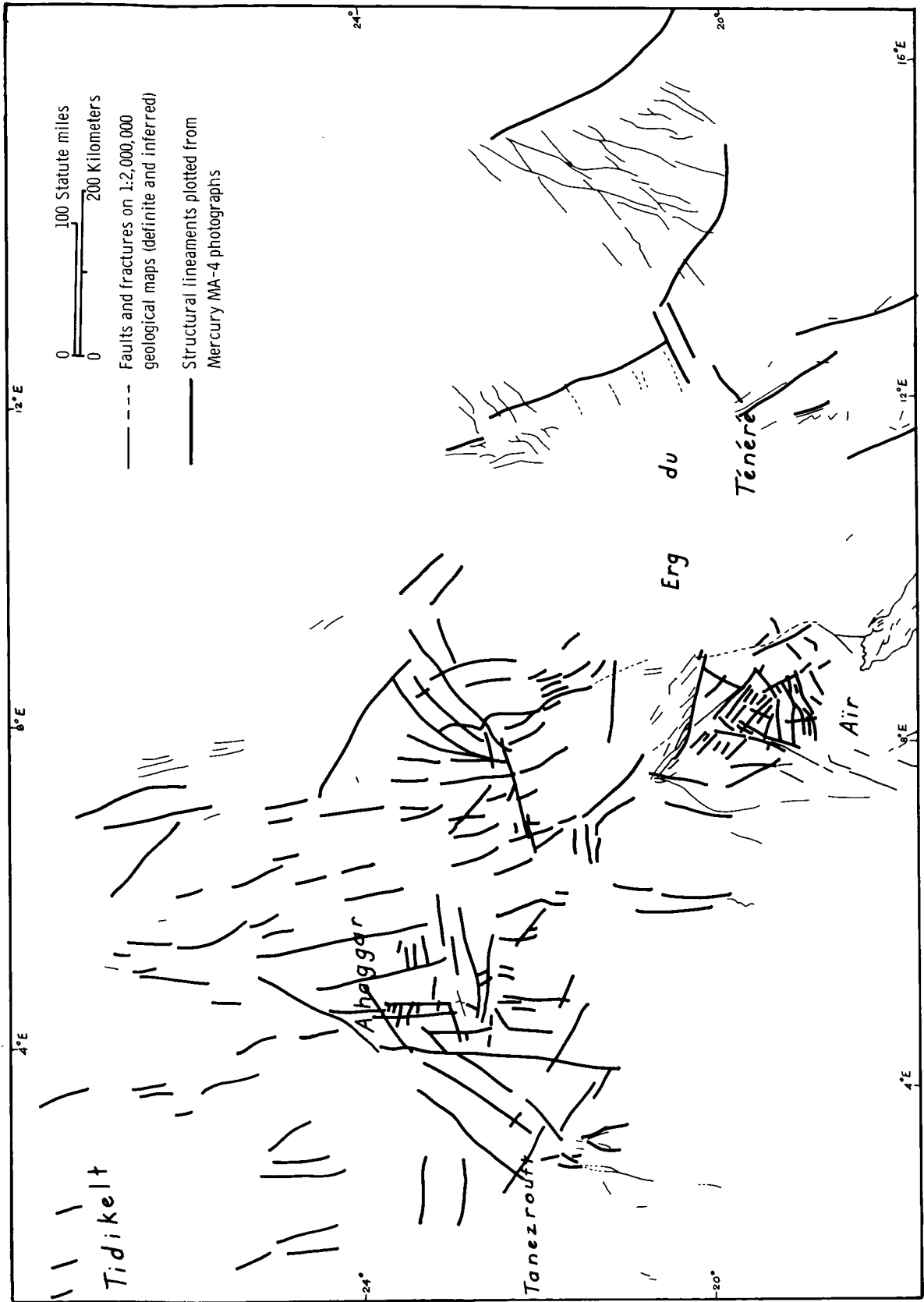


Figure 33. Structural lineaments of the central Sahara.

do not include known bedding contacts, nor of course linear features known to owe their direction entirely to wind-action. In the Ahaggar and Ahr however, many of the lineaments plotted may be the strike of schistosity rather than the fractures and faults which most of the lineaments are believed to represent.

Figures 32 and 33 are maps of structural lineaments mapped from the space photos, with the addition of all faults and fractures marked on the existing 1:2,000,000 geological maps. The most striking feature is the series of northwest-trending lineations extending from the Moroccan coast to beyond the Eglab area, apparently not previously mapped. These run parallel to the northwesterly trend of the Ougarta folded ranges, formed in the early part of the Hercynian orogeny. If produced, this trend would also parallel the 1000 km. long, strikingly linear portion of the Niger River's course. Other trends are visible and are mentioned in the commentaries on individual photos.

Rock-type can be inferred to some extent from tone and texture. The tones representing various rock types are summarised in table 4. On the other hand, some possible clues to rock-type such as gully-density and details of vegetation are not very evident on the space photos. Moreover, the weathering of surfaces of different rock-types into a uniform 'desert varnish' tends to reduce tonal differences. Color occasionally gives information on rock-type which would not be evident in black-and-white. On 198, longitudinal dunes (D), pinkish in color, can be distinguished from elongated strips of blueish hamada formation (T) only by their color. On 239 and 243, pediments surrounding the inselbergs Adrar Madet and Mt. Sirret (granite, etc.) can be distinguished from the surrounding depositional areas (q and D) only by the slightly warmer color of the latter.

Very little can be deduced about the absolute age of the rocks from the photos alone. Relative age is often evident from the structure, while broadly speaking sedimentary rocks appear to increase in darkness of tone with age in this area. In the case of dune sands there is reason to think that the redder dunes were formed in the early Quaternary whereas the paler dunes are younger, and a similar distinction may apply to gravel deposits (ref. 25, pp. 137-138).

The space photographs do not generally suggest that large changes are needed in the existing geological maps of the area, though they do not everywhere agree with them exactly. Differences between maps and photos in the apparent positions of geological boundaries are indicated on the overlays by broken or chain lines, as defined in figure 8.

Small differences do not necessarily mean that the maps are inaccurate, nor that the photo-interpretation is in error. It may be that a change in rock color on the space photos does not correspond to a major stratigraphic boundary, located by the use of fossils, and shown on the map. The map may be generalised for the sake of simplicity. Details shown on the map may be obscured on the photo because of its obliqueness. In areas where bedrock is covered by a thin veneer of drift, the maps may show the bedrock distribution as deduced from small, scattered outcrops examined on the ground, whereas

TABLE 4 - GREY TONES REPRESENTING VARIOUS ROCK TYPES

TYPE OF ROCK	TONE	AS SHOWN ON PHOTOS
Wadi beds: damp, vegetated, or irrigated	Dark	<u>185</u> , <u>223</u>
Wadi beds: dry sand and gravel	Light or white	<u>190</u> , <u>192</u> , <u>223</u> , <u>236</u>
Gravel and sand of depressions in djebel areas	Light or white	<u>187</u> , <u>192</u>
Dune sand	Light	<u>198</u> , <u>202</u>
Gravel of reg areas	Light to medium	<u>210</u> , <u>216</u> , <u>223</u>
Salt-flats (sebkras)	White or light	<u>192</u> , <u>195</u>
Deltas and lagoon deposits (clayey, limey, etc.)	Light	<u>192</u> , <u>216</u> , <u>239</u> , <u>257</u>
Limestones etc. of Plio-Pleistocene hamadas	Light to medium	<u>190</u> , <u>192</u> , <u>195</u> , <u>202</u>
Weathered limestones etc. of the Cretaceous hamadas	Dark	<u>210</u> , <u>216</u>
Primary sandstones etc. of tassilis	Dark to medium	<u>216</u> , <u>223</u> , <u>230</u> , <u>236</u>
Primary sandstones etc. of djebels	Dark to medium	<u>187</u> , <u>192</u>
Precambrian metamorphic rocks	Medium	<u>198</u> , <u>202</u> , <u>223</u> , <u>230</u>
Volcanic rocks, all ages	Dark to black	<u>198</u> , <u>230</u> , <u>239</u> , <u>257</u>

from space the area may appear to be entirely covered by drift.

Nevertheless, the photos have a contribution to make. Photo 236 shows an apparently simple pattern of Primary sedimentary outcrops, striking east-west, abutting against Precambrian basement rocks, and overlain in places by Quaternary deposits. This pattern is not at all apparent on the 1:2,000,000 maps presumably compiled from traverses by several different workers in an area crossed by the political boundary between Algeria and

former French West Africa. Photo 230 shows a striking linear escarpment, certainly a major structural and topographic feature, and maybe a lithological boundary too. None of the geological and topographic maps of the area mark a major continuous feature in this location. A field account of the area shown in 202 describes rhyolite outcrops, surrounded by aureoles of microgranite, in a granite country rock. All three types can be outlined on the photos, though the rhyolites are not separated from the microgranites on the map.

The geological detail which can be interpreted can be gauged by the width of the narrowest geological unit which can be distinguished in the nearer parts of the photograph. Where there is adequate tone contrast, for example in 187, this appears to be about 800 m., when the outcrops run perpendicular to the direction of view, or 400 m. when they run parallel to the direction of view, as judged from measurements on both maps and photos. In 187 in general these smallest visible units appear to be groups of formations approximately equivalent to series, for example the Viséen series. In some places, individual formations can be seen. Whether a particular size of stratigraphic unit is distinguishable in a specific area will of course depend on the true thickness of the unit, its dip, the surface slope, and the tone contrast with adjacent units, as well as other factors.

The figure of 400-800 m. given above is larger than the 'ground resolution' of the photographs. Rather it represents the smallest geological unit which could be mapped from the photographs. In photographs where units as small as this are frequent a map scale of about 1:500,000 would be needed to show all the information in the foreground of the photographs, even though the scale there is only about 1:3,500,000 on the original transparencies, or 1:1,300,000 on the reproductions in this report. On other photographs, where the geologic pattern is less intricate, a map scale of 1:2,000,000 would be fully adequate to record all the geologic data.

Landforms

For most of the statements above about geological interpretation, a parallel statement can be made about landform interpretation.

From the space photographs certain characteristics of the physical features of the Sahara would be obvious even to one who had not previously studied the area. Examples are the alternation of basins and massifs as on 236 and 230, analogous in form with the basin-and-range topography of the American Southwest, but on a vastly greater scale; and the patterns typically formed by sand dunes (198, 206, 257), and wadis (190, 236). On the other hand a visitor from another planet might misinterpret some features. The elongated fragments of hamada formation in 202 could be mistaken for wadi beds, the dark basalt flows of Tibesti in 257 for a lake, the transverse dunes in 247 for water-formed ripple-marks, and the curving longitudinal dunes in 206 for some kind of crevasses.

The clear view of the broad landform patterns in plan allows one rapidly

to form and test theories of genesis. For example, to what extent is the Hamada du Dra in 190 being eaten into by headward erosion by wadis which flow into the Atlantic, and to what extent by deflation or solution not dependent on the nearness of the base level of the Ocean? Could the peculiar pattern in the foreground of 230 be formed by wind action, or is it solely due to rock structure?

The three-dimensional form of surface features is much more difficult to determine from these photographs than is their two-dimensional pattern. This is mainly because of the small stereo-effect obtainable, mentioned above, and often also because of the small areal extent of the individual features making up the broad patterns. Moreover, contrasts in brightness between opposite sides of a ridge due to differences in illumination or to true shadows are at a minimum. This is because (a) the sun was directly behind the camera and (b) the film used is sensitive to blue light which forms the main part of the diffuse skylight which mainly illuminates the sides of ridges away from the sun. For example a sand dune would be recognised as such mainly by its two-dimensional shape, its tone, and the pattern it forms with other dunes. A salt-flat would be recognised by its tone and shape. The existence of cliffs round a hamada (190) would be deduced from the narrowing of rock outcrops along the hamada edge. The slope of an alluvial fan would have to be deduced from the pattern of streambeds on it. Sometimes it would be difficult to be certain whether a series of parallel rock outcrops forms an alternation of scarps and vales or merely a flat plain. Though tone and pattern may allow us to identify volcanic necks and dykes in places, it is difficult to say whether they are expressed in the topography as elevations, depressions, or not at all.

If limited reference is made to maps and field reports, the usefulness of the space photographs in landform interpretation is increased. For example, in 230, geological maps show that the lowland in the foreground is made up of the same type of rocks as much of the Ahaggar massif in the background. The broad view given by the space photo is helpful in deciding between alternative theories to account for the abrupt dividing line: is it a fault-scarp, or is it the product of scarp retreat under desert conditions?

Only one detailed landform map is available covering most of the area shown in these photographs. This is Raisz' map (ref. 53) on a scale of about 1:5,000,000 compiled chiefly from oblique aerial photographs. It agrees closely with the impression given by the space photographs.

Examination of Raisz' map also suggests that all the information about landform patterns contained in the photos could be plotted on a map on a scale of about 1:4,000,000 to 1:5,000,000. If individual dunes, cuervas, etc. were to be plotted, a larger scale, of about 1:1,000,000 to 1:500,000 would be needed.

The smallest landforms visible include dunes, wadis, river beds (261), and pillars of rock isolated from escarpments (223). It is not possible to measure accurately the dimensions of any of these on the available maps, but measurements on the photos suggest that for objects which contrast well with

their surroundings the smallest which could be mapped are 1/2 - 1/4 mile (800-400 m.) in width, depending on their relationship to the direction of view of the photographs.

Vegetation

Since most of the area photographed is desert, it is not surprising that there is no sign of vegetation on the majority of the photos, apart from a slight darkening along some wadis, which may or may not be due to vegetation. South of the desert darker tones clearly indicate vegetation. It is surprising though that there is no sign of vegetation in the northwestern part of the flight-line where a sparse vegetation cover does exist. This may be because in the north, September, when the photos were taken, is the end of the dry season; or because the vegetation does not form a continuous cover; or because it is densest on the mountains which are composed of dark rock or are obscured by clouds.

The vegetation south of the desert shows up in part because it is darker in tone than most desert surfaces. Thus sub-desert steppe (250) is light in tone, wooded steppe (257) medium, and savanna (268) dark. These areas also appear to have distinct textures or patterns. In the sub-desert steppe areas this is the pattern of fixed dunes, with vegetation between, more plentiful in the wooded steppe. In the savannas the pattern is that of alternating woodland and grassland areas, the latter probably due to burning and clearing.

Because of the large area shown on each of these photographs, the whole of the transition from one vegetation zone to the next may appear in one frame. Examination of 250 to 268 suggests that vegetation boundaries in this area do have validity. There does appear to be a more rapid change in tone and pattern between vegetation zones than there is within zones. The apparent boundaries do not seem to correspond to geological boundaries, but they may be in part illusions due to perspective, or temporary boundaries marking the northern limits of rainfall from individual showers immediately preceding the photography. Whether these boundaries could be traced all the way along the desert margin can only be determined when similar photographs of other parts of this zone are available. The permanence of the boundaries could only be established by repeated photography of the same areas. In both these respects comparison with Tiros photography is indicated.

Land use

This series of space photographs is very poorly suited for demonstrating the undoubted possibilities of space photography for small-scale land-use mapping. Man-made features are lacking in most of the regions photographed, while those that do exist are small, such as houses, desert tracks, or tiny cultivated plots at oases, none of which can be distinguished on the photographs. Thus the land-use information they provide is mainly negative.

Some idea of the possibility of land-use mapping from satellite photos is given by photo 268. The patchwork pattern of woodland and grassland is probably at least partly man-induced. If the photo had been taken vertically, and the areas had been say, cultivated land and forest, it would have been a simple matter to outline them and have ready-made a land-use map on a scale of about 1:1,000,000.

PROPERTIES DESIRABLE IN GEOGRAPHIC SPACE PHOTOGRAPHY

Although the specifications for a space photographic system involve numerous interdependent variables such as focal length, negative size, and satellite altitude, the properties being aimed for in the resulting photography may be reduced to the following seven, which may be independently specified.

Area covered by a single frame

In discussing the minimum area to be covered by a single frame, the applications of space photography may be divided into the two following categories.

(1) For photography of unchanging features from space to be worthwhile, the area covered by a single frame must be larger than could be covered by a single air photo of the same tilt. A typical vertical air photo might be taken from 6 km. with a 90° lens, and cover about 4^2 km^2 . The extreme limit for aerial photography may be a height of 30 km. and a 120° lens, which would produce a vertical photograph covering about 75^2 km^2 . Let us say then that the minimum area a space photograph should cover is 50^2 km^2 per frame if intended for the study of unchanging distributions. It is implied that a single space photo has an advantage over a mosaic of air photos.

(2) Space photography of features which change may be justified by the frequent repetition of coverage it can yield, so that there need not be any lower limit to the area covered by a single photograph. In fact the frequency of coverage and the ground resolution may be more critical controls on the design of the system.

The maximum useful area covered by a space photograph is limited only by the extent of the largest pattern it is desired to pick out. Judging mainly from examination of MA-4 photos, the range of useful areas may be as given in table 5. In each case the optimum area is about a quarter the linear dimensions of the maximum area.

Tiros photos, when pointing down vertically, cover an area about 700^2 km^2 (medium angle lens) or 1000^2 km^2 (wide angle lens), and areas planned to be covered by Nimbus pictures are about the same. Therefore it appears that the range which could most usefully be covered by Mercury-type photos is 50^2 to 700^2 km^2 for vertical photos.

TABLE 5

DISTRIBUTION TO BE MAPPED	SIZE OF AREA USEFULLY INCLUDED IN ONE FRAME (KM ²)
(1) Relatively permanent distributions	
Geology	50 ² - 2000 ²
Landforms	50 ² - 1000 ²
Vegetation belts and soil zones	100 ² - 2000 ²
Land use	50 ² - 500 ²
(2) Ephemeral distributions	
Extent of rain from individual storms	200 ² - 500 ²
Effects of rain from individual storms	less than 500 ²
State of vegetation for grazing	less than 300 ²
Extent of savannas burned each year	less than 200 ²

Ground resolution (including scale)

Study of the MA-4 photography suggests that the smallest mappable units are 2 to 4 times the ground resolution, and that these units when mapped have to appear about 2 to 4 times the size they appeared on the original photo.

Ground resolution should be maximised for all purposes, but the minimum acceptable ground resolution for mapping varies greatly with the purpose. Judging from MA-4:

- Lithology: 1/4 - 1/2 width of the narrowest unit to be separately mapped.
- Structure, folds etc., individual: about $\frac{1}{16}$ - $\frac{1}{8}$ the dimension of the structure being mapped.

- Structure pattern: about $1/2 - 1$ times the 'wavelength' of the pattern.
- Structure, fractures etc.: no specific resolution criteria. Optimum conditions are when entire feature is just in one frame.
- Landforms; individual, areal e.g. stacks, inselbergs: $1/8$ size of objects to be mapped.
- Landforms; individual, long e.g. wadis, scarps, dunes: $1/4 - 1/2$ width of objects.
- Landforms, patterns e.g. dune fields, wadi patterns: $1/2 - 1$ times 'wavelength' of pattern.
- Vegetation boundaries: $1/8 - 1$ times distance across boundary, depending on amount of tone contrast.

Nadir angle

Vertical photos are preferable on most counts. They facilitate comparison with maps, and plotting of distributions from landmarks on maps. Stereoimage, if any, can be obtained over the whole photo at once. Curvature of the earth's surface would not raise serious problems with simple methods of interpretation and plotting until areas of 1000^2 km^2 are approached.

Obliques may be preferable if altitude or orbital inclination is limited, so as to cover a larger area. But because of non-uniform scale, some of the information in an oblique will be wasted. Obliques are easier to understand at first glance and therefore may be preferable for 'general interest' photos.

High obliques are preferable to low obliques in simple plotting methods, because the position of the principal line can be easily found.

Overlap and convergence

For stereo-vision in vertical photos 60% overlap is needed. In obliques, if stereo-vision is not wanted, it is enough to ensure continuous cover, by aiming for a 10% overlap at the greatest distance at which it is intended to use the photos.

Number of wavebands used

Other things being equal, the more wavebands used, the more information obtained.

Date and frequency

For particular applications, the date or the frequency of photography may be critical in the design of a satellite photographic system.

Regions photographed

The system must obviously be capable of photographing those regions of the earth which are of interest for a particular application.

POSSIBLE MODIFICATIONS OF THE MA-4 PHOTOGRAPHIC SYSTEM

This section considers only what would be the effects on the results produced by the MA-4 photographic system, if small changes were made in each of the many photographic variables, one at a time. It is not a discussion of the optimisation of satellite photographic systems in general. The desirability of each possible modification will be judged only by the seven criteria outlined in the previous section; the many aims of Project Mercury other than photography of the earth's surface will be ignored.

Orbital elements

A greater inclination of the orbit to the Equator is desirable because it would allow photography of higher latitudes and more complete coverage of the earth's surface. At present it is desirable to photograph as many and varied areas as possible.

Moderate increases in the mean altitude of the satellite would probably bring more advantages than disadvantages. The area covered by a single frame would be increased, which would be an advantage if vertical photos were being taken. The deterioration of ground resolution due to decreased scale would be partly offset by the smaller orbital speed. A higher orbit would have a longer life or, alternatively, less critical launch requirements. On the other hand, large increases in altitude would bring the film increasingly within the radiation belts.

A small orbital eccentricity is desirable. All frames in a sequence will then have roughly the same ground resolution, areal coverage, and overlap, and other design problems are simplified.

The initial location of perigee and apogee on the orbit is not important as long as the eccentricity is small.

Desirable values of the remaining orbital elements, right ascension of the ascending node and ascending node time, are implied below under 'Timing'.

Orientation of principal axis

Nadir angle of principal axis. It has been indicated on p. 115 that vertical photos are preferable for most purposes. The exactness of vertical orientation needed depends on how the photos are to be used. For plotting of distributions against an adequate background of landmarks, nadir angles as high as 10° might be accepted. For low obliques, from altitudes similar to MA-4, a rule-of-thumb might be that the most distant areas included in the picture should have a nadir angle of about 60° . Judging from the MA-4 photos it would not be possible to plot much detail in areas more distant than this. On high obliques the nadir angle should be no larger than is needed to ensure that the apparent horizon is included in most frames. The depression of the apparent horizon, which was about 13° on MA-4, should be allowed for.

Azimuth of principal axis, if the photograph is not vertical, should ideally be perpendicular to the azimuth of the orbit, as in MA-4. This gives the best combination of area covered and ground resolution, for a given altitude and nadir angle.

Spin angle. It is convenient if one pair of edges of the resulting negatives represents a direction parallel to the orbit. In the case of high obliques there is an argument in favor of arranging the camera so that the horizon just appears in the top corner, as in MA-4, but this results in discontinuous coverage in the foreground.

Camera mounting

For photography from a spacecraft in orbit, cameras do not need to be mounted to overcome vehicle vibration during each exposure. Rather the aim should be to reduce the number of surfaces the light encounters, since each reflection or refraction reduces the amount of light and increases distortion.

Therefore the mirror in the optical train is undesirable. Baumann and Winkler (ref. 4) attribute the improved definition in Viking 12 over Viking 11 pictures in part to the removal of a 45° prism used as a mirror in the optical system. The camera should be mounted so that the optical axis is normal to the window whenever possible.

The windows used in the Mercury capsules were of a high standard of flatness, and had good wavelength transmissivity for photography, with maximum transmissivity between 0.5 and 0.9 microns. But they consisted of four elements, one set at an angle of 6° to the others. To reduce reflections and distortions, windows should be made of the minimum number of elements, set parallel to each other. Consideration should also be given to dispensing with the window entirely. The best rocket photographs have been obtained with the camera pressurised but the capsule not. To decide whether, in a particular case, a similar method could be used in a satellite, a study would be needed

of the temperature and humidity conditions which would be experienced both inside the camera and at the outer surface of the lens after exposure to the space environment for the intended duration of the flight.

Cabin lighting. Precautions should be taken to see that no cabin lighting enters the lens.

Camera

Frame size, angle of view and focal length are closely inter-related.

Increases of frame size over the "70 mm", (57 x 57 mm.) format used for MA-4 would be desirable if the volume and weight available for camera and film were increased. Such increases could be used either (1) to give a wider angle of view and hence larger coverage, if used with a lens of the same focal length but larger field angle, or (2) to give larger scale and hence better ground resolution, if used with a lens of the same field angle but longer focal length. The former might be more desirable for vertical pictures, the latter for obliques, if the pictures are for general geographical purposes. If the increased volume and weight was not used as above, it could be used to carry a greater length of film of the same size, allowing a longer period of photography.

If the volume and weight of the camera and film had to remain the same, then either ground resolution or area covered could be improved at the expense of the other, by reciprocal changes in the focal length and field angle of the lens. Apart from this, increased coverage could be obtained from the MA-4 system merely by using a wider-angle lens, since the whole 57 x 57 mm. frame is not within the field of the lens used.

The exposure time, relative aperture, and film speed are closely inter-related.

During the exposure time used, 1/500 second, image motion in the MA-4 photos was not greater than about 0.004 mm., assuming an orbital speed of 7.42 km/sec., a foreground scale number of 3.5×10^6 , and no vehicle vibration. If the resolution achieved is only in fact about 0.1 mm., exposure time is evidently not a limiting factor on resolution, and the exposure time could probably be increased without prejudicing the system's resolution. This would allow use of a film with lower film speed, which could have better definition characteristics and hence might improve system resolution.

The exposure given to the MA-4 film, as determined by a relative aperture of f/8 and an exposure time of 1/500 sec., was probably ideal for highly reflective surfaces such as clouds and cloud-free desert areas. An exposure about one stop larger would have given better rendering of thickly vegetated areas such as those in 268. Probably more detail would have been visible in 270 to 333 if a still larger exposure could have been given, since here most of the ground, though not covered by cloud, lay in the long shadows cast by tall cumulus clouds in the setting sun. Though prints from the latter

- ✓ type of negative could be improved by electronic dodging, it would be advantageous to be able to vary the exposure during the flight. It would be difficult to do this adequately unless the spacecraft were manned, since there is not a direct relationship between light-meter readings and optimum apertures. The pilot would have to be thoroughly briefed on the problems of exposure if the results were to be an improvement on using a constant aperture.

Film and filter

The characteristics of the film-filter combination chosen will affect especially the ground resolution of the system.

Film speed and definition characteristics (resolving power, granularity, sharpness etc.) have already been mentioned.

The wavelength sensitivity of the film, together with the wavelength transmissivity of the filter(s) will determine the light wavelengths used to transmit information from ground to film and hence the amount of contrast between features it is desired to distinguish. In the case of MA-4 the wavelength range was approximately that of visible light. Two factors enter into the choice of wavelengths: (1) maximising differences in reflectivity between ground features; and (2) minimising atmospheric scattering which would tend to reduce these differences. The second factor suggests that the longest possible photographic wavelength, i. e. the near infra-red ($0.76 - 1.0\mu$), should always be used, but the first factor would often suggest that infra-red should not be used, since infra-red light is reflected strongly by many surfaces, including green vegetation, most desert surfaces, and clouds. The ideal for a given purpose will usually be some combination of wavelengths in the range 0.55 to 1.0μ . (refs. 1, p. 20; 9, p. 223; 11). A combination with appreciable sensitivity to blue light ($0.4 - 0.5\mu$), as in MA-4, cannot usually be justified in space photography of ground features.

Using color film is equivalent to using three wavebands instead of one. It is capable of carrying up to three times as much information in favorable conditions. All three light-sensitive emulsions receive the same exposure. In the case of MA-4 the light entering the lens was relatively strong in blue, and weak in green and red, compared with the light for which the film was designed. In effect the green-and-red -sensitive emulsions were grossly underexposed while the blue-sensitive was correctly or overexposed, giving most emphasis in the result to blue light scattered from the atmosphere. Consequently the information recorded by the color film may even have been less than would have been recorded by a properly-exposed single waveband (i. e. black-and-white) film.

This does not mean that color films could not give acceptable results in space photography. A color film designed for aerial photography, for example Kodak Ektachrome Aero, with blue light heavily filtered, might be worth trying. It is more likely to give acceptable colors in verticals than in

obliques. Better still would be a color film sensitive to infrared, red, and green light, but not to blue, for example Kodak Ektachrome Infrared Aero. This produces color diapositives in false colors. Either film should carry more information than a black-and-white film of the same wavelength sensitivity, filmspeed, and definition.

Development procedures for a color film such as was used in MA-4 do not allow much scope for variation, though changes in the color balance of subsequent copies can be made by the use of filters. If a black-and-white film were used, the graininess and gamma (gradient of the exposure/density curve) could be modified appreciably by changes in the method of development.

Keeping properties and general robustness of the emulsions and base were not critical in photography from Mercury capsules since the interiors of these are not subjected to extremes of temperature, humidity, acceleration, nor vibration, nor to immersion in sea-water. In photography from unmanned capsules, where the environmental conditions may be extreme during flight or while awaiting recovery, the delicacy of color and infrared emulsions may be an argument in favor of ordinary black-and-white film (ref. 1, pp. 19-20).

Timing of photography

Launch time. Photographs of a particular area in daylight can be taken from a spacecraft in orbit only on certain orbital passes. For example, a Mercury capsule launched at the same local time as MA-4 would have to continue in orbit for at least 24 passes to photograph all possible areas. Roughly speaking, it could photograph Northwest and Central Africa on passes 1 and 2, North America on 1 to 4, South America on 5 to 9, Australia on 12 to 18, Asia on 20 to 24, South Africa on 21-23, and Northeast Africa not until 24-28. On a Mercury-type flight of limited duration it is therefore desirable to vary the launch time so that different areas are favored on different flights.

The exposure interval of 6 seconds used for MA-4 produced an unnecessarily large overlap even in the middle-distance. A longer interval would allow a larger area to be photographed with the same amount of film. This would not apply to vertical photography. For this a 60% overlap should be the aim, making the exposure interval quite critical.

Programming. For geographic photography it would be desirable to conserve film by photographing only over cloud-free land areas in daylight. The cloud-free condition would require either the capability to command the camera in flight, or a pilot, either of which might use more weight and space than they would save. But the camera could be made to photograph only over land areas in daylight by quite a compact and simple preset timing device.

July, 1964. McGill University, Montreal, Quebec.

REFERENCES

(a) Space photography (In order of publication)

1. Holliday, C. T.: Preliminary Report on High Altitude Photography. Photographic Eng., vol. 1, no. 1, Jan. 1950, pp. 16-26.
2. Holliday, C. T.: The Earth as Seen from Outside the Atmosphere. In The Solar System, vol. 2, The Earth as a Planet. Ed. by Kuiper, (Chicago), 1954, pp. 713-725.
3. Baumann, R. C. and Winkler, L.: Photography from the Viking 11 Rocket at Altitudes Ranging up to 158 Miles. Rocket Research report no. XVIII. U.S. Naval Research Lab. report 4489, Feb. 1955.
4. Baumann, R. C. and Winkler, L.: Photography from the Viking 12 Rocket at Altitudes Ranging up to 143.5 Miles. Rocket Research report no. XXI. U.S. Naval Research Lab. report 5273, April 1959.
5. Hubert, L. F., Fritz, S., and Wexler, H.: Pictures of the Earth from High Altitudes and their Meteorological Significance. In Space Research. Proc. 1st International Space Science Symposium (Nice) 1960. Ed. by H. Kallmann Bijl (Amsterdam), 1960, pp. 3-7.
6. Fujita, T.: A Technique for Precise Analysis for Satellite Data; vol. 1, Photogrammetry. Meteorological Satellite Lab. report no. 14. U.S. Weather Bureau, Jan. 1963.
7. Kiss, E.: Bibliography on Meteorological Satellites, 1952-1962. U.S. Weather Bureau, 1963. Also Supplementary Bibliography on the Use of Satellites in Meteorology. Met. & Geostrophysical Abstracts vol. 14, 1963, pp. 870-936.
8. Tepper, M., Singer, S. F., and Newbauer, J., Eds.: Weather Satellite Systems. Astronautics and Aerospace Eng., vol. 1, no. 3, April 1963, pp. 22-96.
9. Fisher, L. R., Armstrong, W. O., and Warren, C. S.: Special Inflight Experiments. In Mercury Project Summary including Results of the Fourth Manned Orbital Flight. NASA SP 45, Oct. 1963, pp. 213-229.
10. O'Keefe, J. A., Dunkelmann, L., Soules, S. D., and Lowman, P. D. Jr.: Observations of Space Phenomena. In Mercury Project Summary including Results of the Fourth Manned Orbital Flight. NASA SP 45, Oct. 1963, pp. 327-347.

11. Soules, S. D.: Spectral Reflectance Photography of the Earth from Mercury Spacecraft MA-8. Meteorological Satellite Lab. report no. 22. U.S. Weather Bureau, Nov. 1963.
12. Merifield, P.M.: Geologic Information from Hyper-altitude Photography. Ph.D. Thesis, Univ. of Colorado, 1963.
13. Grimwood, J.M.: Project Mercury, a Chronology. NASA SP 4001, 1963.
14. Bird, J.B. and Morrison, A.: Space Photography and its Geographical Applications. Geog. Rev. Oct. 1964.
15. Lowman, P.D. Jr.: Photography of the Earth from Sounding Rockets and Satellites: a Review. Photogrammetric Eng. (in press).
16. Bird, J.B., Morrison, A., and Chown, M.C.: World Atlas of Photography from Tiros Satellites I to IV. NASA CR-98, 1964.

(b) Literature on the whole flightline
(in order of reference)

17. Keay, R.W.J.: Vegetation map of Africa south of the Tropic of Cancer, Explanatory notes accompanying map. Oxford Univ. Press, 1959, pp. 5-11.
18. Shantz, H.L., and Marbut, C.F.: The Vegetation and Soils of Africa. National Research Council and the American Geographical Society (New York) 1923.
19. Menchikoff, N.: Les Grandes Lignes de la Géologie Saharienne. Rev. Géog. Phys. et de Géol. Dyn., Série 2, vol. 1, fasc. 1, 1957, pp. 37-45.
20. Perret, R.: Le Relief du Sahara. Rev. Géog. Phys. et de Géol. Dyn., vol. VIII, fasc. 3, 1935, pp. 211-254, fasc. 4, pp. 363-409.
21. Bernard, A.: Géographie Universelle, Tome XI, Afrique Septentrionale et Occidentale, Part II, Sahara - Afrique Occidentale. Librairie Armand Colin (Paris), 1939.
22. Gautier, E.F.: Sahara: the Great Desert. Columbia Univ. Press (New York) 1935.
23. Capot-Rey, R.: Le Sahara Français. Presses Universitaires (Paris), 1953.
24. Lelubre, M.: Conditions Structurales et Formes de Relief dans le Sahara. Trav. de l'Institut de recherches sahariennes, vol. 8, 1952, pp. 189-239.

- 25. Alimen, H.: The Prehistory of Africa. Hutchinson (London), 1957.
- 26. Smith, H. T. U.: Eolian Geomorphology, Wind Direction, and Climatic Change in North Africa. AFCRL-63-443. U.S. Air Force, March 1963.

(c) Literature on small areas
(in order from northwest to southeast)

- 27. Sougy, J.: West African Fold Belt. Geol. Soc. Amer. Bull., vol. 73, July 1962, pp. 871-876.
- 28. Rod, E.: Fault Pattern, northwest corner of Sahara Shield. Amer. Assoc. Petr. Geol. Bull. vol. 46, 1962, pp. 529-534.
- 29. Joly, F.: Etudes sur le Relief du S-E Marocain. Trav. de l'Institut Scientifique Cherifien, Séries Géol. et Géog. Phys., 10, (Rabat), 1962, 508 pp.
- 30. Godard, A.: Morphologie des Socles et des Massifs Anciens. Rev. Géog. de l'Est, vol. 3, fasc. 1, 1963, pp. 75-92.
- 31. Choubert, G.: Note sur la Géologie de l'Anti-Atlas. XVIII International Geological Congress, (G.B.), 1948. Part XIV, 1951, pp. 29-44.
- 32. Gentil, L.: L'Anti-Atlas et le Djebel Bani. Rev. Géog. Phys. et de Géol. Dyn., vol. II, fasc. 1, (with colored geol. map), 1929, pp. 5-69.
- 33. Bourcart, J.: Reconnaissance Géologique dans les Confins Autonomes du Dra. Rev. Géog. Phys. et de Géol. Dyn., vol. VIII, fasc. 2, 1935, pp. 115-132.
- 34. Lavocat, R.J.M.: Vue d'ensemble sur la Géologie et la Paléontologie des Hammadas du Guir et du Dra. XIX International Geological Congress, (Alger) 1952, Sect. XIII, fasc. XV, 1954, pp. 59-63.
- 35. Choubert, G., and Lavocat, R.: Les Deformations et Plis de la Hamada du Dra. C.R. Acad. Sci., tome 231, 1950, pp. 451-453.
- 36. Menchikoff, N.: Recherches Géologiques et Morphologiques dans le Nord du Sahara occidental. Rev. Géog. Phys. et de Géol. Dyn., vol. III, fasc. 2, (with colored geol. map), 1930, pp. 103-247.
- 37. Lapadu-Hargues, P.: Etude Pétrographique du Massif Antécambrien des Eglab. XIX International Geological Congress (Alger) 1952. Section I, fasc. I, 1953, pp. 103-109.
- 38. Admiralty Handbook: French West Africa, vol. II. The Colonies. BR 512A. 1944.

39. Admiralty Handbook: French West Africa, vol. I. The Federation. BR 512, 1943.
40. Urvoy, J.: Structure et Modelé du Soudan français. Annales de Géographie, vol. 45, 1936, pp. 19-49.
41. Monod, T., with Bourcart, J.: L'Adrar Ahnet, contribution à l'Etude Physique d'un District Saharien. Rev. Géog. Phys. et de Géol. Dyn., in 3 parts, vol. IV, fasc. 2, 1931, pp. 107-150, fasc. 3, 1931, pp. 223-262; vol. V, fasc. 3, 1932, pp. 245-296, (with colored geol. map).
42. Grove, A. T.: Geomorphology of the Tibesti Region with special reference to Western Tibesti. Geog. Jour. vol. CXXVI, 1960, pp. 18-27.
43. Grove, A. T.: The Ancient Erg of Hausaland and Similar Formations on the South Side of the Sahara. Geog. Jour., vol. CXXIV, 1958, pp. 528-533.
44. Urvoy, J.: Formes Dunaires à l'Ouest du Tchad. Annales de Géographie, vol. 42, 1933, pp. 506-515.
45. Grove, A. T.: The Former Extent of Lake Chad. Geog. Jour., vol. CXXV, 1959, pp. 465-467.

(d) Thematic maps
(in order of reference)

46. Carte Géologique du Nord-Ouest de l'Afrique, 1:2,000,000. Pub. by La Comité d'Organisation du XIX^e Congrès Géologique International, (Alger) 1952. Sheet 1, Maroc-Algérie, 1952; Sheet 2, Algérie-Tunisie, 1952; Sheet 3, Sahara Occidental, 1956; Sheet 4, Sahara Central, 1954.
47. Afrique Occidentale (former French areas): Carte géologique, 1:2,000,000. Pub. by Bureau de Recherches Géologiques et Minières, 1960.
48. Carte géologique de l'Afrique Equatoriale Française, 1:2,000,000. G. Gerard, Direction des Mines et de la Géologie de l'A.E.F., 1956.
49. Geological map of the Spanish Sahara with adjacent regions, 1:1,500,000. Pub. by Instituto geologico y minero de Espana (Madrid), 1958.
50. Carte géologique du Maroc, 1:500,000. G. Choubert, Service de la Carte Géologique. Sheet 2, Marrakech, 1955-56; Sheet 4, Ouarzazate, 1959.
51. Official Mapping of the Algerian Sahara, 1:500,000. The following sheets have appeared as geological maps: NG 31 NE Amguid, 1954; NG 31 NW In Salah, 1952; NH 30 SE Kerzaz, 1952; NH 30 NW Tindouf, 1960; NH 30 SW Eglab, 1960.

52. Carte Géologique International de l'Afrique, 1:5,000,000. Pub by le Bureau d'Etudes Géologiques et Minières Coloniales (Paris). Sheets 1 and 2. 1st ed., 1952. (2nd ed. expected.)
53. Raisz, E.: Landform map of North Africa (Pub. by the author, 107, Washington Avenue, Cambridge 40, Mass.), 1952.
54. Van Lopik, J. R., and Kolb, C. R.: Analogs of Yuma Terrain in the Northwest African Desert, and Analogs of Yuma Terrain in the Northeast African Desert (hand-colored atlases). U.S. Army Engineer Waterways Experiment Station (Vicksburg, Miss.), Feb, 1958.
55. Keay, R. W. J. and others: Vegetation map of Africa south of the Tropic of Cancer (with explanatory notes), 1:10,000,000. Sponsored by UNESCO. Oxford University Press (London), 1959.

(e) Topographic and general maps
(in order of reference)

56. Africa, 1:1,000,000. Service Géographique de l'Armée (Paris), 1934-38, and Geographical Section, General Staff (London), 1940-43. Sheets NH 29; NG 29, 30, 31, 32; NF 31, 32, 33; NE 32, 33, 34; ND 33, 34
57. World Aeronautical Charts, 1:1,000,000. Sheets 2420, 2451 to 2454, 2537 to 2540, 2570 to 2573, 2662, 2663, 2692.
58. Africa, 1:2,000,000. Geographical Section, General Staff (London), series 2871. Sheets Maroc, Algérie, Mauritanie, Sahara, Fezzan, Soudan Français, Tchad.
59. Bartholomew, J. Ed.: The Times Atlas of the World, Mid-century ed., vol. IV, Southern Europe and Africa, plate 88, Morocco, Algeria and Tunisia; plate 90, Nigeria and Chad; plate 85, Egypt and Libya. 1:5,000,000. The Times (London) 1956.
60. Grosvenor, M. B. Ed.: National Geographic Atlas of the World. National Geographic Society (Washington, D. C.), 1963.

(f) Photo-interpretation

61. Hemphill, W. R.: Small-scale Photographs in Photogeologic Interpretation. Photogrammetric Eng., vol. 24, 1958, pp. 562-567.
62. Lattman, L. H.: Technique of Mapping Geologic Fracture Traces and Lineaments on Aerial Photographs. Photogrammetric Eng., vol. 24, 1958, pp. 568-576.